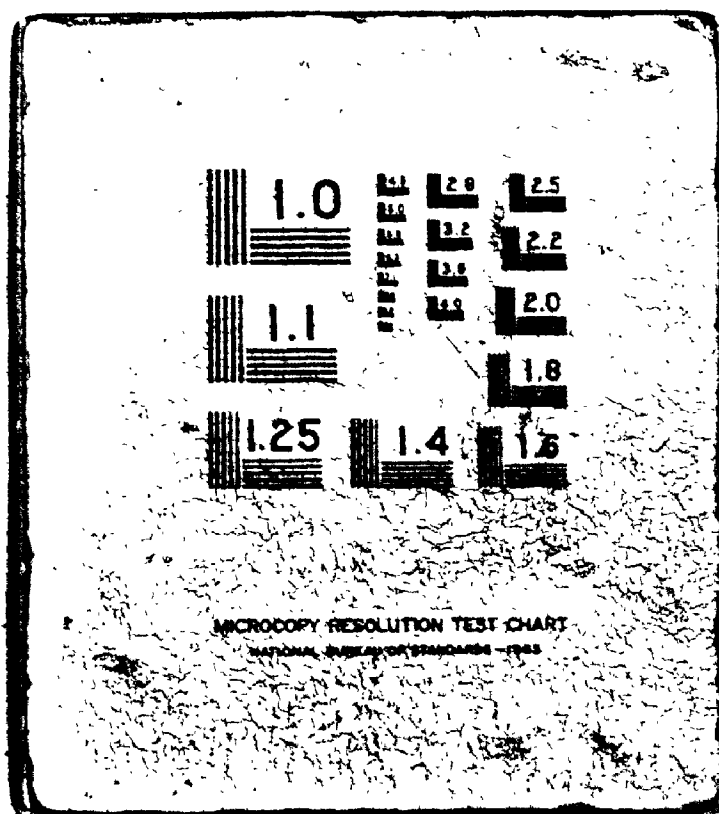


1 2

OF/DE



26595

National Library  
of CanadaBibliothèque nationale  
du CanadaCANADIAN THESES  
ON MICROFICHETHÈSES CANADIENNES  
SUR MICROFICHE

NAME OF AUTHOR/NOM DE L'AUTEUR Joseph Frank Dlouhy

TITLE OF THESIS/TITRE DE LA THÈSE Mössbauer Spectroscopy

UNIVERSITY/UNIVERSITÉ Carleton University

DEGREE FOR WHICH THESIS WAS PRESENTED/  
GRADE POUR LEQUEL CETTE THÈSE FUT PRÉSENTÉE Ph.D.

YEAR THIS DEGREE CONFERRED/ANNÉE D'OBTENTION DE CE DEGRÉ 1975

NAME OF SUPERVISOR/NOM DU DIRECTEUR DE THÈSE D. R. Wiles

Permission is hereby granted to the NATIONAL LIBRARY OF  
CANADA to microfilm this thesis and to lend or sell copies  
of the film.

The author reserves other publication rights, and neither the  
thesis nor extensive extracts from it may be printed or other-  
wise reproduced without the author's written permission.

L'autorisation est, par la présente, accordée à la BIBLIOTHÈ-  
QUE NATIONALE DU CANADA de microfilmer cette thèse et  
de prêter ou de vendre des exemplaires du film.

L'auteur se réserve les autres droits de publication; ni la  
thèse ni de longs extraits de celle-ci ne doivent être imprimés  
ou autrement reproduits sans l'autorisation écrite de l'auteur.

DATED/DATE 20.12.1975 SIGNED/SIGNÉ Joseph R. Dlouhy

PERMANENT ADDRESS/RÉSIDENCE FIXE 840 SPRINGLAND DR, APT. 428,  
OTTAWA, ONTARIO K1V 6L6

## INFORMATION TO USERS

THIS DISSERTATION HAS BEEN  
MICROFILMED EXACTLY AS RECEIVED

This copy was produced from a microfiche copy of the original document. The quality of the copy is heavily dependent upon the quality of the original thesis submitted for microfilming. Every effort has been made to ensure the highest quality of reproduction possible.

PLEASE NOTE: Some pages may have indistinct print. Filmed as received.

Canadian Theses Division  
Cataloguing Branch  
National Library of Canada  
Ottawa, Canada K1A 0N4

## AVIS AUX USAGERS

LA THESE A ETE MICROFILMEE  
TELLE QUE NOUS L'AVONS RECUE

Cette copie a été faite à partir d'une microfiche du document original. La qualité de la copie dépend grandement de la qualité de la thèse soumise pour le microfilmage. Nous avons tout fait pour assurer une qualité supérieure de reproduction.

NOTA BENE: La qualité d'impression de certaines pages peut laisser à désirer. Microfilmée telle que nous l'avons reçue.

Division des thèses canadiennes  
Direction du catalogage  
Bibliothèque nationale du Canada  
Ottawa, Canada K1A 0N4

MÖSSBAUER SPECTROSCOPY

by

Joseph Frank Dlouhy

A thesis submitted to the Faculty of  
Graduate Studies in partial fulfilment  
of the requirements for the degree of  
Doctor of Philosophy

Department of Chemistry

Carleton University

Ottawa, Ontario


K1S 5S6

© Joseph Frank Dlouhy 1976

The undersigned recommend to the Faculty  
of Graduate Studies acceptance of the thesis  
"Mössbauer Spectroscopy"  
submitted by Joseph Frank Dlouhy, in partial  
fulfilment of the requirements for the degree  
of Doctor of Philosophy.

  
.....  
Thesis Supervisor.

  
.....  
Chairman, Department of Chemistry

  
.....  
External Examiner

Carleton University

## ABSTRACT

A constant acceleration Mössbauer spectrometer was constructed and its long time stability and operating parameters studied. With this spectrometer a variety of technical and chemical problems were examined: for example, systematic deviations in spectrum shapes, chemical changes caused by grinding common inorganic salt hydrates, the occurrence of numerous small peaks in the background spectra, and the occurrence of narrow peaks in spectra of samples in solution in viscous solvents.

A new version of Mössbauer spectroscopy, called Integral Mössbauer Spectroscopy, was developed, whereby changes in Mössbauer absorption over selected energy ranges could be observed as a function of time. It was established from calculations of an optimum signal to noise ratio as a function of the integration interval that this method is phenomenologically independent of conventional Mössbauer spectroscopy. Applications of Integral Mössbauer Spectroscopy were demonstrated in the study of the kinetics of solid-solid and solid-liquid chemical reactions, and in the study of solid-solid and solid-liquid phase transitions. The existence of large non-Mössbauer resonance absorption was discovered. This absorption was observed for many materials even under conditions where the conventional Mössbauer effect does not occur as, for example, in liquid solutions. This absorption was found to be much stronger than normal (integrated) Mössbauer absorption, and to vary greatly (by up to 20%) from one compound to another. It is also found to have either a positive or negative temperature dependence in different compounds.

## ACKNOWLEDGEMENTS

The thanks of the author go to the faculty and staff of the Chemistry and Physics Departments for the technical help and for providing creative surroundings. Specifically the help of L. Raffler and E. Grey from the Science Workshop and P. Bertels from the Chemistry Workshop in the construction of equipment is greatly appreciated.

Discussion with and advice from Dr. G. J. Thiessen and Dr. H. S. Word from the National Research Council and D. W. Carson from the Department of Energy, Mines and Resources, Mines Branch, were equally very helpful. The last kindly made available the listing and the card deck for the curve fitting routine.

The financial support from the National Research Council is acknowledged.

Special thanks go to my supervisor Dr. D. R. Wiles for his patience, trust, deep personal understanding and for making this work possible.



## TABLE OF CONTENTS

ABSTRACT .....	i
ACKNOWLEDGEMENTS .....	ii
TABLE OF CONTENTS .....	iii
LIST OF FIGURES .....	vi
LIST OF TABLES .....	viii
INTRODUCTION AND THEORY .....	1
RESONANCE RADIATION PROCESSES .....	3
RESONANCE ABSORPTION CROSS-SECTION .....	4
DEBYE-WALLER FACTOR .....	5
THE MÖSSBAUER EFFECT .....	7
Isomer Shift .....	11
Quadrupole Splitting .....	13
Magnetic Hyperfine Splitting .....	14
Combined Interaction .....	16
Line Width .....	17
Relative Intensities .....	18
Chemical Applications .....	20
INTEGRAL MÖSSBAUER SPECTROSCOPY .....	21
Applications .....	29
NON-MÖSSBAUER RESONANCE ABSORPTION .....	32
EXPERIMENTAL PART .....	34
CONSTANT ACCELERATION MÖSSBAUER SPECTROMETER .....	34
INTEGRAL MÖSSBAUER SPECTROMETER .....	43
SOURCES AND ABSORBERS .....	45

CELLS .....	46
EVALUATION OF MÖSSBAUER SPECTRA .....	48
CALCULATIONS .....	50
RESULTS AND DISCUSSION .....	53
MÖSSBAUER SPECTROSCOPY .....	54
Standard Absorbers .....	55
Inorganic Compounds .....	65
Determination of Zero Velocity Position .....	67
Determination of the Phase Shift .....	69
INTEGRAL MÖSSBAUER SPECTROSCOPY .....	71
Apparent Shift in Spectral Characteristics .....	72
Shift in Position of Parabola .....	73
Shift in Position of Peaks .....	74
Integral Reaction Spectra .....	75
Solid-Solid Reactions:	
Ligand Transfer .....	76
Dehydration .....	87
Oxidation and Reduction .....	87
Solid-Liquid Reactions:	
Ion Exchange .....	90
Complex Redox and Exchange .....	93
Reprecipitation .....	94
Integral Thermal Scans:	
$\alpha$ -Fe <sub>2</sub> O <sub>3</sub> .....	96
Fe(ClO <sub>4</sub> ) <sub>2</sub> ·6H <sub>2</sub> O .....	100
Stainless Steel .....	102
(NH <sub>4</sub> )Fe(SO <sub>4</sub> ) <sub>2</sub> .....	103

NON-MÖSSBAUER RESONANCE ABSORPTION .....	105
CONCLUSIONS .....	111
PERSPECTIVES .....	115
APPENDIX 1 Signal-to-noise Ratio .....	117
APPENDIX 2 Definition of $\Delta A$ for Pure Compounds .....	119
REFERENCES .....	121

# LIST OF FIGURES

Figure 1a:	Mössbauer spectrum. Single peak.	9
Figure 1b:	Mössbauer spectrum. Quadrupole splitting.	9
Figure 2 :	Balance of radiation	10
Figure 3 :	Symmetric integration for $\delta = 0$ and $\gamma \neq 0$	24
Figure 4 :	Asymmetric integration	25
Figure 5 :	Offset integration	26
Figure 6 :	Symmetric integration with coincidence	28
Figure 7 :	Mössbauer spectra, velocity and displacement	35
Figure 8 :	Block diagram of Mössbauer spectrometer	40
Figure 9 :	Sample printout of 128 channels spectrum	49
Figure 10:	Determination of zero velocity position	70
Figure 11:	Dependence of signal-to-noise ratio on interval of integration	79
Figure 12:	Integral reaction spectrum $\text{FeSO}_4 \cdot 7\text{H}_2\text{O} + 6\text{KCN}$	81
Figure 13:	Integral reaction spectrum $\text{FeSO}_4 \cdot 7\text{H}_2\text{O} + 5\text{KCN}$	81
Figure 14:	Integral reaction spectrum $\text{FeSO}_4 \cdot 7\text{H}_2\text{O} + 6\text{KCNS}$	83
Figure 15:	Integral reaction spectrum $\text{FeSO}_4 \cdot 7\text{H}_2\text{O} + 6\text{KCNO}$	83
Figure 16:	Integral reaction spectrum $(\text{NH}_4)_2\text{Fe}(\text{SO}_4)_2 \cdot 6\text{H}_2\text{O} + 6\text{KCNS}$	86
Figure 17:	Integral reaction spectrum $(\text{NH}_4)_2\text{Fe}(\text{SO}_4)_2 \cdot 6\text{H}_2\text{O} + 2\text{Mg}(\text{ClO}_4)_2$	86
Figure 18:	Integral reaction spectrum $2\text{FeSO}_4 + (\text{NH}_4)_2\text{S}_2\text{O}_8$	89
Figure 19:	Integral reaction spectrum $\text{NH}_4\text{Fe}(\text{SO}_4)_2 \cdot 12\text{H}_2\text{O} + \text{KI}$	89
Figure 20:	Integral reaction spectrum adsorption of $\text{Fe}^{3+}$ on Dowex 50W	92
Figure 21:	Integral reaction spectrum $3\text{FeOx} \cdot 2\text{H}_2\text{O} + 2\text{K}_3[\text{Fe}(\text{CN})_6]_{\text{aq}}$	92

Figure 22:	Integral reaction spectrum $\text{FeOx} \cdot 2\text{H}_2\text{O} + \text{Na}_2\text{S}_{\text{aq}}$	95
Figure 23:	Integral reaction spectrum $\text{FeOx} \cdot 2\text{H}_2\text{O} + \text{Na}_2\text{S}_{\text{aq}}$ (agar-agar)	95
Figure 24:	Temperature profile for cryostat	97
Figure 25:	Integral thermal scan $\alpha\text{-Fe}_2\text{O}_3$	98
Figure 26:	Integral thermal scan stainless steel	98
Figure 27:	Integral thermal scan $\text{NH}_4\text{Fe}(\text{SO}_4)_2$ aq (agar-agar)	104

## LIST OF TABLES

Table 1:	Relative Intensities for Mössbauer Multiplet Spectra of $^{57}\text{Fe}$	19
Table 2:	Mössbauer Spectrometer Components	37
Table 3:	Mössbauer Spectral Parameters of Selected Iron Absorbers	56
Table 4:	Mössbauer Spectral Parameters of Selected Iron Absorbers	57
Table 5:	Mössbauer Spectral Parameters of 0.001" Iron Foil Standard	58
Table 6:	Mössbauer Spectral Parameters of 0.001" Iron Foil Standard	60
Table 7:	Mössbauer Spectral Parameters of $\alpha\text{-Fe}_2\text{O}_3$ Standard Absorber Material	61
Table 8:	Mössbauer Spectral Parameters of Sodium Nitroprusside Dihydrate	62
Table 9:	"Self-Absorption" Data for Two Sodium Nitroprusside Dihydrate Absorbers	63
Table 10:	Mössbauer Spectral Parameters of 0.0002" Stainless Steel 310 Standard Absorbers	64
Table 11:	Lorentz and Integrated Lorentz Functions	77
Table 12:	Symmetrical Integration of Lorentz Function	78

## INTRODUCTION AND THEORY

The Mössbauer effect, or gamma ray resonance fluorescence, is the resonant absorption and re-emission of a nuclear gamma ray made possible by the quenching of the usual nuclear recoil. Since its discovery in 1958, the Mössbauer effect has been the subject of a large number of publications and books, as well as many international conferences and symposia. The research is carried out mainly in two disciplines, namely Chemistry and Physics, with further applications in Mineralogy and Biochemistry. The effect is observed almost exclusively in the form of Mössbauer absorption (transmission) spectra or of Mössbauer emission (scattering) spectra.

While in principle resonance absorption is straightforward, it is uncommonly met in cases of nuclear  $\gamma$ -ray transitions. The reasons for this lie in that the  $\gamma$ -ray as emitted from a nucleus is usually of a lower energy than the transition energy, because of the recoil of the emitting (and absorbing) nucleus. This discrepancy is usually very large compared to the width of the  $\gamma$ -ray transition. It is useful to compare the energies of recoil ( $E_R$ ) from emission of various photons, as in the following table:

	$\text{Na}_D$ (optical)	$^{57}\text{mFe}$ ( $\gamma$ -ray)
$E$ (keV)	0.0021	14.39
$E_R$ (eV)	$10^{-10}$	$2 \cdot 10^{-3}$

In certain cases of low energy  $\gamma$ -transitions, the nuclear recoil energy can be taken up by the solid surrounding the atom, and

resonance absorption becomes possible. In this case, it is also possible to modulate the energy of the  $\gamma$ -ray by adding a Doppler motion to one of the nuclei concerned, and effectively scan back and forth over a very narrow energy region so as to study subtle chemical effects on the nuclear energy levels. Such scans represent the main application of Mössbauer spectroscopy.

While most of the studies to date involve materials assumed to be unchanging during the course of the measurement this need not be so. The object of the present study is to describe methods for performing time-dependent measurement of the Mössbauer absorption, and to show some results from its use. This method is quite novel and without precedent in the literature, except for some few papers describing so called "thermal scans" done under rather restricted conditions.

In order to explain the existence and nature of the Mössbauer effect, it is useful to deal first with optical resonance effects. Here the recoil energies are very low, so that the transition widths are much greater than the energy discrepancy. Further, the Debye-Waller factor must be described in order to interpret the magnitude of the Mössbauer effect. This factor, coming from early studies in X-ray diffraction by crystals, accounts for the "rigidity" of the crystal and its consequent ability to take up the recoil energy of a single atom. Later the method of the Integral Mössbauer spectroscopy will be treated.



# RESONANCE ABSORPTION PROCESSES

Optical resonance processes were predicted in the late nineteenth century by Rayleigh, and first found experimentally in 1904 (Wood). They are based on the fact that the energy of an emitted photon equals the energy of the photon required to effect the reverse transition. In practical cases the transition concerned is between the ground state and an excited state. There is, strictly speaking, an energy difference caused by nuclear recoil, as is shown in Equation 1, but this difference is negligible in most cases, and was not even suspected at that time.

$$E = E_{\text{upper}} - E_{\text{lower}} = E_Y + \frac{E_Y^2}{2Mc^2} \quad [1]$$

Because of the finite lifetime of an excited state, the energy of such a transition has a distribution with a Lorentzian shape as given in Equation 2, which describes the relation between the normalized intensity  $I(E)$  and the energy  $E$  in a peak where maximum intensity is at  $E_0$ .

$$I(E) = \frac{(\Gamma/2)^2}{(\Gamma/2)^2 + (E - E_0)^2} \quad [2]$$

This shape is fully described by its 'full width at half maximum' ( $\Gamma$ ) which is usually called the 'natural line width' and is given by the Heisenberg Uncertainty Principle:

$$\Gamma = \hbar/\tau = 6.6 \times 10^{-16} \frac{\ln 2}{t_{1/2}} \quad (\text{eV})$$

where  $\tau$  is the lifetime of the excited state in seconds and  $t_{1/2}$  is the half life of the excited state in seconds. The relative normalized probability  $W(E)$  of the occurrence of resonance absorption is thus

$$W(E) = \frac{(\Gamma/2)^2}{(\Gamma/2)^2 + (\Delta E)^2}$$

where  $\Delta E$  is the energy difference between the measured energy and the resonance energy.

### RESONANCE ABSORPTION CROSS-SECTION

The maximum resonance cross-section per atom ( $\sigma_0$ ) is given by the formula

$$\sigma_0 = \frac{2 I_e + 1}{2 I_g + 1} 2\pi \lambda^2 = \frac{2 I_e + 1}{2 I_g + 1} \frac{2.45 \times 10^{-15}}{E_0^2} \quad (\text{cm}^2)$$

where  $I_g$  and  $I_e$  are the spin quantum numbers for the ground state and the excited state, respectively,  $E_0$  and  $\lambda$  are respectively the energy (in keV) and the wavelength (in cm) of the photon.

In the case of a nuclear transition, the probability for re-emission of a gamma quantum is decreased, because of the possibility of internal conversion. The effective maximum resonance cross-section is then

$$\sigma_0 = \frac{2 I_e + 1}{2 I_g + 1} \frac{2.45 \times 10^{-15}}{E_0^2} \frac{1}{1 + \alpha} \quad (\text{cm}^2)$$

where  $\alpha$  is the internal conversion coefficient.

# DEBYE-WALLER FACTOR

While atomic recoil associated with optical resonances can be ignored, the recoil energy from higher energy emission (or absorption) is no longer negligible. For example Bragg reflection of X-rays occurs only with those photons scattered coherently - that is, without loss of energy by the recoiling of the scattering atom. In this case, the intensity of the Bragg X-ray lines is dependent on the rigidity of the lattice and this is strongly influenced by the temperature of the scattering crystal. The temperature dependence of this intensity is usually expressed as

$$I = I_0 f \quad [3]$$

$$f = e^{-2W} \quad [4]$$

where  $W$  is the Debye-Waller factor, and expresses the temperature dependence.

The Einstein model of the solid state leads to an expression for this Debye-Waller factor

$$W = \frac{1}{2} \frac{E_r}{k\theta_E} \quad [5]$$

where  $E_r$  is the recoil energy and  $\theta_E$  is the characteristic temperature, derived from the relation  $k\theta_E = \hbar\omega_E$ . This model, however, does not satisfactorily account for the observed temperature dependence. The Debye model of the solid state leads to the equation

$$W = 3 \frac{E_r}{k\theta_D} \left[ \frac{1}{4} + \left( \frac{T}{\theta_D} \right)^2 \int_0^{\theta_D/T} \frac{x dx}{e^x - 1} \right] \quad [5a]$$

where  $\theta_D$  is the Debye temperature defined as  $k\theta_D = \hbar\omega_D$  and  $x$  is the component of the mean square vibrational amplitude of the emitting particle in the direction of emission. This formula is simplified for the low temperature region, where  $T \ll \theta_D$

$$W = \frac{1}{2} \frac{E_r}{k\theta_D} \left( \frac{3}{2} + \frac{\pi^2 T^2}{\theta_D^2} \right) \quad [5b]$$

and at absolute zero to

$$W = \frac{3}{4} \frac{E_r}{k\theta_D} \quad [5c]$$

In the high temperature region ( $T > \frac{1}{2}\theta_D$ ) the dependence can be reduced to

$$W = 3 \frac{E_r T}{k\theta_D^2} \quad [5d]$$

When an appropriate expression for  $W$  (Equation 5a-d) is used in Equation 4, the variation of the intensity of Bragg reflection lines as a function of temperature is correctly given by Equation 3.

The relevance of this Debye-Waller factor to Mössbauer spectroscopy is that the value of  $f$  (in Equation 3) gives the probability of the recoil-free photon emission, or absorption. This in turn of course leads to an understanding of the probability of  $\gamma$ -ray resonance absorption -- the Mössbauer effect.

## THE MÖSSBAUER EFFECT

The occurrence of resonant scattering of  $\gamma$ -rays was predicted already in 1929 by Kuhn, but not discovered at that time. More recent attempts to achieve  $\gamma$ -ray resonance approached the problem by attempting to compensate for the nuclear recoil by adding a large Doppler motion. Thus, Moon (1950) achieved resonance absorption for the first time in  $^{198}\text{Hg}$ , by the use of a Doppler velocity of about  $10^5 \text{ cm sec}^{-1}$ .

A special case of resonant emission and absorption of  $\gamma$ -rays was discovered by physicist Rudolf F. Mössbauer during his graduate work in Heidelberg (Max Planck Institute for Medical Research) in 1957. The subject of his study (thesis advisor H. Maier-Leibnitz) was the scattering of 129 keV  $\gamma$ -rays of  $^{191}\text{Ir}$  by Ir and Pt and its increase for Ir by the lowering of the temperature. This observed scattering increase was contradictory to current predictions.

Already in the first publication (Mössbauer, 1958) the contradiction was explained in terms of the Lamb theory of elastic scattering of thermal neutrons (a recoilless process) known since 1937. In fact, Mössbauer had accomplished resonance absorption not by compensating for the recoil, but by eliminating it by altering the Debye-Waller factor. In his second work, he added small Doppler velocity ( $v$ ) to the source (in a way paralleling Moon experiment) and so altered the energy of the emitted  $\gamma$ -ray by  $\Delta E$  as given in the following equation

$$\Delta E = \frac{v}{c} E_{\gamma}$$

[6]

By altering the velocity he was able to scan over the energy range

of the resonance so as to study the shape of the resonance absorption peak. In practice, of course, one measures the transmission. This transmission as a function of the Doppler velocity has come to be known as a Mössbauer spectrum. While the effect was discovered first for  $^{191}\text{Ir}$ , a large number of other nuclides display the same effect. The overwhelming majority of Mössbauer studies are done using  $^{57}\text{Fe}$  as absorber of a  $\gamma$ -ray whose ultimate source is  $^{57}\text{Co}$ .

The transmission spectrum for a single line is given as Figure 1a. On one axis is the modulation Doppler velocity, energy or simply the channel number of a multichannel pulse analyser. On the other axis is the transmission or absorption or just the counting rate. The correct setting of the 100% transmission is possible only in the case of curve fitting of the results, although in practice the off-resonance baseline is used instead. Also shown in Figure 1a is the nuclear isomer shift ( $\delta$ ), to be described below. Figure 2 demonstrates the balance of radiation in the source-absorber system. Scattering and other effects of the surroundings are ignored. First there is a self-absorption in the source of both resonant and non-resonant radiation. Part of the radiation leaving the source is lost by absorption in the medium and another part of mainly resonant but also non-resonant radiation is the measured transmission.

This description is not fully exact because, for example, part of radiation is lost by resonance absorption in the source, since the source contains  $^{57}\text{Fe}$  in quantities which, though small, increase with increasing age of the source. Another secondary disturbance is the re-emission of  $\gamma$ -rays by the absorber. This effect is important

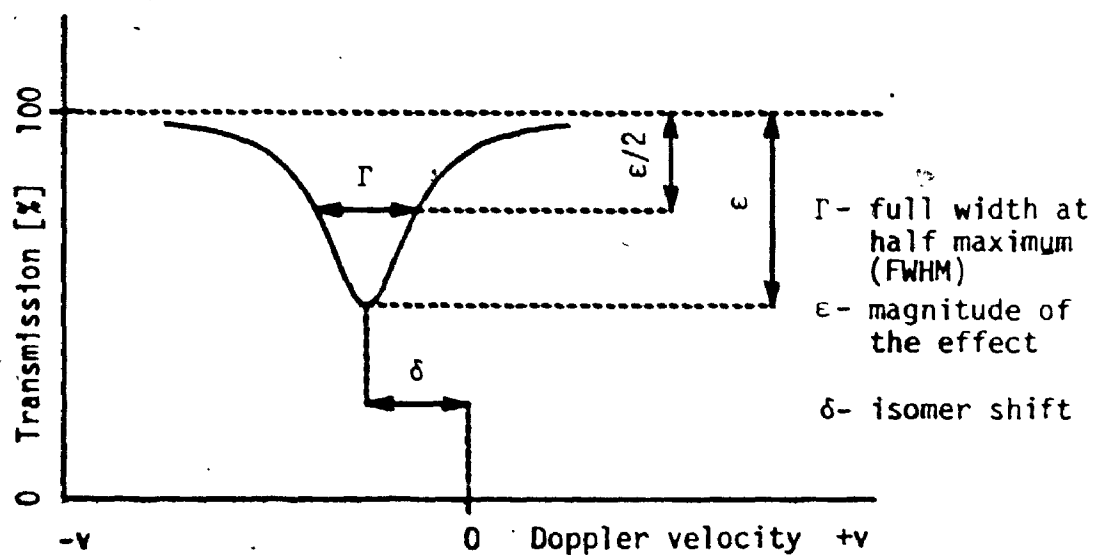


FIGURE 1a Mössbauer spectrum. Single peak.

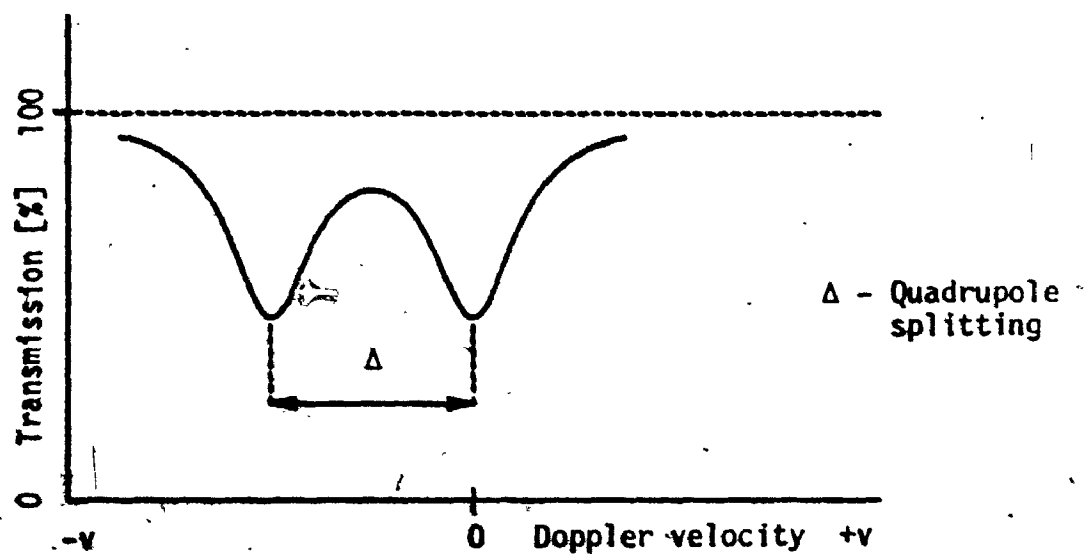


FIGURE 1b Mössbauer spectrum. Quadrupole splitting.

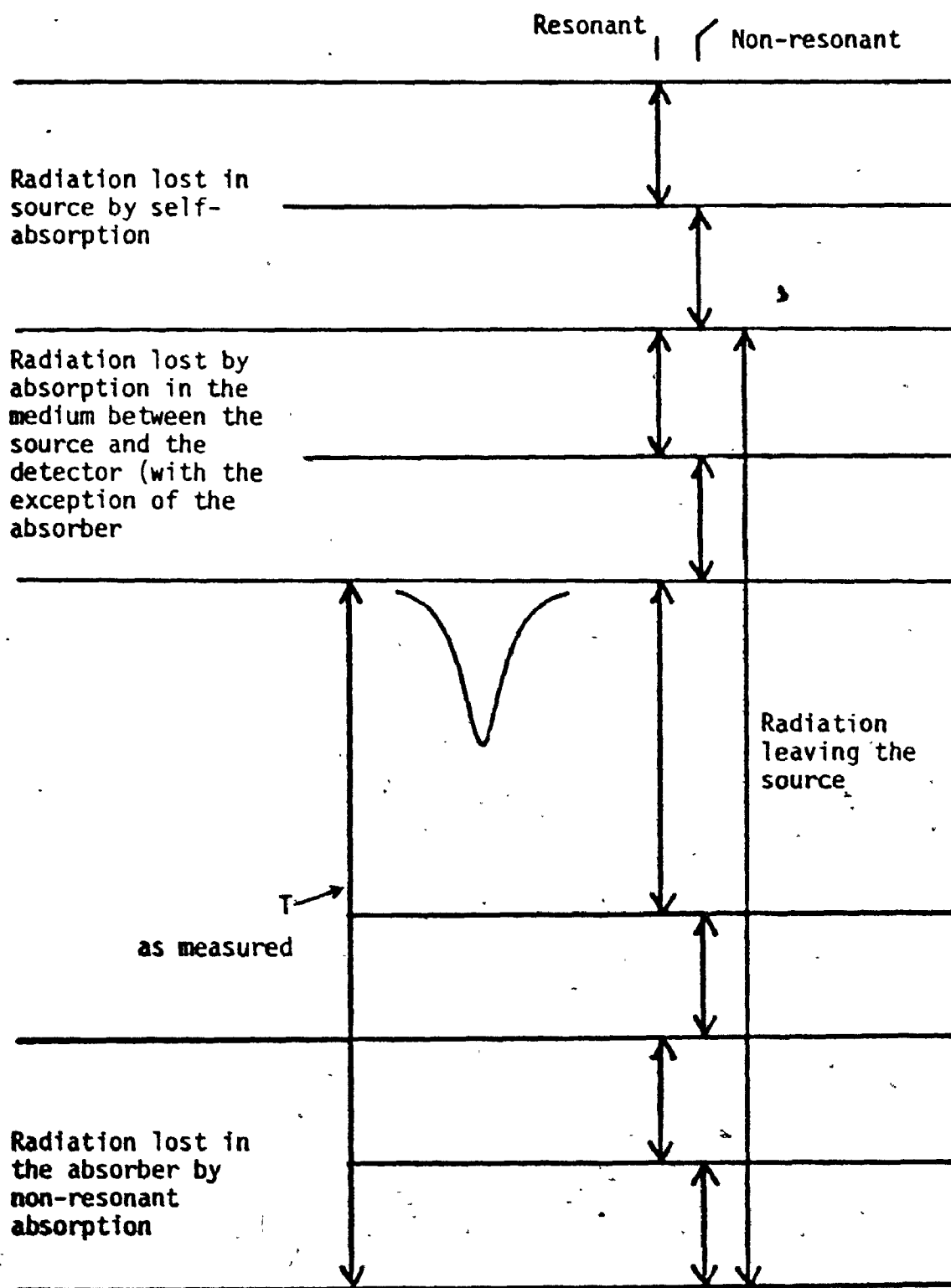


FIGURE 2 Balance of radiation



for selecting of the geometry of an experiment and critical in certain "difficult" experiments.

### Isomer Shift

The nuclear isomer shift ( $\delta$ ), called also chemical shift, is the energy difference between the energy of Mössbauer transition in the source and in the absorber. It was first identified by Kistner and Sunyar and its magnitude was calculated by Solomon.

The energy of the nuclear level is changed as a result of the interaction between the finite nucleus and the electron cloud by an amount given by

$$E = \frac{2}{3} \pi e |\psi(0)|^2 \int \rho(x_1, x_2, x_3) r^2 dV \quad [7]$$

where  $|\psi(0)|^2$  is the density probability of the s-electrons at the nucleus

$\rho(x_1, x_2, x_3)$  is the nuclear charge density at the  $(x_1, x_2, x_3)$ .

Introducing the mean square radius as

$$\langle r^2 \rangle = \frac{\int \rho(x_1, x_2, x_3) r^2 dV}{\int \rho(x_1, x_2, x_3) dV} \quad [8]$$

and using the relation  $\int \rho(x_1, x_2, x_3) dV = Ze$ , the energy of an emitted gamma quantum is then

$$E_{\gamma, s} = E_0 + \frac{2}{3} \pi e^2 Z |\langle r^2 \rangle_e - \langle r^2 \rangle_g| \cdot |\psi(0)|_s^2 \quad [9]$$

where indices s, e, g denote the source, excited state and ground state, respectively.  $E_0$  is the energy of the gamma quantum for the bare nucleus.

A similar expression is valid for the absorber

$$E_{\gamma,a} = E_0 + \frac{2}{3}\pi e^2 Z |\langle r^2 \rangle_e - \langle r^2 \rangle_g| \cdot |\psi(0)|_a^2 \quad [10]$$

Finally, the isomer shift is equal to

$$\delta = E_{\gamma,a} - E_{\gamma,s} = \frac{2}{3}\pi e^2 Z |\langle r^2 \rangle_e - \langle r^2 \rangle_g| (|\psi(0)|_a^2 - |\psi(0)|_s^2) \quad [11]$$

Assuming that the nuclear charge density is constant within the radius (R) of the nucleus leads to

$$\rho = \frac{3Ze}{4\pi R^3} \quad [12]$$

and therefore

$$\langle r^2 \rangle = \frac{\rho \int r^2 dV}{\rho \int dV} = \frac{3}{5} R^2$$

The difference between the mean square radii is then

$$\frac{3}{5}(R_e^2 - R_g^2) = \frac{3}{5} \Delta R^2 \approx \frac{6}{5} R \Delta R$$

Substitution into Equation 11 leads to

$$\delta = \frac{4}{5}\pi e^2 Z R^2 \frac{\Delta R}{R} (|\psi(0)|_a^2 - |\psi(0)|_s^2)$$

For a given transition this equation can be simplified to the following form

$$\delta = \text{const} (|\psi(0)|_a^2 - |\psi(0)|_s^2)$$

Mössbauer spectroscopy experiments are usually performed with a given source (or absorber) and the corresponding wave function is then also constant. This gives the final expression

$$\delta = \text{const} |\psi(0)|_a^2 - \text{Const} \quad [13]$$

This equation or the previous one can be used to prove the invariance of differences of  $\delta$  for various compounds measured with different sources, which is heavily used to recalculate measured  $\delta$  values to a selected standard.

### Quadrupole Splitting

The quadrupole splitting ( $\Delta$ ) is the lifting of the degeneracy of nuclear levels (with the nuclear spin of  $3/2$  or greater). It is caused by the interaction of the nuclear quadrupole moment ( $Q$ ) with the gradient of electric field ( $V_{ij}$ ), and was first observed by Kistner and Sunyar.

The energy difference ( $\Delta E$ ) between the original and the shifted nuclear levels (Wegener; Townes and Shawlow) is

$$\Delta E = \frac{e^2 q Q}{4I(2I - 1)} [3m_I^2 - I(I + 1)] \left(1 + \frac{\eta^2}{3}\right)^{1/2} \quad [14]$$

where  $eq$  is the maximum value of the electric field gradient (on the  $Z$  axis)

$I$  is the nuclear spin

$m_I$  is the nuclear magnetic quantum number (projection of  $I$  on the  $Z$  axis)

$\eta$  is the asymmetry parameter defined as  $\eta = (V_{xx} - V_{yy})/V_{zz}$  and the convention  $|V_{zz}| > |V_{yy}| > |V_{xx}|$  means that  $\eta \leq 1$ .

Because the  $m_I$  is present only as the square, the degeneracy is not completely lifted:

$$\Delta E(+m_I) = \Delta E(-m_I)$$

The  $^{57}\text{Fe}$  in the ground state has a nuclear spin of  $1/2$  and

therefore has a spherical nuclear charge distribution. The absence of a nuclear quadrupole moment means that  $\Delta E = 0$ . The nuclear spin for the first excited state is  $3/2$ . Then  $m_I$  has the values  $3/2$ ,  $1/2$ ,  $-1/2$  and  $-3/2$ . Substitution for  $m_I$  and  $I$  in Equation 14 leads to the results

$$\Delta E\left(\frac{3}{2}, \pm\frac{3}{2}\right) = \frac{1}{4}e^2qQ\left(1 + \frac{n^2}{3}\right)^{\frac{1}{2}} \text{ and}$$

$$\Delta E\left(\frac{3}{2}, \pm\frac{1}{2}\right) = -\frac{1}{4}e^2qQ\left(1 + \frac{n^2}{3}\right)^{\frac{1}{2}}$$

Finally, the quadrupole splitting ( $\Delta$ ) equals

$$\Delta = \Delta E\left(\frac{3}{2}, \pm\frac{3}{2}\right) - \Delta E\left(\frac{3}{2}, \pm\frac{1}{2}\right) = \frac{1}{2}e^2qQ\left(1 + \frac{n^2}{3}\right)^{\frac{1}{2}} \quad [19]$$

This partial degeneracy is the reason for the formation of a doublet only. The centroid of the doublet gives the position of the unsplit level, and the isomer shift thus remains fully defined. A quadrupole split spectrum is shown in Figure 1b.

### Magnetic Hyperfine Splitting

The magnetic hyperfine splitting ( $\Delta E$ ) is the lifting of the degeneracy of nuclear levels (usually in the absorber) caused by the interaction of the internal magnetic field ( $H$ ) with the nuclear magnetic moment ( $\mu$ ). It was first observed by Pound and Rebka.

The theoretical treatment of magnetic hyperfine splitting was given by Abragam. The magnetic field splits the nuclear level of spin  $I$  into  $(2I + 1)$  levels,  $m_I$ . For  $^{57}\text{Fe}$  the excited level ( $3/2$ ) is split into four and the ground level ( $1/2$ ) into two non-degenerate substates. The selection rule  $\Delta m_I = 0, \pm 1$  limits the number of lines

for one iron species to six as shown in the Figure. The splitting for the two levels will be different and in each case equal to

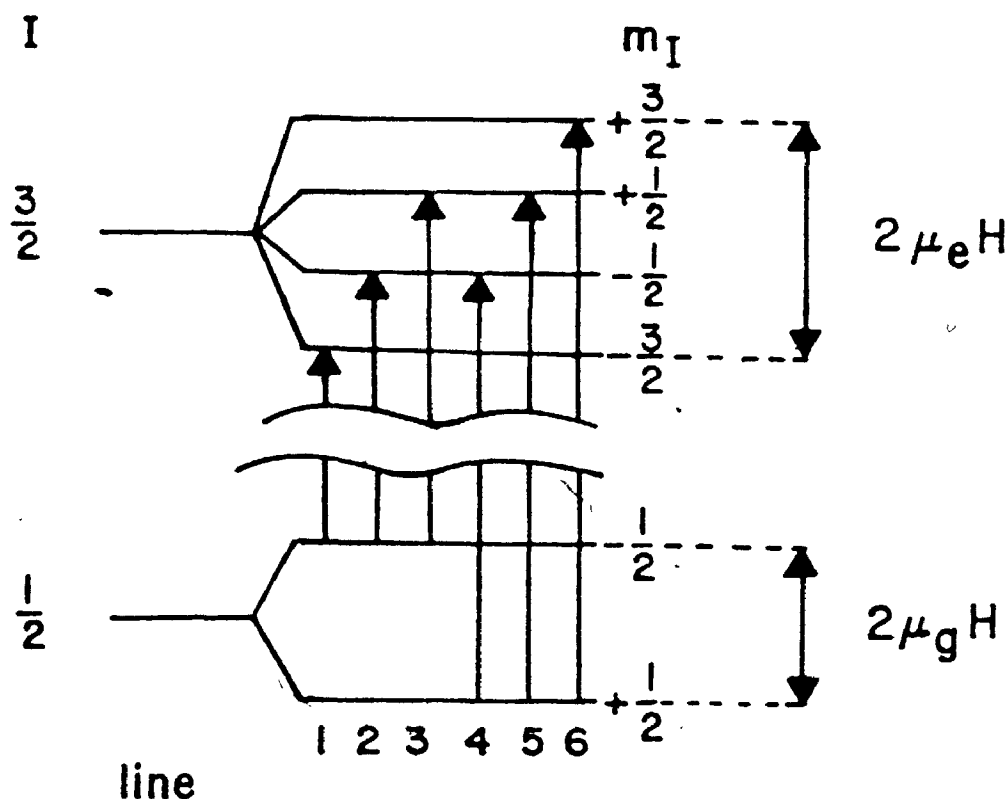
$$\frac{\mu_e H}{I_e} \rightarrow \frac{2}{3} \mu_e H \neq \frac{\mu_g H}{I_g} = 2 \mu_g H$$

where  $\mu$  is magnetic moment of the nucleus

$H$  is the magnetic field

$I$  is the nuclear spin

$e$  and  $g$  denotes the excited and ground state respectively.



The energy ( $E_{ij}$ ) of the transition is equal to

$$E_{i,j} = E_0 + \delta - g_0 \mu_N H m_{j,g} + g_e \mu_N H m_{i,e}$$

and the energies for the individual hyperfine lines are

$$\Delta E_{i,j} = \delta - g_0 \mu_N H (m_{j,g} - \frac{g_e}{g_0} m_{i,e})$$

where  $\delta$  is the isomer shift

$E_0$  is the energy of the emitted gamma quantum

$\mu_N$  is nuclear magneton

$m_I$  is nuclear magnetic quantum number

$g$  is gyromagnetic ratio (nuclear g-factor); index 0 means ground state

The degeneracy is now completely lifted because  $m$  is present to the first power only.

Magnetic field can originate either within the atom itself, within the crystal via exchange interactions or as a result of an external magnetic field. (For  $^{57}\text{Fe}$  it must be about 30 kG to have a significant effect.)

### Combined Interactions

The chemical isomer shift does not cause a change in separation of the resonance lines of quadrupole spectra or magnetically split spectra. But the combined quadrupole and magnetic interaction causes changes in separation. Only simple cases can be treated analytically. Kistner and Sunyar were the first who analyzed the combined magnetic and electric hyperfine interactions in the absorption spectrum of  $\alpha - \text{Fe}_2\text{O}_3$ .

### Line Width

The natural line width ( $\Gamma$ ) was already introduced on page 3. The formula given there is valid only for a thin source or absorber. In a real experiment the measured  $\Gamma_{\text{exp}}$  is the sum of the widths of the source and of the absorber which are assumed for simplicity to be equal to each other where the thicknesses are not great and for most cases equal to the natural line width. Therefore

$$\Gamma_{\text{exp}} = 2\Gamma .$$

For a thicker absorber with an effective thickness ( $T$ ) the measured line is broader (Frauenfelder and others):

$$\Gamma_{\text{exp}} = \Gamma(2.00 + 0.27T) \quad 0 < T \leq 5$$

$$\Gamma_{\text{exp}} = \Gamma(2.02 + 0.29T - 0.005T^2) \quad 4 \leq T \leq 10$$

where  $T = f_a n_a a_a \sigma_0 t_a$

and  $f_a$  is the recoil-free fraction for the absorber

$n_a$  is the number of atoms of the element studied, per  $\text{cm}^3$   
in the absorber

$a_a$  is the relative abundance of the Mössbauer active isotope

$\sigma_0$  is the resonance absorption cross-section

$t_a$  is the thickness of the absorber in cm

There are other causes of the broadening of a line. One is the diffusional broadening (studied for viscous liquids and solids); another is the broadening caused by the presence of a magnetic field which is not large enough to cause the hyperfine splitting,

still another involves apparent broadening caused by, for example, an unresolved quadrupole doublet.

### Relative Intensities

The relative intensities of lines in multiplet Mössbauer spectra are not all equal and in some cases differ markedly. According to Fagg and Hanna, an angular dependence of the intensities is displayed, which is in turn dependent on changes in the nuclear angular momentum or in the nuclear magnetic quantum number in the transition occurring. The relative intensity values are given in Table 1 for the case of magnetic hyperfine splitting and quadrupole splitting for single crystals of selected orientation. It was also found that the relative intensities for assemblies of randomly oriented small crystals are different and can be calculated as an average over all crystals. These values are also given in the Table.

For isotropic compounds the lines in the magnetic hyperfine split spectra have relative intensities 3:2:1:1:2:3, and for quadrupole spectra the two peaks have the same intensities.

For anisotropic compounds the ratio in dependence on  $\theta^*$  is 3:x:1:1:x:3, where  $x \in (0,4)$  is the ratio  $4 \sin^2 \theta / (1 + \cos^2 \theta)$  and for quadrupole splitting  $x:3$ , where  $x \in (1,5)$  and  $x = (2 + 3 \sin^2 \theta) / 3(1 + \cos^2 \theta)$ . In all cases the sum of the absolute intensities

---

\*  $\theta$  is the angle between the magnetic field and the direction of propagation of the radiation.



TABLE 1 Relative Intensities for Mössbauer Multiplet  
Spectra of  $^{57}\text{Fe}$

Transition $m_i \rightarrow m_j$	$C^2*$	A b s o r b e r s			
		Anisotropic $\theta^\dagger$	0°	90°	Isotropic
Magnetic Hyperfine Spectra					
$\frac{1}{2} \rightarrow \frac{3}{2}$	3	$1 + \cos^2 \theta$	3	3	3
$\frac{1}{2} \rightarrow \frac{1}{2}$	2	$2 \sin^2 \theta$	0	4	2
$\frac{1}{2} \rightarrow -\frac{1}{2}$	1	$1 + \cos^2 \theta$	1	1	1
$\frac{1}{2} \rightarrow -\frac{3}{2}$	1	$1 + \cos^2 \theta$	1	1	1
$-\frac{1}{2} \rightarrow -\frac{1}{2}$	2	$2 \sin^2 \theta$	0	4	2
$-\frac{1}{2} \rightarrow -\frac{3}{2}$	3	$1 + \cos^2 \theta$	3	3	3
Quadrupole Spectra					
$\pm \frac{1}{2} \rightarrow \pm \frac{1}{2}$	1	$2 + 3 \sin^2 \theta$	1	5	1
$\pm \frac{1}{2} \rightarrow \pm \frac{3}{2}$	1	$3(1 + \cos^2 \theta)$	3	3	1

The normalization of numerical values is arbitrary.

\*  $C^2$  is the angular-independent intensity term

†  $\theta$  is the angular dependent term

must be a constant unless the formal angular dependence of the overall intensity is introduced on account of saturation effects.

Numerous spectra have been published as having the two lines of quadrupole split spectra with different intensities. The validity of observations, claimed to be described as the Goldanskii-Karyagin effect, has been contested (Housley, Gonser and Grant). The asymmetry may well result from an instrumental artefact.

### Chemical Applications

Mössbauer spectroscopy has been widely applied and has, in fact, become almost a routine method in physical inorganic chemistry of substances which contain iron or any of the other Mössbauer-active elements. Virtually all of the studies which have been made concern stable materials, in which the sample remains unchanged during the course of the measurement. In nearly all of these cases the object of the study was to understand the structure or bonding of a single material or the usual spectroscopic identification.

In some few cases, studies have been made in which a reacting system has been studied. This has been done either by selecting a very slow reaction, such that the time measurement can effectively be made at a point in time, or by quenching a reaction which proceeds only at a higher temperature. In the present work, a method is described by which chemical and other transformations can be studied directly while they occur, that is, by the method of Integral Mössbauer Spectroscopy, whereby the transmission of gamma radiation through a selected part of the Mössbauer spectrum is followed as a function of time.

## INTEGRAL MÖSSBAUER SPECTROSCOPY

Although Mössbauer spectroscopy is used in Chemistry almost exclusively to study molecular and crystal structures, it has also been used to study chemical reactions. This is possible in cases when the duration of the reaction is much longer than the time necessary to accumulate a Mössbauer spectrum. For practical purposes this means that one can study reactions with lifetime of tens of days and longer. For example, Wittmann, Pobell and Wiedemann studied changes in ferrites over a period of seven hundred days.

Faster reactions can be studied, but only if it is possible to stop them by cooling or other means and measure the Mössbauer spectrum after the reaction has been stopped. That has been done, for example, by Gallagher, Johnson and Schrey in a study of the thermal decomposition of  $\text{FeSO}_4 \cdot 7\text{H}_2\text{O}$  and  $\text{FeSO}_4 \cdot \text{H}_2\text{O}$  and by Bancroft, Dharmawardena and Maddock, who studied the thermal decomposition of  $\text{K}_3\text{Fe}(\text{C}_2\text{O}_4)_3 \cdot 3\text{H}_2\text{O}$ .

Another use of Mössbauer spectroscopy in following chemical and physical changes involves measurements of Mössbauer spectra at different constant temperatures. This is mainly used to study the phase changes. A very good example of this work was done by Gibb, Greenwood and Sastry on  $\text{NH}_4\text{Cl}$  using  $\text{FeCl}_2$  as a probe. In both these latter cases the amount of work involved is rather prohibitive.

Some authors therefore developed the technique of "thermal scans". These can be realized in two ways. The simplest method, limited to compounds with the absorption peak of interest close to

zero velocity, consists of using a stationary source and a stationary absorber. Transmitted photons are registered with a simple counter and plotted against the temperature. An example of such type of work is the study of frozen solutions of  $\text{Fe}(\text{ClO}_4)_3$  by Keszthelyi, Cameron, Nagy and Kacsóh. A more sophisticated method uses a constant velocity Mössbauer spectrometer, where the peak can be located at any velocity. One early example of such study is perhaps found in the work of Preston, Hanna and Heberle who used this method for the study of phase transitions in iron. Both of these latter mentioned methods can be also used for constant temperature measurements.

For thermal scans the disadvantage of the above mentioned methods lies in the combination of two effects: the change in the intensity of the peak and the change in the position of the peak.

Therefore a new spectroscopic method which avoids this disadvantage, is proposed and realized in this thesis, for which the name Integral Mössbauer Spectroscopy is suggested. For both constant temperature and variable temperature measurements, this method gives a better signal to noise ratio (See Appendix 1).

Integral Mössbauer spectroscopy involves measuring the counting rate over a selected velocity interval for successive time intervals which are integer multiples of the period of motion or which are long in comparison with the period of motion. The basic idea of the Integral Mössbauer Spectroscopy is to count over the entire area of one selected peak or group of peaks.

The measurements can be accomplished in various ways. The

simplest version is for the case when the integration interval is symmetrical around the zero velocity of the source. Then the source moving with constant acceleration will sweep through the interval from  $-v_{\max}$  to  $+v_{\max}$  equivalent to the corresponding energy values. This gives optimum results for peak located at the centre of the Mössbauer spectrum (see Figure 3). If the peak is shifted from this position, then the integration interval has to be enlarged so as to include the whole peak. This diminishes the sensitivity. Broadening the velocity range to accommodate an isomer shift  $\delta$  equal to  $\Gamma$ , will cause the diminishing of the effect to one half. To maintain the sensitivity it is necessary to keep the source at constant velocity located at the maximum of the peak and either move the absorber over the entire width of the peak or to modulate the constant velocity by such motion (see Figure 4). This modulatory motion must have a frequency which is a whole multiple of the basic frequency or be high by comparison. The whole process can, of course, be inverted (source — absorber). For integrations which are not symmetric around the origin, greater time utilization can be achieved through the use of an asymmetric wave form. It is also possible to use a velocity signal of more complicated shape, where the velocities outside the region of interest are passed over with a higher acceleration (see Figure 5). With such a velocity signal, time utilization and signal-to-noise ratio in the integration are optimized for any value of the isomer shift and at the same time only the source (or the absorber) need be moved. The motion is relatively simple in comparison to that of the previous version.

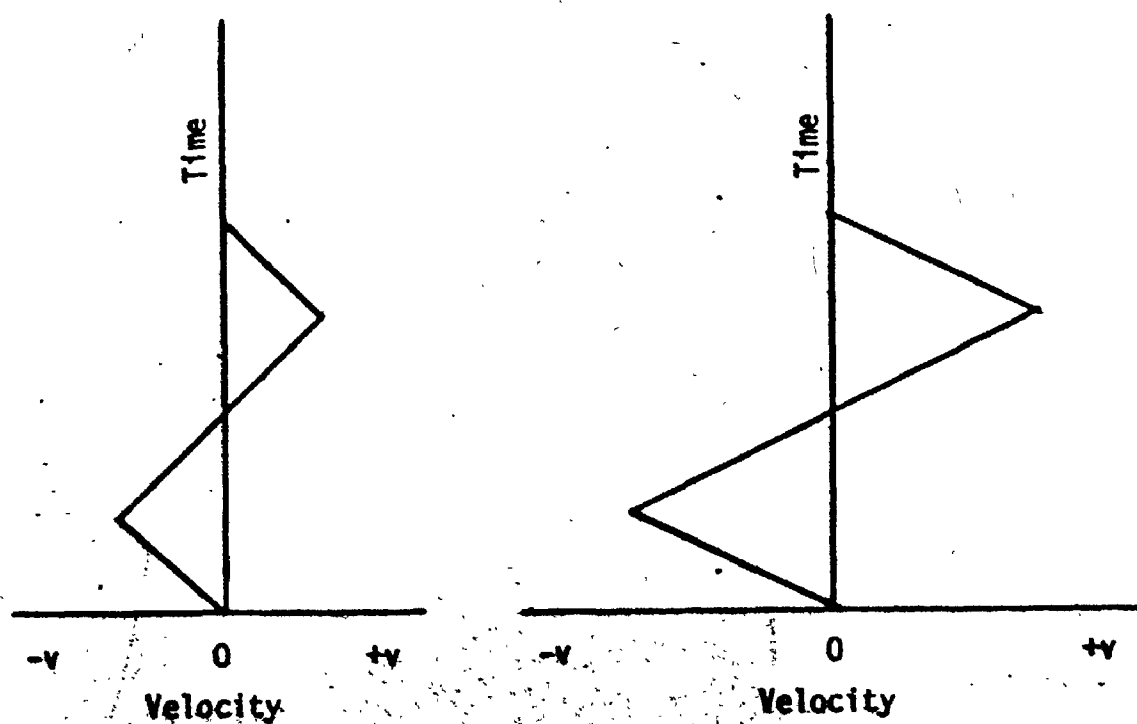
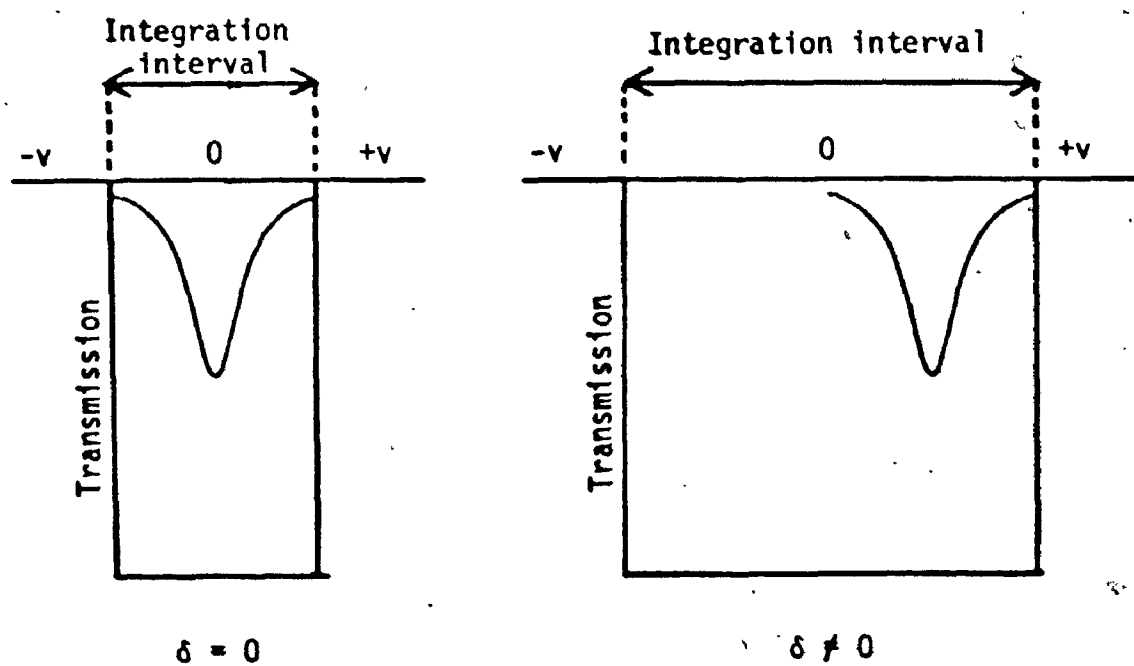


FIGURE 3 Symmetric integration for  $\delta = 0$  and  $\delta \neq 0$

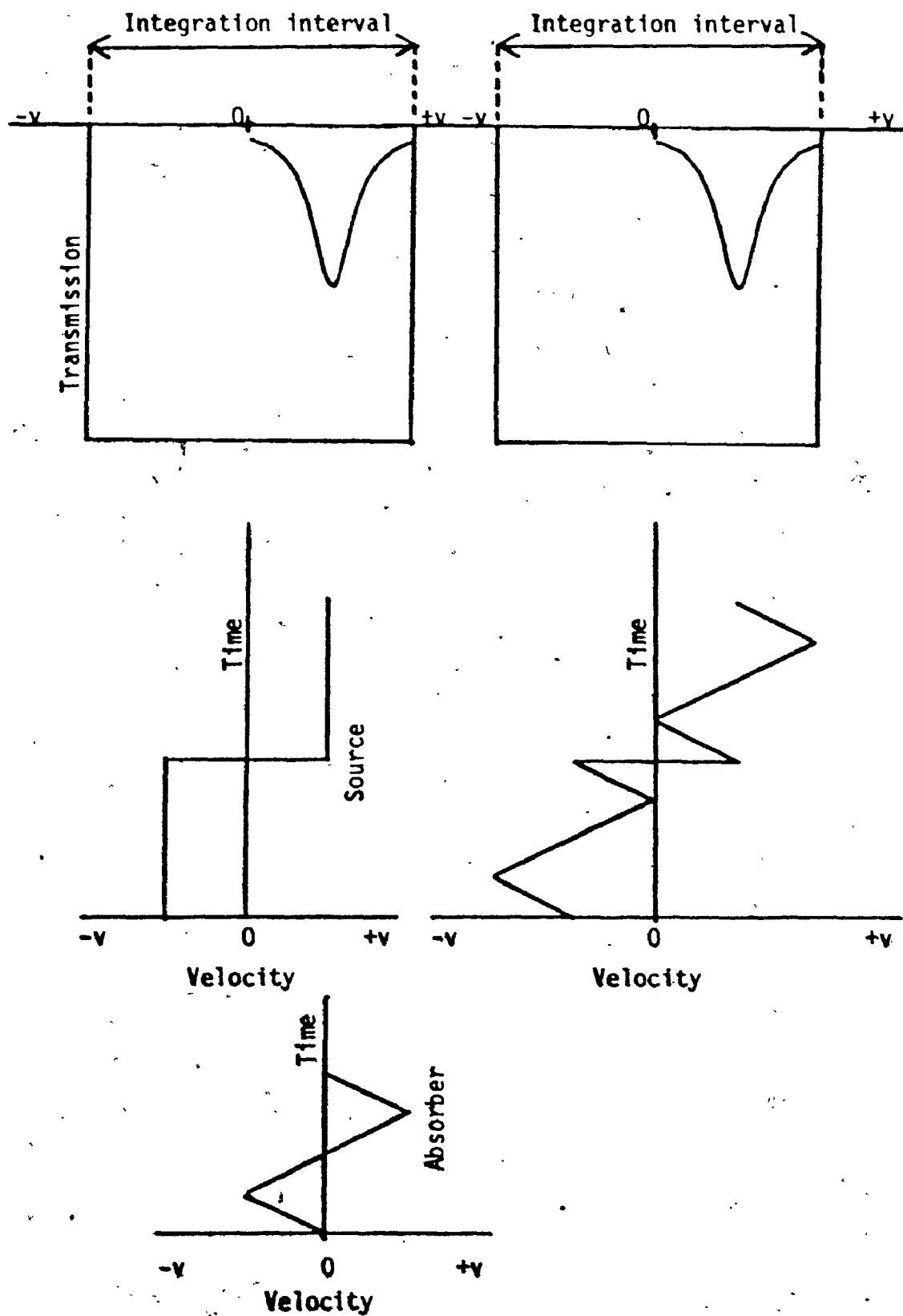


FIGURE 4 Asymmetric integration.

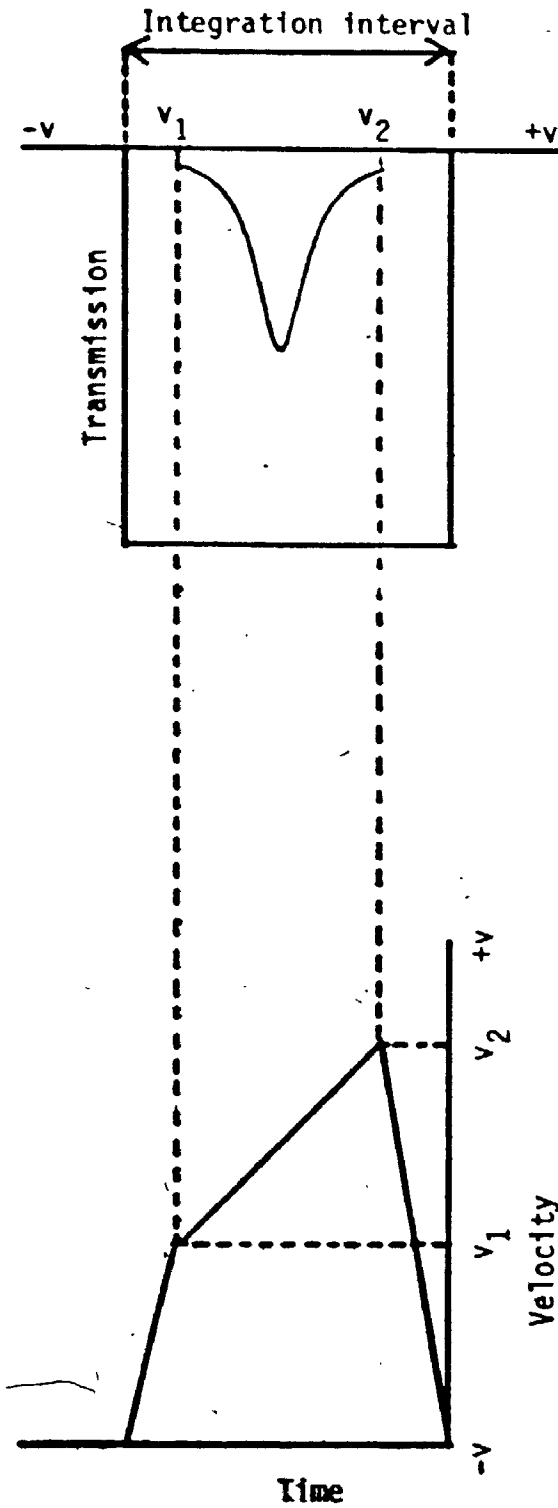


FIGURE 5 Offset integration



Electronically the simplest solution for an asymmetrical integration is to work in a constant acceleration mode and use conditions such that the last channel coincides with the highest required velocity. Using a DC coincidence circuit now makes it possible to integrate over only the desired velocity interval. (See Figure 6). The motion of the source (or absorber) is still fully symmetrical and the integration is optimized for these conditions.

Time utilization suffers by this method of course. Where slow drift in peak position is anticipated, it is helpful to use a larger integration interval to ensure that the changes occurring actually do proceed within the interval under observation.

Processes which can be studied by Integral Mössbauer Spectroscopy are of different types. The first type is characterized by the disappearance (or appearance) of a peak from a given position as result of a reaction or phase change. A second type is based on the change in the area of a peak resulting from a change in the Mössbauer-Lamb factor. Furthermore most measurements in practice are done in the area of non-linearity of absorption ( $\mu > 10 \text{ mg Fe cm}^{-2}$ ) therefore the diminishing of  $\Delta E$  and overlapping of the two peaks which were formerly separated (still both within the integration interval) leads to the diminishing of the absorption and vice versa. The obvious case of changes of absorption by the change of mass in the path of radiation which is valid for all radiations is not treated here.

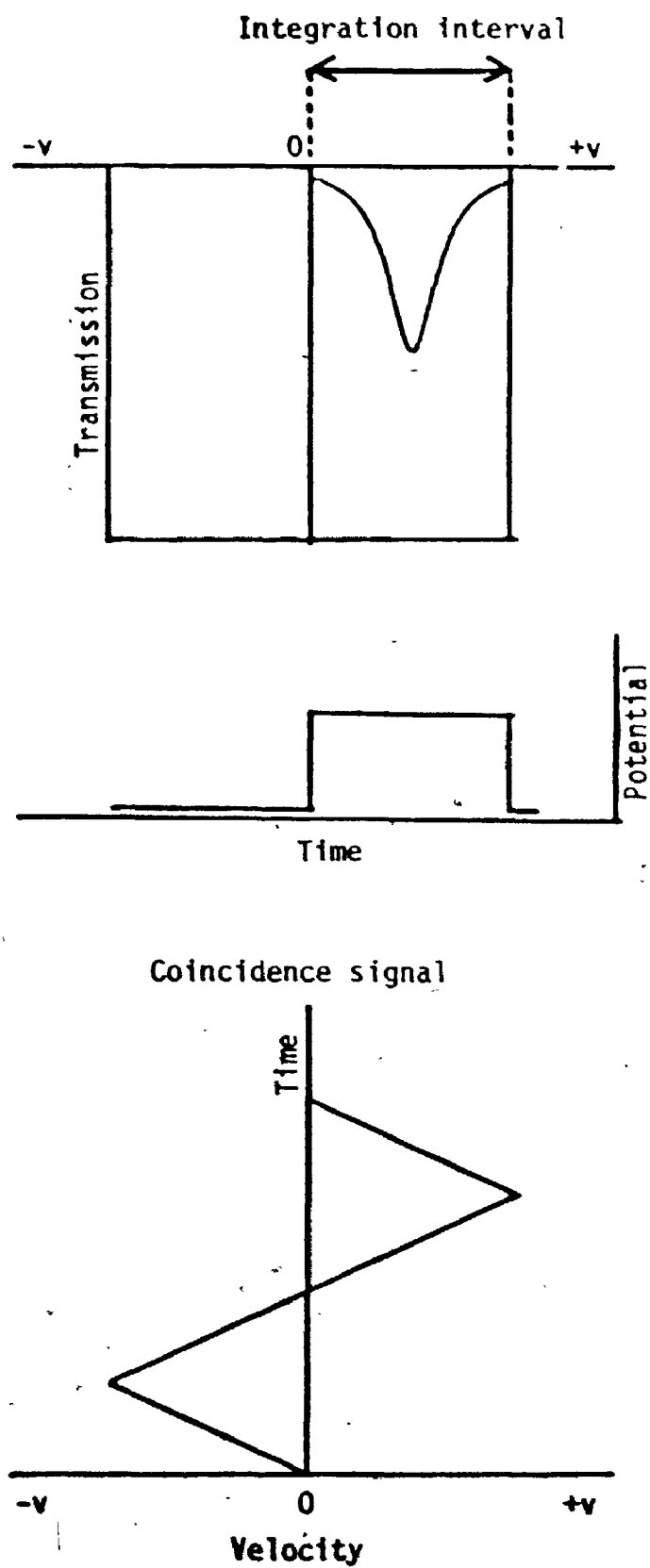


FIGURE 6 Symmetric integration with coincidence

## Applications

Every new experimental technique must have some advantage e.g. opening a new area of research, making such area better, (or more conveniently) accessible, making the research more economical or offering a better quality of information.

Taking as an example a spectroscopic technique, infrared spectroscopy, it underwent large changes over the years. The three main difficulties - the source, the dispersive element and the detector - were overcome and the technique found its way in more physical laboratories and after the beginning of commercial production of infrared spectrometers in chemical laboratories also because its usefulness for chemical research was easily recognized. The recent development, the introduction of Fourier transform infrared spectroscopy, is apparently bringing in only the better quality of information (better signal-to-noise ratio due to Fellgett advantage), but the impact on chemical research is rather large.

Another example from the field of spectroscopy is the  $\gamma$ -ray spectroscopy. The magnetic spectrometer with its high resolution and price is up to now used only in limited number of physical laboratories. The development of photomultipliers and scintillators led to the construction of scintillation  $\gamma$ -spectrometers (with the resolution worse by more than two orders of magnitude), but the economic accessibility caused it to "overflow" from physical laboratories to many chemical laboratories. Economically still much more convenient gray-wedge analyzers based on the same principles remained only a laboratory curiosity (due to the necessity to process and evaluate the photographic material). The next development

leading to the introduction of multichannel analyzers with their convenience of operation and quality of information (again Fellgett advantage) overcame the larger expense and nowadays there is no  $\gamma$ -spectrometry laboratory without at least one such unit. The last development (semiconductor detectors) brought only better resolution (by almost two orders of magnitude) but its significance is manifold.

The new technique of Integral Mössbauer Spectroscopy fulfills all four earlier mentioned criteria. Up to the present time there is not a spectroscopic technique available, that makes a measurement of a heterogenous reacting or changing system including solid phase(s) possible. The most common spectroscopic techniques UV, visible and IR spectroscopy can be used (in the reflection version) to study the surface reactions only and can not measure the bulk properties (due to the combination of dispersion and absorption and partly also the dilution effects).

To measure the bulk properties in such polydisperse systems a higher energy radiation is necessary. (Usually in the region of more than few keV.) Up to the present time only two techniques are available in such energy interval. (The Mössbauer spectroscopy and the X-ray diffraction.) The difference between the Mössbauer spectroscopy and the Integral Mössbauer spectroscopy was explained previously. The X-ray diffraction can not be used because the conditions for diffraction are not fulfilled (grain size must be in the order of 1  $\mu\text{m}$  or larger).

The absence of a proper method caused that the research in the area of the above mentioned systems was almost entirely neglected, with the exception of small number of rather difficult studies using

the Mössbauer spectroscopy. Some examples are given on pages 21 and 22.

It is necessary to stress that also other systems not including the solid phase(s) can be studied by the proposed and described method of the Integral Mössbauer spectroscopy and complement other methods commonly used for these systems.

## NON-MÖSSBAUER RESONANCE ABSORPTION

In evaluating different effects encountered in the measurement of Integral Mössbauer spectra (see pages 77 and ff) it became clear that another resonance effect (non-Mössbauer resonance absorption) is present and in some systems its influence is much larger than that of Mössbauer resonance absorption.

A similar (?) effect was noticed in another type of measurement - in the "thermal scans" at constant velocity far off the Mössbauer resonance - by Brunot, Hauser and Neuwirth and by Fröhlich and Keszthelyi. The explanation given by the first group (change in X-ray diffraction caused by the change of Debye-Waller factor) was contested by the second group. Their explanation renders the effect to trivial change in X-ray scattering caused by the confirmed appearance and disappearance of random cracks in supercooled liquid. The randomness of crack formation is causing the absence or presence of the effect and in the case of presence also the change of sign of the effect. The question mark at the beginning of this paragraph means that the authors should have observed the non-Mössbauer resonance absorption but unfortunately the eventually present non-Mössbauer resonance effect ( $\text{FeCl}_2$  in frozen solution can have a small or zero effect) was totally obstructed for both groups by the formation of random cracks as explained above.

Due to different experimental technique (Integral Mössbauer spectroscopy) and larger experimental basis (Integral reaction spectra and Integral thermal scans on materials in different

aggregate states) it is necessary to state that there exists a non-trivial non-Mössbauer resonance absorption. This statement is also supported by the results of calculations of non-Mössbauer resonance absorption from the "background" of Mössbauer spectra (see, page 107).

The non-Mössbauer resonance absorption can be caused at least in some cases by the diffusion of measured species, which will partly lead to the decrease (or increase) of the resonance absorption, because the average isotropic motion will contribute to "non-selective" changes in absorption. There are some easy experiments which will make the measurement of this contribution possible.

## EXPERIMENTAL PART

## CONSTANT ACCELERATION MÖSSBAUER SPECTROMETER

The most common instrument for the measurement of Mössbauer spectra is the constant acceleration Mössbauer spectrometer. It works through modulation of the energy of the Mössbauer active line of the source by the Doppler effect. The record of number of counts stored in successive channels of a multichannel analyzer in dependence either on time (the so-called multiscaler or time mode operation) or on velocity (analogue mode operation) repeatedly for successive identical sweeps through the entire selected region of velocities constitutes the spectrum.

In the case of symmetrical harmonic motion the time mode operation potentially leads to the storage of two Mössbauer spectra, one of which is reversed (version i). Alternatively, if only one of these spectra is stored, the overall time efficiency is less than 50% (version ii). To approach 100% efficiency, the wave form must be asymmetrical (version iii). These three versions of operation are illustrated in Figure 7.

- In more complex systems the so-called folding operation is performed where the two spectra are instrumentally added together after proper inversion of the second spectrum (version iv).

The three latter systems (ii, iii and iv) have obvious disadvantages (e.g. economics and reliability of operation). To decide between the first two versions is rather a simple task. If the resolution is adequate and there is the usual need for improved statistical and overall validity of derived parameters (and if



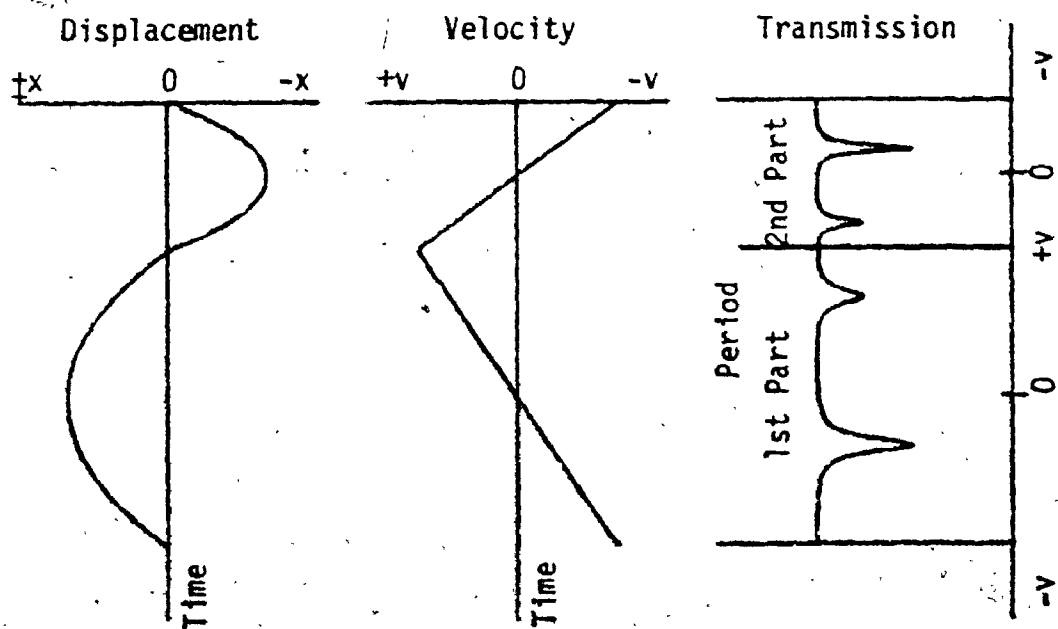
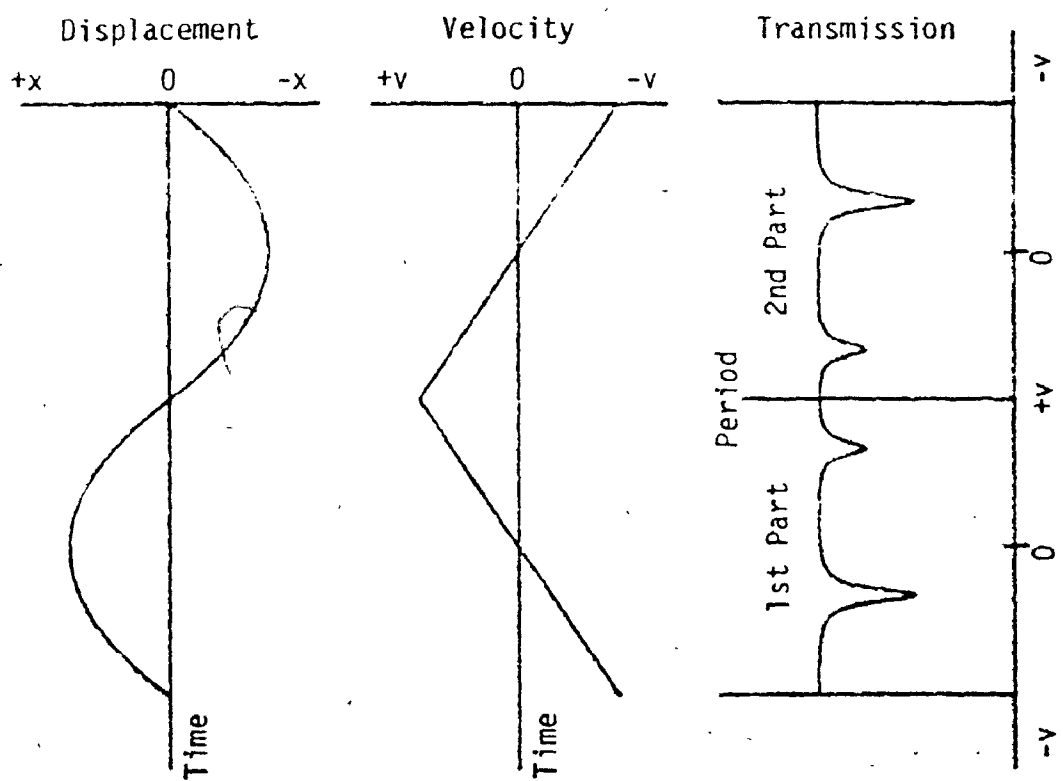


FIGURE 7 Mössbauer spectra, velocity and displacement

enough computing capacity is available), two spectra should be used. Where higher resolution is desired or only limited curve fitting can be done, only one spectrum should be stored.

Many different constructions and principles have been used for building Mössbauer spectrometers. Adequate descriptions are available in review articles and in most of the monographs (Greenwood, Gibb).

The first (constant acceleration) spectrometer already available in this laboratory was operating in the analogue mode. Such a system has two main disadvantages. The inevitable delay (in the region of 2-10 msec) of the velocity signal behind the real motion of the source causes the doubling (for smaller differences only broadening) of peaks. That can be removed by using only one branch of the velocity signal (thus losing approximately 50% of the counting time). Moreover the real motion is of higher quality than the electronic signal derived from such motion, which is usually non-linear and contains electronic noise mainly from the 60 hz line frequency.

Therefore a new spectrometer was built which operates in the time mode. It consists of parts and instruments included in Table 2.

The instruments used should ideally represent an optimum selection. However they were mainly chosen on account of their availability, and as a consequence it is certain that their parameters are not matched. Better instruments are, or have been, available from these same and other manufacturers.

It was found by direct observation of the amplified velocity signal from the detector coil of the transducer that a motion of

TABLE 2 Mössbauer Spectrometer Components\*

1. Mössbauer source ( $^{57}\text{Co} + ^{57\text{m}}\text{Fe(Pd)}$ ) (New England Nuclear Co.)
2. Mössbauer absorber
3. Mössbauer drive unit (Carleton University, Science Workshop)
4. Power amplifier (Hewlett-Packard, 6823A)
5. Triangle generator (Hewlett-Packard, 3300A)
6. Detector (Reuter-Stokes, RSG-61-M2)
7. Preamplifier (Simtec, P-10)
8. High voltage source (Phillips, PW 4025/10)
9. Pulse amplifier (Hamner, NA-15)
10. Single channel analyzer (Hamner, NC-11)
11. Analog-to-digital converter (Northern Scientific, NS-622)
12. Memory unit (Northern Scientific, NS-633)
13. Readout control (Northern Scientific, NS-621)
14. Teletype (Northern Scientific, 102)
15. Acoustically insulated box (Carleton University, Chemistry Workshop)

\* For assembly diagram see Figure 8

the source occurs even when no signal is applied to the system. This motion is caused by accoustical and mechanical vibrations and the sensitivity of the velocity measuring circuitry is such that the motion is detected without difficulty. A deformation of the Mössbauer spectra, mainly broadening of the peaks, is caused by these two types of vibration.

A series of experiments were performed in order to suppress the mechanical vibrations. Various materials were investigated to separate the bench top from the mounting bench of the Mössbauer drive unit. Evaluation of this vibrational isolation was done in different ways, the most advantageous was by the recording of the amplified signal from the velocity measuring coil of the transducer by a fast strip chart recorder.

The frequencies found for these extraneous vibrations were 2.5, 6 and 30 Hz. The finding of extraneous vibrations was independently confirmed (Word) and the frequencies corroborated and identified as those of building vibrations. Two other commonly observed major building vibrations (at 0.7 and 60 Hz) were not detected by this method. A program to measure and analyze the vibrations of other laboratories on different floors of the building was suggested (Word) but was not carried out mainly because in any case it would not be possible to move the Mössbauer spectroscopy laboratory. Considerable improvement was made by enclosing the system in an accoustically isolated box. After some experiments with an open or closed glove box, an accoustically isolated box was constructed of plywood, lead and glass fibre tile (Thiessen). At the same time 2 mm layer of lead works as a radiation protection.

The inertia of the box and material used for its construction diminish the amplitude of all vibrations.

A block diagram of the spectrometer is given in the next Figure 8. Diagrams for instruments which were obtained commercially are not included here.

### Selection of Operating Conditions

- (1) Selection of the proper distance between the source and the detector.

Two contradictory requirements have to be reconciled. First, the distance between the absorber and the detector should be the maximum available to suppress deformation of the spectrum by fluorescence in the absorber. Second, the distance between the source and the absorber should be the maximum possible to suppress the cosine deformation of the spectrum. Obviously, at the same time, the source-detector distance, should be as small as possible, to obtain high detection efficiency. The absorber was consequently located in the middle, between the source and the detector.

- (2) Setting of the detector high voltage.

The detector voltage must be close to the maximum because the signal from 14.4 keV  $\gamma$ -ray is small. The optimum gain of the preamplifier is the highest available. (Since in this spectrometer the quality of the preamplifier used is better than that of the amplifier.)

- (3) Setting of the amplifier gain.

The Mössbauer active peak (14.4 keV) of the pulse height

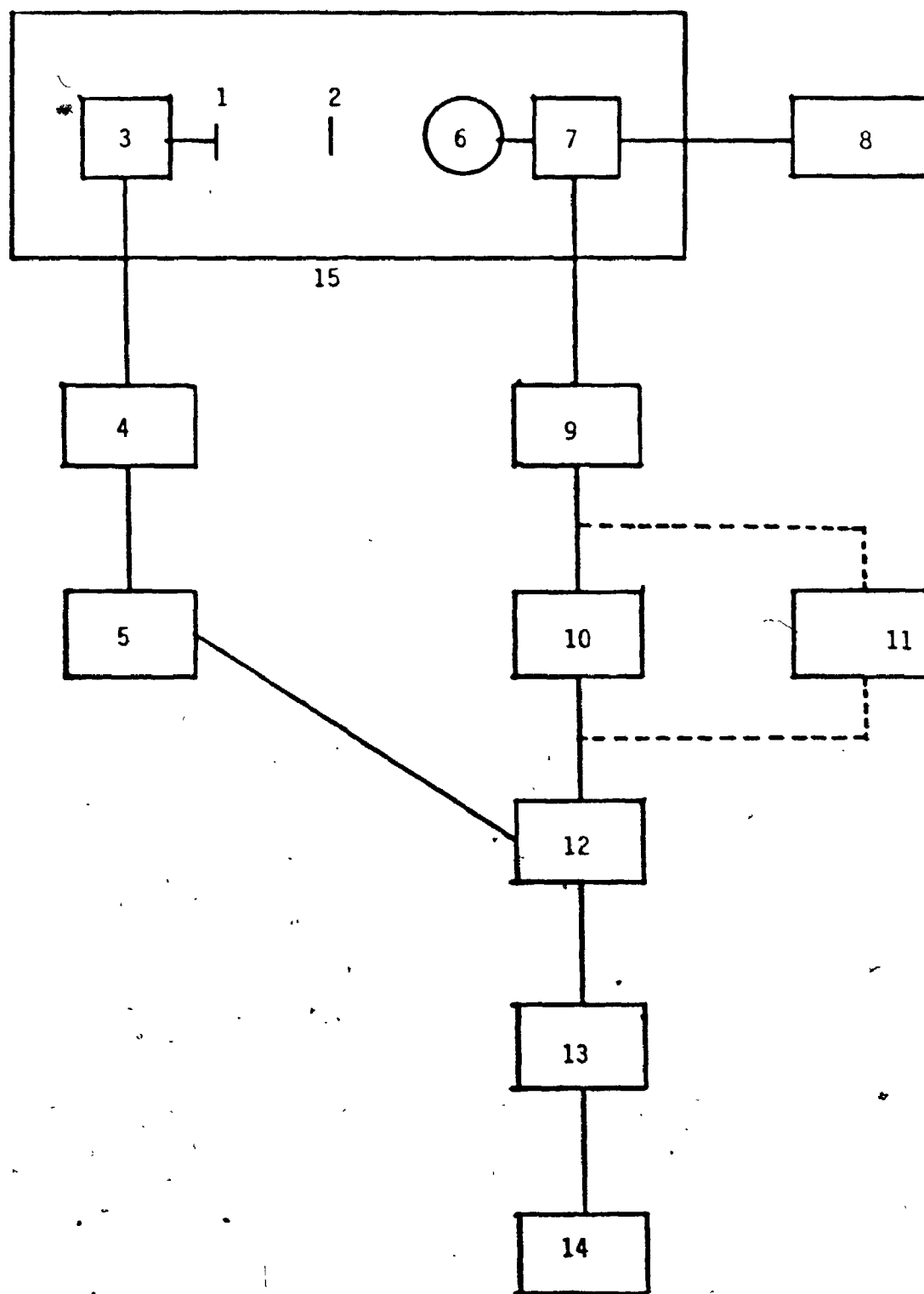


FIGURE 8 Block diagram of Mössbauer spectrometer  
see page 37

spectrum is conveniently set within the third quarter of the memory. The position of the peak for this system changes with the change of counting rate and changes of gain are required to compensate for this in any individual absorber. Changes in overall gain can be achieved by changes in the high voltage but there the current through the detector system will change, therefore the temperature will change and there will be inevitable changes in the position of the peaks.

(4) Setting of the single channel analyzer.

The low level discriminator and the window have to be set by means of an external pulse generator, so that they span the third quarter of the memory, and encompass the Mössbauer peak.

(5) Setting of the triangle generator and the memory unit.

For regular work the selection of the frequency, the dwell time and the number of channels of the memory unit has to be done such that the velocity change per channel and the velocity range are satisfactory for the observed spectrum (about  $0.003 \text{ cm sec}^{-1} \text{ ch}^{-1}$  and  $3 \text{ cm sec}^{-1}$ ). For a given velocity range, a higher frequency gives a smaller displacement of the source and thus reduces the parabolic background of the spectrum. The frequency, number of channels and dwell time must fulfill the following expression:

$$\frac{1}{f} > N \cdot \tau$$

where  $f$  is the frequency ( $\text{c sec}^{-1}$ )

$N$  is the number of channels

$\tau$  is the dwell time ( $\text{sec ch}^{-1}$ ).

For 10 hz and 1024 channels this relation requires a dwell time of about  $100 \mu\text{sec ch}^{-1}$ . The number of channels used can normally be changed (diminished) only by factors of two and the dwell time only by integers within the given order. Therefore the proper number of channels and the dwell time are selected and finally the (continuously variable) frequency is adjusted to fulfill the above condition. This is easily checked visually by following the stop indicator of the memory unit.

The intensity of the triangular signal from the generator and hence the velocity range, can be set using a proper absorber. With enriched iron foil it can be done visually. The parameters described in this point were selected in such a way that the velocity increment per channel is about  $0.003 \text{ cm sec}^{-1}$ . This value is a reasonable compromise between the requirement of the highest resolution (it is equal to about 1/7 of the FWHM) and the contradictory requirements of the highest statistical validity of the accumulated counts per channel and an acceptable value of the velocity interval for the constant number of available channels.

#### (6) Setting of the memory unit.

The memory unit operates in a single sweep mode. The triggering for each new sweep is done externally from the triangle generator. The number of sweeps is stored in channel 0.

The start and the end of the measurement must be done manually. The measurement is usually terminated after accumulation of circa one million counts in the background.



## INTEGRAL MÖSSBAUER SPECTROMETER

Operation of a Mössbauer spectrometer in the integral mode requires the use of much larger dwell time -- up to 900 sec per channel is convenient. This is readily accomplished by a simple divider circuit activated by a toggle switch. This is the only change required in the circuitry to give integral capability.

OPERATION

- (1) The setting of the intensity of the triangular signal can be easily done visually, using a proper absorber. It was done using the iron foil enriched in  $^{57}\text{Fe}$  so that one of the inner peaks was entirely in the spectrum and the second one was cut off at its maximum.
- (2) The setting of the dwell time depends on the rate of the chemical reaction under observation and must also be long enough in comparison to the period of the Doppler motion so that incomplete scans will not cause the systematic deformations of the Integral Mössbauer spectra. This latter is only a minor problem which can, if necessary, be solved simply by including an independent period counter to trigger the address advance externally. In this version of operation the dwell time multiplier described above is not necessary any more. The lowest achievable limit is the channel advance for every sweep, that is, about  $100 \text{ msec ch}^{-1}$ . It is necessary to bear in mind that there are other limitations as well (e.g. counting rate). Thus a dwell time of 60 sec per channel was used in most cases.

- (3) All other operating conditions are kept as in the regular Mössbauer spectrometer, although some parameters are no longer critical. For example, it is possible to decrease the distances and use a poorer quality Mössbauer spectrum.

## SOURCES AND ABSORBERS

Throughout this work five sources of  $^{57}\text{Co}$  +  $^{57\text{m}}\text{Fe}$  were used. All but one were in a palladium matrix which gives better resolution and high Mössbauer fraction. Their basic parameters are:

Source Number	Producer Number	Activity (mC)	Date	Recoilless Fraction (%)	FWHM (mm sec <sup>-1</sup> )
4	1189	10	10.2.1971	44	0.24
5	1683	11	28.8.1973	43	0.25

With the exception of source #5 all were supplied in the form of a foil which was cemented onto the polymethyl methacrylate support. Source #5 was mounted by the manufacturer, because in some previous cases cracks ultimately developed in the polymethyl methacrylate because of the cement used.

In addition to the experiments done with  $^{57}\text{Co}$  +  $^{57\text{m}}\text{Fe}$  a few experiments were done with  $^{119\text{m}}\text{Sn}$  source. The source was prepared by grinding coarse crystals of  $\text{SnMg}_2$  in an agate mortar and fixing the ground material with a cement on a polymethyl methacrylate disc.

Absorbers used were metallic foils (supplied by various manufacturers), crystalline powders, solutions, sheets and in one case a monocrystal. Whenever possible the thickness of the absorber was selected so as to have about  $10 \text{ mg cm}^{-2}$  of Fe, which corresponds to about  $200 \text{ } \mu\text{g cm}^{-2}$  of  $^{57}\text{Fe}$ . Materials were taken as often as possible in the available form. Any unavoidable grinding was done in an agate or porcelain mortar or in an agate vibration mill. Low melting hydrates and other compounds which may decompose during grinding were

handled under an inert liquid (usually hexane) whose boiling point is lower than the decomposition temperature of the compound. This liquid serves to control local temperature, to suspend the solid in the cell and to reduce losses of water from the surface. The slurry is transferred into a Teflon cell with mica windows. Solutions were either filled into appropriate cells or absorbed in a filtration paper and placed in the cell. The main advantage of the second version is the prevention of settling of an eventual precipitating solid phase.

#### CELLS

Different types of cells were used through the work. In most cases they were mounted on the cell holder with the help of two springs. In the case of thermal scans the cells were pushed into the slit of the thermally isolated block.

The paper cells were used first on account of their availability in the laboratory. For some absorbers they were quite adequate. Their main advantage is the low price (and low weight). The opening of the cell was covered with cellulose tape, then the absorber was introduced in selected quantity, spread so as to fill the cell and closed with another piece of the adhesive tape. The main disadvantage, caused by the fixed thickness of the cell, is that the amount of each absorber is difficult to regulate and attempts to use small amounts give packing problems. No attempt was made to prepare a variable thickness cell. A second disadvantage, appearing only for some materials is the electrostatic charge of the tape which causes

the repulsion of some materials.

For the measurement of the slurries a special cell with mica windows and Teflon spacer was used. One window was cemented (Epoxy resin) to the Teflon spacer, the second window was held by pressure applied via two mounting plates.

A third type of the cell was a rectangular copper cell with a one inch diameter opening. Closing was done with two inch wide cellulose tape. Copper was selected because of its high thermal conductivity. These cells were initially used for measurements at low temperature and for the thermal scans, although later they were used in all cases. On account of their larger thickness, it was occasionally necessary to use one or two filtration paper discs to fill the empty space. A slit on one side is used for a thermocouple. This type of cell is also used for the isothermal reaction studies. In almost all cases a pressure (usually 5 tons/in) is used in the absorber preparation. At least some absorbers must be in a closed system also at the time of pressing.

For thermal scans the cells were inserted into a block of polyurethane foam (wall thickness 2") with 300 ml of coolant. To prevent the leakage of liquid nitrogen onto the absorber, the liquid nitrogen was filled in a polyethylene bag, which was in close contact with the top of the Cu-cell. In such way it was possible to reach liquid nitrogen temperature in the cell holder within less than 1 minute. With the full amount of liquid nitrogen a temperature of  $-196^{\circ}\text{C}$  could be maintained for more than 30 min before it started to rise. Within about 6 h the laboratory temperature was reached.

The temperature was measured with a differential Cu-Constantan thermocouple connected to a Hewlett-Packard recorder (type 17500A).

### EVALUATION OF MÖSSBAUER SPECTRA

The evaluation of Mössbauer spectra is done in various ways depending on the requirements of the experiment. In the simplest case the very presence of a Mössbauer spectrum as seen on the CRT display is sufficient. In other cases the position of the peak(s) is read from the CRT, the eventual presence of quadrupole or magnetic hyperfine splitting is observed and therefore in many cases the identity or the structure of the compound is obtained or confirmed.

The next form of evaluation is the permanent record of the spectra, which is useful in all other cases. The permanent record is either a photograph of the CRT display or a plot taken with an X or XY recorder. Pictures can also be obtained from the digital plotter after some computer operations. For any type of more serious work a numerical printout of the data is necessary. The most convenient way is to obtain a page printout. An example of the 128 channels spectrum printout is in Figure 9. The first column represents the channel number (so-called address) of the next column. In the next five columns the numbers of counts per channel are tabulated channel after channel. In channel zero is the number of sweeps. There are other formats of printout with or without the address column. The system described seems to be quite satisfactory.

0000	602547	480991	619655	937657	620147
0005	617398	621021	618850	621738	618904
0010	620623	618004	620444	619045	617525
0015	618285	616439	621813	616709	617612
0020	616439	619588	621906	621569	617853
0025	620444	621343	619128	622436	618691
0030	620185	620445	621494	618322	621591
0035	620601	619909	617850	620057	622437
0040	619785	620504	619119	621357	617795
0045	617224	620822	618315	622392	618104
0050	620103	619053	622360	621975	618583
0055	622298	619940	620992	619850	621811
0060	622018	619216	617193	623897	619930
0065	620624	620420	619426	621940	619871
0070	620280	620823	617787	621638	618697
0075	621228	623108	619659	621397	620783
0080	622711	621742	622829	620223	620037
0085	621452	617579	620676	619395	619625
0090	621105	621808	620383	621673	618702
0095	618550	622503	620931	621871	622432
0100	618713	620918	622758	624449	623133
0105	623041	622465	620724	621698	622309
0110	619179	623365	620547	622546	620927
0115	620417	620803	620495	621629	621168
0120	621396	618621	623779	623288	620600
0125	623615	619213	624020		

FIGURE 9 Sample printout of 128 channels spectrum  
Illustration of the page format.

Quantitative evaluation, with the exception of the simplest one (i.e. plotting of the intensity of the maxima) has to be done by digital computer. The data can be submitted to the computer in different forms. The most economical form is to extract the data on the punched tape and either read them in the computer through a computer terminal in timesharing mode or convert them to the form of punched cards or magnetic tape. First and third form were used in this laboratory. The best but most expensive way is to output the data directly on a magnetic tape. An added advantage of having the data on tape is the possibility of introducing the spectrum back in the memory for additional studies.

Some multichannel Mössbauer spectrometers have so-called "computer interface" which in most cases is practically identical with a timesharing terminal. The only part which is "saved" is the paper tape punch or magnetic tape drive.

The most modern versions of the regular Mössbauer spectrometers are digital minicomputers which can not only store and display the spectra but do a large amount of editing and data reduction (Window, Dickson, Routcliffe and Srivastava).

#### CALCULATIONS

The calculations in the field of Mössbauer spectroscopy are basically of two types. First there are the calculations of the spectra of monocrystals (both splittings) which are done by physicists and in most cases consist of variation of parameters until the agreement with the experiment is satisfactory. One such



example including the computer program was published by Czerlinsky. The second type of calculation is the curve fitting of the Mössbauer spectra. There are many programs available, some quite sophisticated (but only one program corrects the cosine smearing Kankeleit). The selection of adequate program and the proper interpretation is rather difficult (Pfeiffer and Lichtenwalner). The older programs usually do the correction of the background using a sinusoidal function what is originating from the time when constant acceleration spectrometers were not in broad use and the background was de facto sinusoidal. Some of these programs are still in use. The fault caused by their use is small only in the case of proper geometry.

Within this work three different approaches to the calculations of the second type were used.

The first approach uses the approximate linearization of the general formula by neglection of non-linear terms after Taylor expansion (see Rhodes, Polinger, Spijkerman and Christ). The card deck and listing was supplied by Carson. The program had to be rewritten and adapted before it was usable on the Carleton University Sigma 9 computer. Revisions of the computer program must be made frequently, either on account of the changes in the computer hardware or software or as a result of the demand of the work (larger number of peaks processed, greater convenience etc.). The main program has been changed extensively and the plotting subroutine is entirely new.

In addition to the usual plot, a plot of differences between the calculated and experimental values is obtained. That has proven

to be very important because it made it possible to discover systematic deviations in all spectra up to June 1971 and subsequent solution of that problem.

On account of the great problems with the analysis of spectra with so-called "hidden" peaks (either small peaks present within the area of large peaks or close unresolved doublets) which show up sometimes only as systematic deviations in the difference spectrum, two additional programs were used. One is the program using interactive calculations combined with the display of the experimental and suggested spectra on the visual display terminal (TV-terminal). This program is also very useful for checking of the data files before the submission of more time consuming calculations. The faults in data files are of different origin and cannot be conveniently detected in any other way.

The last program is the large multipurpose optimization program "Hillclimbing" available in the Science Program Library. In this case a short program including necessary subroutines has to be written defining the variables, the initial guesses and the studied function. Only this program has made it possible to find the correct solutions of the close doublets.

## RESULTS AND DISCUSSION

Different problems were encountered and subsequently solved during this work. Some of them were instrumental, others of a chemical or physical nature. Altogether five different multichannel analyzers were used (one 512-channel analyzer, one 100-channel analyzer and three 400-channel analyzers) and adequate Mössbauer spectra obtained, before the final delivery of a 1024-channel analyzer. All five analyzers operated in the analogue mode. The first orientation measurements on the 1024-channel analyzer were done also in the analogue mode, before the external triggering system was installed and time mode measurements became possible. The complementary electronics and other peripherals were changed at the same time. All changes led to an improved and more compact Mössbauer spectrometer.

Results and discussion are presented in three separate parts. The first one deals with the results obtained by Mössbauer spectroscopy. The second and third part under the headings of Integral Mössbauer spectroscopy and non-Mössbauer resonance absorption describe a new spectroscopy for which the name Integral Mössbauer spectroscopy is proposed and a new  $\gamma$ -ray resonance effect (studied within this work almost exclusively as an absorption effect) for which the name non-Mössbauer resonance absorption (effect) is suggested, in order to express the relations between the three  $\gamma$ -ray resonance processes (Moon type resonance, non-Mössbauer resonance and Mössbauer resonance).

## MÖSSBAUER SPECTROSCOPY

Some results of Mössbauer spectroscopy measurements are included later, specially in the part of Integral Mössbauer spectroscopy, when it was necessary for the discussion of effects encountered there. None of them have any substantial significance in this part. The only deviation, from the point of view of the importance of results obtained and their presentation under proper headings, occurred in the case of calculations of non-Mössbauer resonance absorption of pure compounds (in distinction from the reaction mixtures) from the background of Mössbauer spectra, which phenomenologically does not belong into the realm of Mössbauer spectroscopy anyhow.

After the selections, changes and realization of the final constant acceleration Mössbauer spectrometer (with the time mode of operation) which was used through this work the main problem was the identification and the correction of systematic deviations of spectra from the theoretical Lorentzian shape. There were different reasons for this difficulty: impurities were present in the iron foil  $^{57}\text{Fe}$  enriched, and  $\text{FeSO}_4 \cdot 7\text{H}_2\text{O}$  etc., a single peak was incorrectly assigned to a given spectrum (stainless steel 310) which really has a close non-resolved doublet. This situation was complicated by the asymmetry of the FWHM for the outside peaks in the iron spectrum and disagreement of the relative intensities in the iron spectrum.

Therefore all spectra at the time of the accumulation of the first analyzed spectra were in disagreement with the theory in the

shape, FWHM and intensity.

### Standard Absorbers

Iron, stainless steel 310, sodium nitroprusside dihydrate, and  $\alpha$ -ferric oxide were or are commonly used as standard absorbers in Mössbauer spectroscopy (see Herber). All these compounds were repeatedly measured and satisfactory results were found in all cases.

Iron is now used as the basic standard for the isomer shift and velocity calibration. The results of some early measurements from this work on different iron foils and iron sponge are in Table 3. The spectra are not symmetrical, in that the fifth and sixth peaks are broader than the corresponding first and second peaks although the  $\epsilon$  values are correct. The use of the acceleration  $65 \text{ cm sec}^{-2}$  solved this problem (see Table 4). The reason is that the motion of the source is better defined using higher acceleration. After final evaluation including the differences in the position of the centroids of corresponding peaks, the acceleration  $65 \text{ cm sec}^{-2}$  was accepted as the better one for all future measurements, but in order to preserve the necessary resolution and the velocity range the dwell time was changed to  $50 \text{ } \mu\text{sec}$ . Thus only one spectrum was stored within 1000 channels. The results for  $0.001''$  iron foil measured under these conditions are given in Table 5. The calculated values of the ratio of the splitting for the ground state and the excited state (1.747 and 1.744) are in good agreement with the best literature value (1.750).

TABLE 3 Mössbauer Spectral Parameters of Selected Iron Absorbers

Fo11 Thickness	Peak 1		Peak 2		Peak 3		Peak 4		Peak 5		Peak 6	
	P	$\Gamma$	P	$\Gamma$	P	$\Gamma$	P	$\Gamma$	P	$\Gamma$	P	$\Gamma$
0.001"	112.2	8.00	180.5	7.48	250.4	7.20	302.8	7.44	374.8	7.96	448.2	8.90
	112.6	8.26	181.1	7.76	251.0	7.54	303.4	7.52	374.8	8.10	447.4	9.22
	112.9	8.00	181.3	7.54	250.6	7.08	302.7	7.14	374.1	7.96	446.3	8.96
	112.2	7.86	180.2	7.54	249.5	7.08	301.7	7.22	373.2	8.08	445.7	9.04
	112.3	8.12	179.9	7.36	248.9	7.22	301.1	7.42	373.1	8.06	445.6	9.10
0.001" *	112.0	8.18	180.4	7.28	249.8	7.16	302.2	7.30	374.4	8.00	447.0	9.00
	113.1	8.12	181.4	7.56	250.8	7.08	302.8	7.30	374.1	7.88	446.3	8.86
0.0005"	113.2	7.18	181.0	6.88	250.3	6.60	302.4	6.90	373.7	7.28	445.7	7.80
0.00025"	112.2	6.38	180.4	6.48	250.1	6.72	302.6	6.70	374.7	7.22	448.2	7.34
	113.0	6.52	180.9	6.64	250.1	6.52	302.3	6.52	373.7	7.14	445.8	7.38
sponge	112.8	7.42	181.4	7.24	251.0	7.10	303.4	7.46	374.5	7.48	447.1	8.22

P is the channel number of the peak maximum

$\Gamma$  is the full width at half maximum in channel numbers

Acceleration  $32 \text{ cm sec}^{-2}$ ; dwell time  $100 \text{ } \mu\text{sec}$

\* Fo11 loaned by P. W. Carson

TABLE 4 Mössbauer Spectral Parameters of Selected Iron Absorbers

Foil Thickness	Peak 1		Peak 2		Peak 3		Peak 4		Peak 5		Peak 6	
	P	$\Gamma$	P	$\Gamma$	P	$\Gamma$	P	$\Gamma$	P	$\Gamma$	P	$\Gamma$
0.001"	193.8	4.26	227.5	3.96	261.4	3.68	287.2	3.68	322.4	4.04	357.4	4.32
	192.9	4.22	227.2	3.94	261.2	3.76	287.0	3.74	322.2	4.08	357.5	4.28
	193.0	4.24	227.3	3.86	261.4	3.70	287.1	3.76	322.3	4.10	357.5	4.24
0.0005"	194.4	3.88	228.8	3.64	262.8	3.44	288.6	3.70	323.7	3.54	358.6	3.66
0.00025"	193.3	3.46	227.7	3.40	261.6	3.28	287.5	3.50	322.8	3.64	357.9	3.40
sponge	194.0	3.94	228.3	3.90	262.8	3.40	288.7	3.60	323.6	3.76	358.6	3.82

P is the channel number of the peak maximum

$\Gamma$  is the full width at half maximum in channel numbers

Acceleration  $65 \text{ cm sec}^{-2}$ ; dwell time  $100 \text{ } \mu\text{sec}$

TABLE 5 Mössbauer Spectral Parameters of 0.001" Iron Foil Standard

Peak 1 P	$\Gamma$	Peak 2 P	$\Gamma$	Peak 3 P	$\Gamma$	Peak 4 P	$\Gamma$	Peak 5 P	$\Gamma$	Peak 6 P	$\Gamma$
387.2	8.44	456.0	7.82	524.1	7.34	575.5	7.20	645.8	7.78	715.5	8.34
387.9	8.64	456.6	8.12	524.8	7.42	576.5	7.26	646.9	7.62	716.4	8.34
387.5	8.52	456.1	7.92	524.2	7.26	575.6	7.14	645.8	7.62	715.0	8.26
386.6	8.48	455.7	7.92	523.4	7.40	575.7	7.28	645.1	7.80	714.2	8.48

P is the channel number of the peak maximum

$\Gamma$  is the full width at half maximum in channel numbers

Acceleration  $65 \text{ cm sec}^{-2}$ ; dwell time 50  $\mu\text{sec}$



Table 6 gives a survey of the average parameters for the 0.001" selected standard iron foil measured under different conditions. On account of partial magnetization of the samples the theoretical ratio of the values (3:2:1:1:2:3) was not achieved.

In order to obtain a spectrum with theoretical intensity ratios  $\alpha\text{-Fe}_2\text{O}_3$  was measured. The first sample contained <10% of  $\alpha\text{-Fe}_2\text{O}_3$ . The results for three authentic  $\alpha\text{-Fe}_2\text{O}_3$  samples are in Table 7. The sample with the smallest amount of  $\alpha\text{-Fe}_2\text{O}_3$  gave the ratio 1:1.96:2.76 which was the closest one to the theoretical values. No attempt was made to use samples with still smaller amounts of material to achieve yet better results.

Sodium nitroprusside dihydrate (from NEN) gave a systematic deviation from the Lorentzian shape. Therefore two new samples were prepared from freshly ground larger crystals. Both gave the correct shape. The results are given in Table 8. The fifth measurement was done immediately before the fourth measurement but in a different geometry. The absorber was placed close to the detector. The changes in parameters are smaller than the changes observed within three months. In Table 9 are the results for the measurements of the combination of absorbers #2 and #3. The values are very close. The recalculated baseline is 47% lower than the corresponding baseline for sample #2. Therefore the thickness of the combined absorber is already in the strongly non-linear region of resonance absorption. That can also clearly be seen from the broadening of the two peaks. The increase in the area is about 15% for identical backgrounds and is caused entirely by broadening of the peaks.

TABLE 6      Mössbauer Spectral Parameters of 0.001" Iron Foil  
Standard

Peak	$\Gamma$			$\epsilon$		
	*	†	**	*	†	**
1	0.0257	0.0276	0.0277	20.4	20.5	20.9
2	0.0240	0.0255	0.0258	16.1	16.2	16.5
3	0.0230	0.0242	0.0239	10.8	10.7	10.9
4	0.0235	0.0243	0.0235	10.7	10.8	10.8
5	0.0257	0.0265	0.0250	16.4	16.1	16.3
6	0.0289	0.0278	0.0272	20.7	20.5	20.7

$\Gamma$  is given in  $\text{cm sec}^{-1}$ ,  $\epsilon$  is in percent of absorption.

Each value is the average of at least 3 determinations.

\* acceleration  $0.0032\text{cm sec}^{-1}\text{ch}^{-1}$ ; dwell time 100  $\mu\text{sec}$

† acceleration  $0.0065\text{cm sec}^{-1}\text{ch}^{-1}$ ; dwell time 100  $\mu\text{sec}$

\*\* acceleration  $0.00325\text{cm sec}^{-1}\text{ch}^{-1}$ ; dwell time 50  $\mu\text{sec}$

TABLE 7 Mössbauer Spectral Parameters of  $\alpha\text{-Fe}_2\text{O}_3$  Standard  
Absorber Material

Absorber Thickness $\text{mg cm}^{-2}$	FWHM ( $\text{cm sec}^{-1}$ )					
	Peak 1	Peak 2	Peak 3	Peak 4	Peak 5	Peak 6
Acceleration $32 \text{ cm sec}^{-2}$						
200		0.0267	0.0204	0.0246	0.0283	
44.5		0.0223	0.0229	0.0245	0.0256	
44.5		0.0238	0.0226	0.0234	0.0266	
5.4		0.0213	0.0213	0.0197	0.0228	
Acceleration $65 \text{ cm sec}^{-2}$						
200	0.0303	0.0287	0.0231	0.0254	0.0298	0.0325
44.5	0.0264	0.0256	0.0218	0.0238	0.0259	0.0274
5.4	0.0235	0.0225	0.0190	0.0243	0.0235	0.0248
$\epsilon$ (%)						
Acceleration $32 \text{ cm sec}^{-2}$						
200		12.4	8.62	8.28	12.4	
44.5		8.52	5.34	5.51	8.41	
44.5		8.40	5.10	4.97	8.40	
5.4		3.85	1.99	2.19	3.82	
Acceleration $65 \text{ cm sec}^{-2}$						
200	14.4	12.3	8.35	8.43	12.5	14.2
44.5	10.7	8.34	4.85	5.27	8.43	10.8
5.4	5.23	3.90	2.22	2.01	3.89	5.23

Dwell time 100  $\mu\text{sec}$

TABLE 8 Mössbauer Spectral Parameters of Sodium  
Nitroprusside Dihydrate

Acceleration  $32 \text{ cm sec}^{-2}$ ; dwell time  $100 \text{ } \mu\text{sec}$

Sample	FWHM		$\Delta$ ( $\text{cm sec}^{-1}$ )
	Peak 1 ( $\text{cm sec}^{-1}$ )	Peak 2 ( $\text{cm sec}^{-1}$ )	
1	0.0241	0.0259	0.1728
1	0.0241	0.0259	0.1728
1	0.0243	0.0260	0.1729
1	0.0222	0.0230	0.1706
1*	0.0214	0.0223	0.1711
2	0.0240	0.0253	0.1708
2	0.0238	0.0251	0.1703
3	0.0239	0.0254	0.1711
3	0.0240	0.0255	0.1712
2 + 3	0.0284	0.0296	0.1708

Acceleration  $65 \text{ cm sec}^{-2}$ ; dwell time  $100 \text{ } \mu\text{sec}$

2	0.0246	0.0242	0.1687
2	0.0251	0.0244	0.1691
2*	0.0247	0.0239	0.1689

\* The absorber was immediately in front of the detector.

TABLE 9 "Self-Absorption" Data for Two Sodium Nitroprusside Dihydrate Absorbers

Absorber Number	$\epsilon$ (%)		Baseline/ $10^6$ Sweeps (%)	Area Counts* ( $\times 10^{-4}$ )	
	Peak 1	Peak 2		Peak 1	Peak 2
2	18.6	18.5	100	127	133
3	19.8	19.8	93	135	143
2 + 3	18.0	18.2	53	146	154

Acceleration  $32 \text{ cm sec}^{-2}$ ; dwell time  $100 \mu\text{sec}$

\* Corrected to 100% baseline

TABLE 10      Mössbauer Spectral Parameters of 0.0002" Stainless Steel 310 Standard Absorbers

Absorber Number	$\delta^*$ (cm sec <sup>-1</sup> )	$\Delta$ (cm sec <sup>-1</sup> )	Peak 1		Peak 2	
			$\Gamma$ (cm sec <sup>-1</sup> )	$\epsilon$ (%)	$\Gamma$ (cm sec <sup>-1</sup> )	$\epsilon$ (%)
1	-0.0109	0.0161	0.0257	6.2	0.0280	8.8
2 <sup>†</sup>	-0.0086	0.0165	0.0264	7.2	0.0252	7.8

\* Relative to iron foil centroid

† Foil loaned by D. W. Carson (Department of Energy, Mines and Resources)

All samples of stainless steel 310 had systematic deviations from the single line spectrum. There was a possibility that this is caused by high sensitivity of the motion to distortion near zero velocity. However, such deformation was not observed for the higher energy peak of  $\text{FeSO}_4 \cdot 7\text{H}_2\text{O}$  spectrum which is located in the same position. It was therefore assumed that the spectrum consists of an unresolved doublet. For the analysis two samples were used with the narrowest peak. Both samples have the thickness 0.0002" (from NEN). The results are in Table 10. No systematic deviations remain in the different spectra under the previous simplest possible assumption and the calculated parameters give good agreement with the observed spectrum. Detailed further study of this doublet has not been done since it is somewhat outside the scope of this work.

#### Inorganic Compounds

Mössbauer spectra of inorganic compounds were measured for several different reasons. The original idea was to measure the spectra of simple ferrous and ferric compounds as preparation for the application of Mössbauer spectroscopy to study the fate of Fe species after hot atom reaction or implantation. Such a project was partly realized by Fenger but in some respects proved to be not practicable even with the best existing means (on-line accelerator). It appears, in fact, that ion implantation followed by Mössbauer spectroscopy does not give the means to solve the problems of hot atom chemistry because of the necessity to implant  $10 \mu\text{g cm}^{-2}$  or more of  $^{57}\text{Fe}$ , which causes damage to the matrix and

requires excessive time for implantation. This same makes it impossible to do the implantation on hydrates, where most of the inorganic hot atom studies were done.

Unfortunately also in this case the first calculated sample  $\text{FeSO}_4 \cdot 7\text{H}_2\text{O}$  gave systematic deviations in the difference spectrum for the best fit of the well resolved doublet. The final solution was simple. The sample was found to contain a small amount of other  $\text{Fe}^{2+}$  species with different parameters. The identity of this other compound was not determined. Its presence is obvious, although not mentioned, in results published by Gallagher, Johnson and Schrey. Similar problems were encountered with other hydrates. From the results of repeated measurements on  $\text{NH}_4\text{Fe}(\text{SO}_4)_2 \cdot 12\text{H}_2\text{O}$  it was deduced that some problems are caused by partial melting of the hydrates during grinding. This is unfortunate because most compounds are commonly obtained in such form that the grinding is necessary in order to prepare uniform absorbers of proper thickness.

A different method of grinding was therefore selected. The slow, gentle grinding in an inert liquid whose boiling point is lower than the melting point of the hydrate. Pentane and hexane were the selected inert liquids. The ground sample was then transferred, together with the excess of the liquid, into an airtight cell and measured in a form of a slurry. Under such conditions, a sample of  $\text{FeSO}_4 \cdot 7\text{H}_2\text{O}$  gave almost exactly the pure theoretical doublet. Other samples measured,  $\text{NH}_4\text{Fe}(\text{SO}_4)_2 \cdot 12\text{H}_2\text{O}$  and  $\text{Fe}(\text{NO}_3)_3 \cdot 9\text{H}_2\text{O}$ , gave spectra which differed from the spectra of these compounds prepared under usual conditions. On these samples final non-constrained curve fitting analysis was not achieved.



All other compounds were measured for other reasons (for example, to determine the interval of integration for Integral Mossbauer Spectra measurements) and their computer analysis was not attempted. The original intention to prepare an atlas of spectra of the simple iron compounds measured in this laboratory under identical and therefore comparable conditions was not fulfilled for the abovementioned and other reasons.

#### Determination of Zero Velocity Position

The isomer shift values in the literature are given with respect to some chosen standard absorber. Stainless steel 310 and the centroid of the doublet of sodium nitroprusside dihydrate were formerly commonly used reference absorbers (Herber), but recently the centroid of the iron spectrum has been more widely used.

It is nevertheless important to know the position of the true zero velocity. The channel corresponding to zero velocity can be determined in various ways; for example, by the use of a Moire grating or a Michelson interferometer. In the present work the zero velocity position was determined graphically and by calculation, using the property of the invariance of the zero position with changes of acceleration for given frequency and dwell time. For any position, constant frequency and identical source the relationship

$$\text{position} \cdot \text{dwell time} \cdot \text{acceleration} = \text{const}$$

is valid. In this relationship, "position" refers to the channel number for some identifiable spectral feature, such as a selected absorption peak. For example, given that  $f = 9.1 \text{ Hz}$ , and  $a = 65 \text{ cm sec}^{-2}$ , for source #5 ( $^{57}\text{Co} + ^{57m}\text{Fe (Pd)}$ ) the following data were observed.

Channels used for the spectrum storage	256	1024
1 Dwell time ( $\mu\text{sec ch}^{-1}$ )	200	50
2 Position of the 3rd peak in the iron spectrum (ch)	138.5	554.0
Product 1.2 (msec)	27.7	27.7

It is therefore possible to linearize the previous equation for a given frequency.

$$\text{Position} \propto 1/a$$

Using this equation and experimental data obtained under various conditions, the values in the following Table were obtained.

a (cm sec <sup>-2</sup> )	1/a (cm <sup>-1</sup> sec <sup>2</sup> )	Position of iron peaks 3rd (ch)                  4th (ch)		Zero velocity position calc. (ch)
256 channels, dwell time 200 μsec				
65	0.0154	138.5	151.5	*
30.3	0.033	132	160	144.1
15.4	0.065	120	175	144.2
8.05	0.124	100	205	<u>143.9</u>
		Average		144.1
1024 channels, dwell time 50 μsec				
65	0.0154	554	608	*
4.75	0.2105	278	1018	576

The results for the dwell time  $200\mu$  sec are plotted in Figure 10. Zero velocity position read from the graph (143.2) is in good agreement with the calculated value of 144.1 as seen in Table. The value 144.1 converted to the other dwell time ( $50\mu$ sec) gives 576.4, which is again in very good agreement with the value (576) calculated from direct measurements.

The determination of the zero velocity position is important for various reasons. For calculations it defines the position of the maximum of the background parabola, thus removing one variable. It is not possible to calculate this maximum from measurements using no absorber. For measurements of Mössbauer spectra it is one of the basic factors for the selection of new working conditions.

#### Determination of the Phase Shift

As was mentioned earlier, there is a phase shift between the drive signal for the Doppler unit and the amplified signal from the velocity sensing coil of the transducer. This inevitable phase shift is the cause for the broadening or doubling of the peaks in Mössbauer spectra measured with Mössbauer spectrometers operating in the analogue mode. The delay of the amplified signal was read directly from the oscilloscope and was between 2 and 5 msec.

In the multichannel scaler mode, too, there is a small delay between the scan triggering signal and the real motion of the Doppler unit. In the previous section the zero velocity position

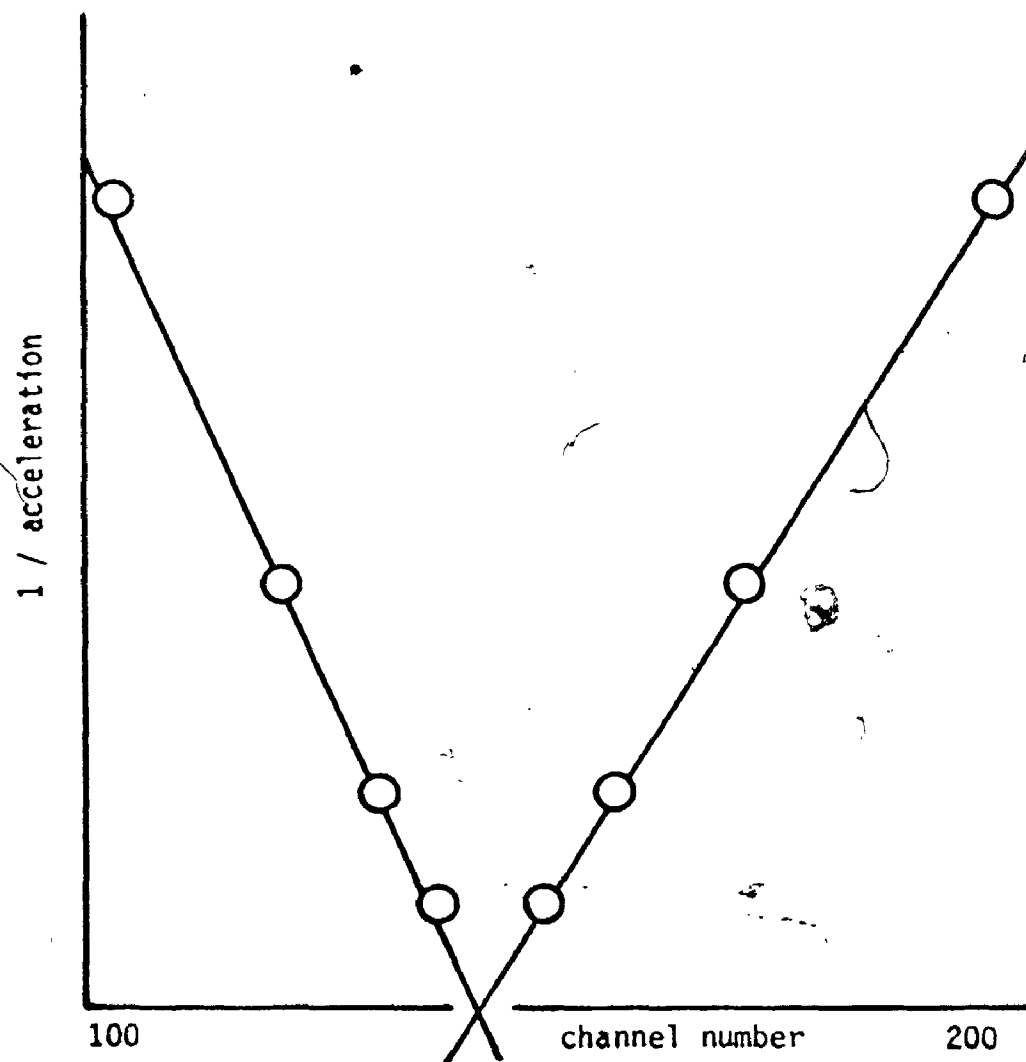


FIGURE 10 Determination of zero velocity position

was calculated. That position is at the channel 576, which for the dwell time used (50  $\mu$ sec), corresponds to 28.8 msec after the sweep start. The zero velocity should be at exactly 1/4 of the period (27.5 msec) after the triggering signal. The difference between these two values is 1.3 msec, equivalent to 26 channels, and is the delay time between the triggering signal and the actual beginning of the spectrum. The first 26 channels thus represent the end of the second spectrum (from the previous scan) which is not stored under the selected operating conditions.

#### INTEGRAL MÖSSBAUER SPECTROSCOPY

The chemical and physical processes studied by the means of Integral Mössbauer spectroscopy were of several general types, and included ligand displacements, dehydrations, oxidations, reductions, processes resulting from temperature change, and other processes. These can be divided into two classifications: measurements at constant temperature and measurements with varying temperature. In the first group a variety of chemical reactions was studied. In all cases where the data were available, the reaction free energy was calculated, to ensure that the reaction would be expected to occur. Several other interesting reactions were rejected on this basis. The second group treated in section Integral thermal scans includes the studies of phase changes (p.96). Most measurements were done with the acceleration of 5 cm sec<sup>-2</sup>. Therefore the velocity interval for integration was from -0.11 cm sec<sup>-1</sup> to +0.14 cm sec<sup>-1</sup>.

### Apparent Shifts in Spectral Characteristics

The presence of the background parabola causes changes in the position of the peak in the Mössbauer spectrum. These changes amount to less than one thousandth of a channel and do not depend on the position of the peak.

The analytical form of a Mössbauer spectrum is given by the following equation

$$y = ax^2 + bx + c - \sum_{i=1}^m C_i \frac{A_i^2}{A_i^2 + (x - B_i)^2}$$

where  $A_i = \frac{\Gamma_i}{2}$  and  $x$  = channel number

$B_i$  = position of the absorption maximum for the  $i^{\text{th}}$  peak

$C_i$  = height of the  $i^{\text{th}}$  peak

$m$  = number of peaks

The first three terms give the background parabola.

For the case of signal averaging and Integral Mössbauer Spectra the integrated equation is

$$Y = \frac{1}{3} ax^3 + \frac{1}{2} bx^2 + cx + \text{const} - \sum_{i=1}^m C_i A_i \arctan \frac{x - B_i}{A_i} + \text{Const}$$

with a definite integral

$$Y_x^{x+n} = n[ax^2 + (an + b)x + \frac{1}{3} an^2 + \frac{1}{2} bn + c] + \sum_{i=1}^m C_i A_i \arctan \frac{nA_i}{A_i^2 + (x - B_i + n)(x - B_i)}$$

where  $n$  is the number of channels in the integration interval.

The regular (constant acceleration) Mössbauer spectrum is "integrated" over each channel in turn and has the consequent analytical form

$$Y_x^{x+1} = ax^2 + (a+b)x + \frac{1}{3}a + \frac{1}{2}b + c - \sum_{i=1}^m$$

$$C_1 A_1 \arctan \frac{A_1}{A_1^2 + (x - B_1 + 1)(x - B_1)}$$

The integration causes an apparent change in positions of maxima of all peaks and of the parabola.

#### Shift in Position of Parabola

The definite integral of a general parabola equation ( $y = ax^2 + bx + c$ ) is

$$Y = anx^2 + (an^2 + bn)x + \frac{1}{3}an^3 + \frac{1}{2}bn^2 + cn$$

The only extremum for this function must fulfill the condition

$$\frac{dY}{dx} = 2anx + an^2 + bn = 0$$

with a solution

$$x = -\frac{b}{2a} - \frac{n}{2}$$

The position of the extremum for the original parabola is  $-b/2a$ . Therefore the position of the extremum for the integrated parabola is shifted by  $n/2$  channels to the left.

### Shift in Position of Peaks

The positions of peaks in the Mössbauer spectrum are also apparently shifted by the integration. Assuming a linear background, the differentiated Integral Mössbauer spectrum for one peak has the form

$$\begin{aligned} \frac{dY}{dx} &= -CA \frac{1}{1 + \frac{n^2 A^2}{[A^2 + (x - B + n)(x - B)]^2}} - nA \frac{(x - B) - (x - B + n)}{[A^2 + (x - B + n)(x - B)]^2} \\ &= nCA^2 \frac{(x - B) + (x - B + n)}{n^2 A^2 + [A^2 + (x - B + n)(x - B)]^2} \end{aligned}$$

As was shown above (see page 72), the first condition (viz. linear background) is acceptable, because the influence of the background parabola is negligible. The second condition, the use of one peak only, does not influence the general validity of the final solution. The above expression must be, for an extremum, equal to zero. That can be fulfilled only if

$$(x - B) + (x - B + n) = 0$$

The position of the extremum is then

$$x = B - \frac{n}{2}$$

Peaks in an integrated Mössbauer spectrum thus appear to be shifted by  $n/2$  channels to the left from the positions of corresponding peaks in a Mössbauer spectrum such as is obtained from the constant velocity Mössbauer spectrometer. This is the reason for



the discrepancies between Mössbauer parameters measured with the two basic versions of Mössbauer spectrometers. In the case of the constant acceleration Mössbauer spectrometer, where the integration is done over one channel, the shift is equal to one half of a channel.

It is clear that the "peak shift" results from the definition of  $x$  as the position of the beginning of the given channel. Clearly then, the middle of a single channel is at  $x + 1/2$  and a middle of a block of  $n$  channels is at  $x + n/2$ . This becomes important however when the method of effecting the integration is considered. The use of a constant velocity spectrometer allows to get  $v_i - \frac{n}{2}$  to  $v_i + \frac{n}{2}$ , so that the peak is still in the middle of the region of integration. If however a constant acceleration spectrometer is used, window need not be set at the original peak position, but at a position  $x_i - \frac{n}{2}$ .

In the following Table 11 are some results of the integration of a single peak, where the shift of the apparent position is clearly seen. The quantitative results of symmetrical integration over one peak are given in Table 12 and Figure 11. The signal-to-noise ratio has an optimum value for the integration interval equal to 1.5 of FWHM.

### INTEGRAL REACTION SPECTRA

Most measurements of Integral reaction spectra were done with an acceleration of  $5 \text{ cm sec}^{-2}$  over all 1023 channels. That means that in all cases the total (integrated) Mössbauer effect absorption should be smaller than 1% for  $\epsilon = 10\%$  (see Table 12 on page 78). The (differential) Mössbauer effect exceeds 10% in only one of the

reaction mixtures to be discussed.

Nevertheless in almost all cases studied the changes in absorption were larger than 1% reaching practically the value of 20% with both signs. That is caused by the existence and presence of a non-Mössbauer resonance absorption, which has different values for different compounds. The simultaneous occurrence of this new  $\gamma$ -ray resonance effect and of the Mössbauer effect, and their changes in the course of the chemical reaction, cause that at the present time the Integral reaction spectra are difficult to evaluate and interpret. (Within the results presented in this work is one case where only non-Mössbauer resonance absorption is present - see page 91.) Simple logical instrumental development can easily eliminate this problem as is mentioned on page 115.

It is perhaps useful to remind at this point that the  $\gamma$ -ray (and X-ray) absorption (due to the photoelectric effect and the Compton effect) does not change in closed systems. Cells with reacting compounds, as used in this work, represent closed systems. Therefore all changes in Integral reaction spectra are caused by changes in the Mössbauer effect and non-Mössbauer resonance effect. For the following discussion the changes in the Mössbauer absorption can in many cases be ignored (being less than 1% as compared to the 20% non-Mössbauer resonance absorption).

#### Solid-Solid Reactions: Ligand Transfer

Typical of the reactions which were studied was that occurring in the system  $\text{FeSO}_4 \cdot 7\text{H}_2\text{O}$  - KCN, which had previously been studied

TABLE 11 Lorentz and Integrated Lorentz Functions

$$y = C \frac{A^2}{A^2 + (x - B)^2} \quad \text{and} \quad y_1 = CA \arctan \frac{nA}{A^2 + (x - B + n)(x - B)}$$

for a peak, FWHM = 2A, maximum height C (\*) in channel B.

x (ch)	y Lorentz Function Value	y <sub>1</sub> Integration over n channels		
		n = 1	n = 2	n = 5
26	0.500	0.568	1.287	4.124
27	0.640	0.719	1.594	4.428
28	0.800	0.875	1.855	4.428
29	0.941	0.980	*1.960	4.124
30	*1.000	0.980	1.855	
31	0.941	0.875	1.594	
32	0.800	0.719	1.287	
33	0.640	0.568		
34	0.500			

The total area of the peak is 12.568.

TABLE 12 Symmetrical Integration of Lorentz Function

Conditions: straight line background, FWHM = 8 channels

Integration Interval (ch)	Lorentz Function Value	Area for Peak for Unit Size	Area (%)	Effect Size Per 10% Peak (%)	Signal to Noise Ratio	
					*	†
0	1.000	0	0	10.00		
1	0.985	0.994	7.9	9.94	0.99	3.16
2	0.941	1.960	15.6	9.80	1.39	4.40
4	0.800	3.710	29.6	9.28	1.86	5.90
6	0.640	5.148	41.0	8.56	2.10	6.65
8	0.500	6.283	50.0	7.85	2.21	7.02
12	0.308	7.862	62.5	6.55	2.26	7.17
16	0.200	8.856	70.5	5.52	2.21	7.02
24	0.100	9.992	79.5	4.15	2.05	6.46
32	0.059	10.608	84.4	3.33	1.88	5.94
36	0.047	10.816	86.2	3.01	1.80	5.70
40	0.038	10.992	87.5	2.75	1.74	5.50
64	0.015	11.564	92.0	1.81	1.44	4.55
80	0.010	11.765	93.6	1.47	1.31	4.15
100	0.006	11.928	95.1	1.19	1.19	3.77
256	<0.001	12.313	98.3	0.48	0.79	----
∞	0.000	12.568	100.0	0.00	0.00	0.00

\* For acceleration  $a$  cm sec<sup>-2</sup>† For acceleration 0.1a cm sec<sup>-2</sup>. The integration interval must be multiplied by ten.

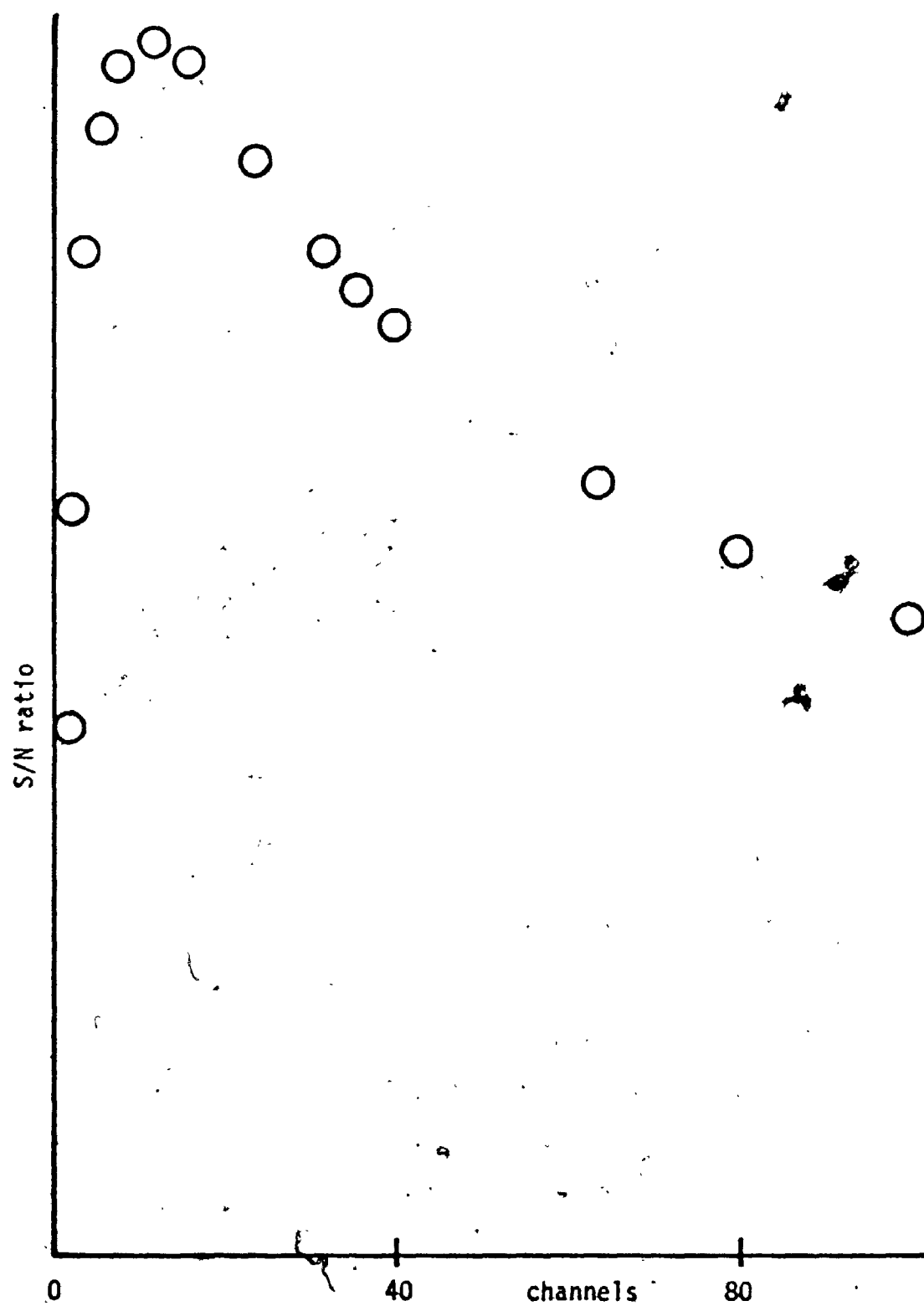
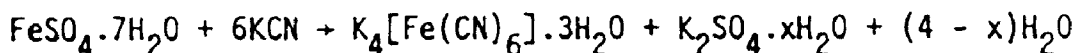


FIGURE 11 Dependence of signal-to-noise ratio on interval of integration.

by Gütlich and Hasselbach by (conventional) Mössbauer spectroscopy.



The solid starting materials were mixed as fine crystals and pressed (5 tons  $\text{in}^{-2}$ ) for one minute. Only one of the two  $\text{FeSO}_4 \cdot 7\text{H}_2\text{O}$  peaks was within the integration interval. Mössbauer spectrum of  $\text{K}_4[\text{Fe}(\text{CN})_6] \cdot 3\text{H}_2\text{O}$  has only one peak, which was also within the integration interval. Therefore, in the observed reaction spectrum the absorption should increase up to a constant final value. Only the first of these expectations was fulfilled, as seen in Figure 12. The absorption increased for about 400 min, and then it was constant for about 100 min. After that period the absorption decreased again. The Mössbauer spectrum, as measured afterwards, shows the main product to be  $\text{K}_4[\text{Fe}(\text{CN})_6] \cdot 3\text{H}_2\text{O}$  with a small amount (less than 10%) of unreacted  $\text{FeSO}_4 \cdot 7\text{H}_2\text{O}$ .

Gütlich and Hasselbach proposed a two-step reaction with the formation of  $\text{K}_3[\text{Fe}(\text{H}_2\text{O})(\text{CN})_5]$  first, which is then converted into  $\text{K}_4[\text{Fe}(\text{CN})_6]$ . The Mössbauer spectrum of  $\text{Na}_3[\text{Fe}(\text{H}_2\text{O})(\text{CN})_5]$  contains a well resolved doublet within the integration interval. Assuming similar absorption cross-sections for both products, the reaction spectrum is compatible with formation of the aquo complex, which will cause an increase in absorption (because it has both peaks within the integration interval). The formation of the final product  $\text{K}_4[\text{Fe}(\text{CN})_6] \cdot 3\text{H}_2\text{O}$ , will be accompanied by a decrease in absorption. The final absorption will remain greater than the original value.

An attempt was made, by using a reduced molar ratio, to stop the reaction and thus isolate the aquo complex.

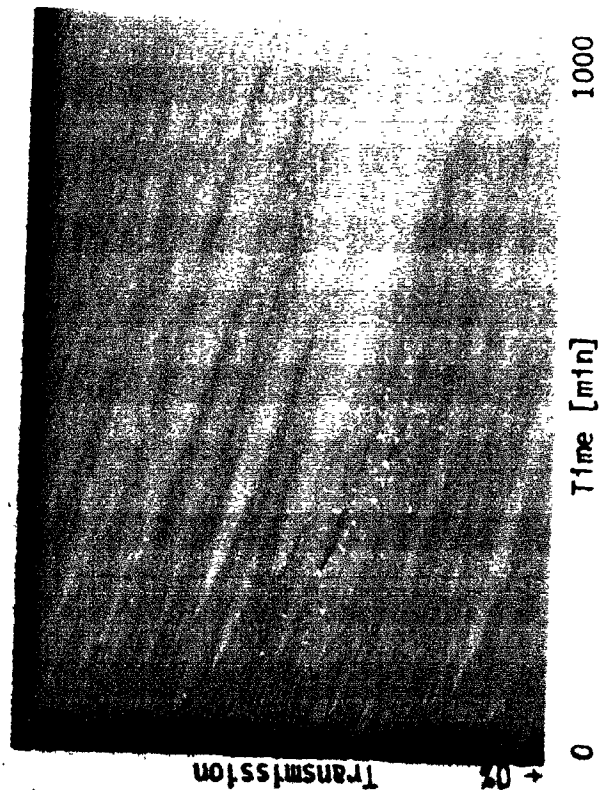


FIGURE 12 Integral reaction spectrum  
 $\text{FeSO}_4 \cdot 7\text{H}_2\text{O} + 6\text{KCN}$

Acceleration:  $5 \text{ cm sec}^{-2}$   
 Dwell time :  $1 \text{ min ch}^{-1}$

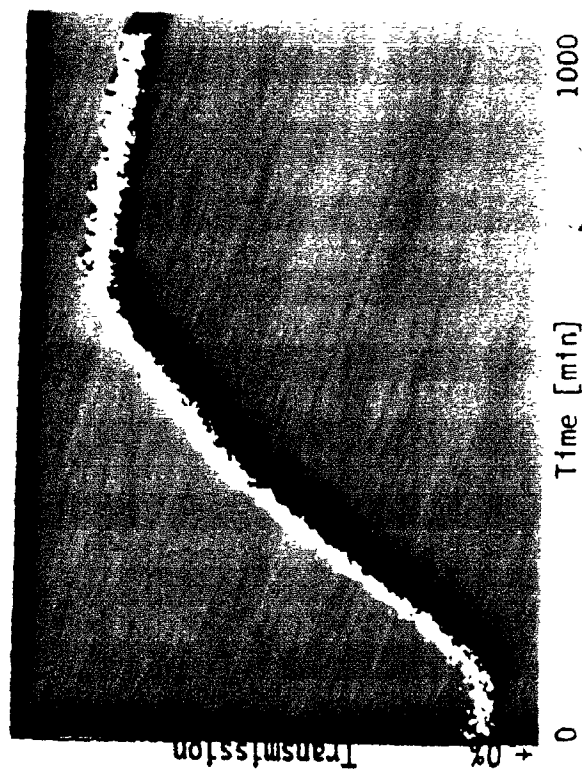
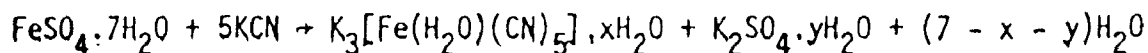


FIGURE 13 Integral reaction spectrum  
 $\text{FeSO}_4 \cdot 7\text{H}_2\text{O} + 5\text{KCN}$

Acceleration:  $5 \text{ cm sec}^{-2}$   
 Dwell time :  $1 \text{ min ch}^{-1}$

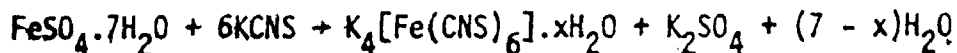


In this experiment the reaction proceeded, but the Integral reaction spectrum was quite different (see Figure 13). After an induction period of about 100 min, the transmission rose for 500 min. (with one change in rate) and only then a reversal in absorption was observed, which did not compensate fully for the original increase in transmission. The Mössbauer spectrum of the reaction product revealed the presence of  $[\text{Fe}(\text{CN})_6]^{4-}$  and of less than 10% of unreacted  $\text{FeSO}_4 \cdot 7\text{H}_2\text{O}$ . Part of the  $\text{Fe}^{2+}$  was bound to  $[\text{Fe}(\text{CN})_6]^{4-}$  as was indicated by the presence of blue coloration.

The Integral reaction spectrum was measured again after six days (under strictly identical conditions). There were no changes in the spectrum and the value corrected for the decay corresponded to the final value of the original reaction spectrum. The reaction was therefore finished within 1000 min.

The same reaction was attempted using NaCN. This reaction did not proceed at all using a pressure of 3 tons or 5 tons. No change occurred in the Integral reaction spectrum and Mössbauer spectra measured subsequently contained only the doublet of  $\text{FeSO}_4 \cdot 7\text{H}_2\text{O}$ .

Replacing the KCN by KCNS but using the 1:6 ratio gave a spectrum similar to that of the previous system.



There was a short induction period and then an increase in transmission (see Figure 14). The Mössbauer spectrum of the reaction products was so weak that it was possible to measure it only after the



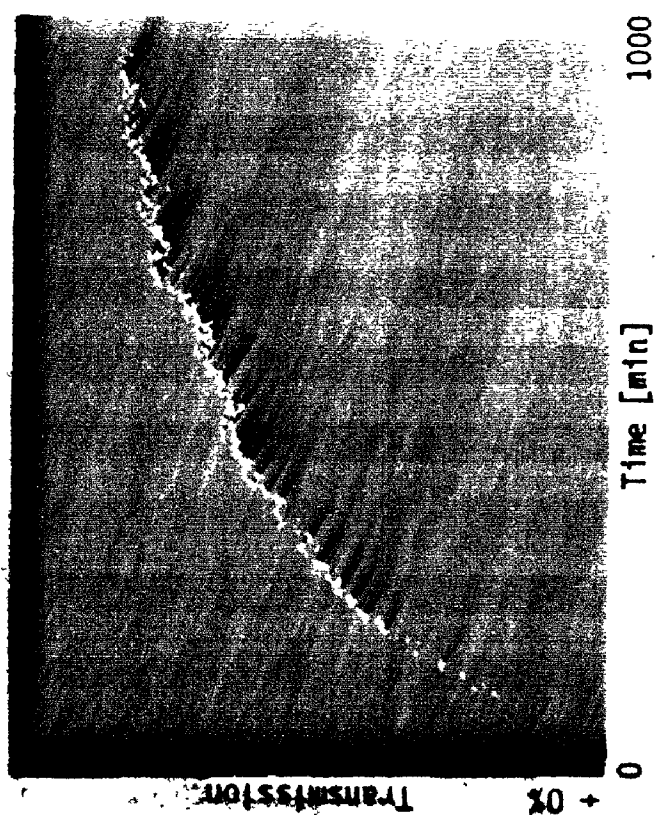


FIGURE 14 Integral reaction spectrum  
 $\text{FeSO}_4 \cdot 7\text{H}_2\text{O} + 6\text{KCNS}$

Acceleration:  $5 \text{ cm sec}^{-2}$   
 Dwell time :  $1 \text{ min ch}^{-1}$

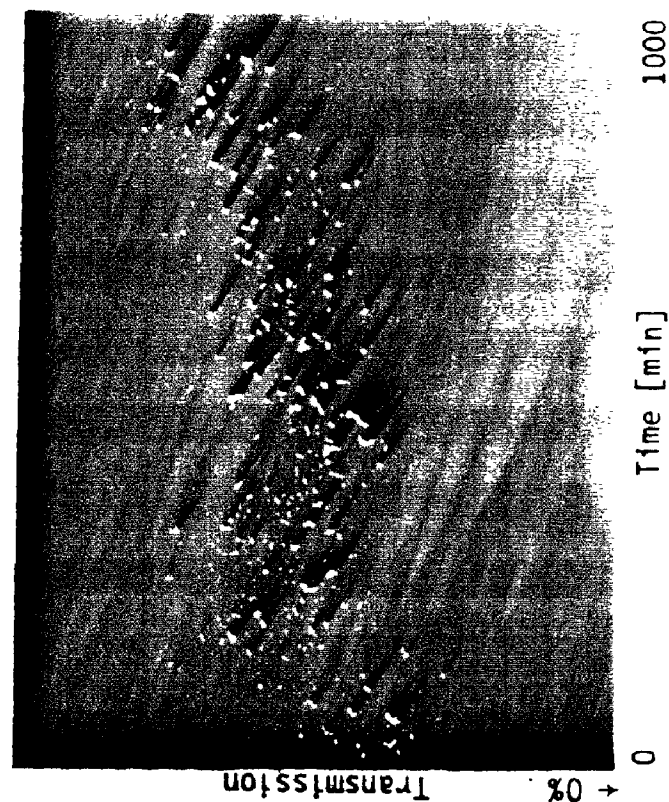


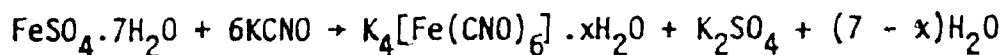
FIGURE 15 Integral reaction spectrum  
 $\text{FeSO}_4 \cdot 7\text{H}_2\text{O} + 6\text{KCNO}$

Acceleration:  $5 \text{ cm sec}^{-2}$   
 Dwell time :  $1 \text{ min ch}^{-1}$

purchase of a new 11 mC  $^{57}\text{Co} + ^{57\text{m}}\text{Fe}$  (Pd) source. It consists of a weak close doublet ( $\epsilon \sim 1\%$ ) and therefore the smooth shape of the integral spectrum is practically only a measure of the disappearance of  $\text{FeSO}_4 \cdot 7\text{H}_2\text{O}$  from the system. Kinetically there is one first order reaction, with a half-life of 216 minutes. But the most important feature of this spectrum is the value of the change in the absorption ( $\Delta A$ ). The  $\Delta A$  between the beginning and the end of the reaction, relative to the end of the reaction, is -18.1%. As was stated on pages 75 and 76, such a large change is unexplained by the changes caused by the Mössbauer effect. Such a situation occurred also in the previous reaction (where it was not mentioned because the reaction product contained iron in two forms).

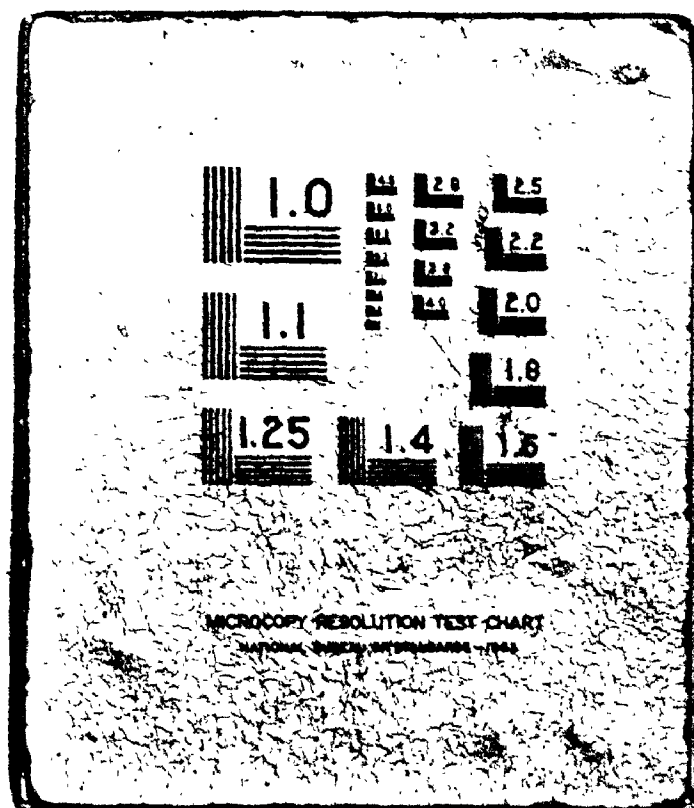
It is rather difficult to measure the initial value of the absorption ("before" the start of the reaction). Therefore the value from the end of the spectrum (after the completion of the reaction) is taken and assigned the value of zero absorption. If the absorption at the beginning was higher, then a negative sign is used for  $\Delta A$  and vice versa. (On account of the logical inversion to the beginning of the process.) The value of  $\Delta A$  stated above is further treated on page 106.

A similar experiment was undertaken using  $\text{KCNO}$ :



The Integral reaction spectrum (see Figure 15) is more complex than in previous cases. The Mössbauer spectrum of the product contains a close doublet of the complex (a weak spectrum with  $\epsilon$  about 1%) and a very weak spectrum from residual  $\text{FeSO}_4 \cdot 7\text{H}_2\text{O}$  ( $\epsilon$  less than 1%).

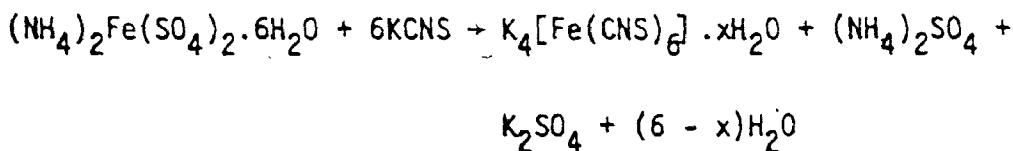
22  
OF/DE



The non-Mössbauer resonance absorption is further detailed on page 106.

The Integral reaction spectra for  $\text{FeSO}_4 \cdot 7\text{H}_2\text{O}$  with KCNS and with K<sub>4</sub>CNO are quite different. That is caused almost entirely by differences in the non-Mössbauer resonance absorption, which is much larger for  $\text{K}_4[\text{Fe}(\text{CNO})_6] \cdot x\text{H}_2\text{O}$  than for  $\text{K}_4[\text{Fe}(\text{CNS})_6] \cdot x\text{H}_2\text{O}$ . The non-Mössbauer resonance absorption of  $\text{FeSO}_4 \cdot 7\text{H}_2\text{O}$  is similar (within about 0.5%) to that of  $\text{K}_4[\text{Fe}(\text{CNO})_6] \cdot x\text{H}_2\text{O}$ .

The formation of  $[\text{Fe}(\text{CNS})_6]^{4-}$  was carried out via the following reaction:



which contains one molecule of  $\text{H}_2\text{O}$  less than in the previous experiment using  $\text{FeSO}_4 \cdot 7\text{H}_2\text{O}$ . The character of the Integral Mössbauer spectrum (see Figure 16) is similar to that of the heptahydrate system, including the weakness of the Mössbauer spectrum ( $\epsilon = 2\%$  on a dried sample). There are two reasons for the presence of a weak Mössbauer spectrum only. First the Mössbauer absorption cross-section is small for the reaction product, secondly it is soluble in water (which is released in the reaction). The increase in transmission in the Integral reaction spectrum amounts to  $\Delta A$  of - 6.6% and demonstrates also in this case the small non-Mössbauer resonance absorption of  $\text{K}_4[\text{Fe}(\text{CNS})_6] \cdot x\text{H}_2\text{O}$ . It will be used again on page 106.

Taking into consideration the high reactivity of KCNS, an attempt was made to prepare the mixed complex  $\text{Na}_3\text{K}[\text{Fe}(\text{CNS})(\text{CN})_5] \cdot x\text{H}_2\text{O}$

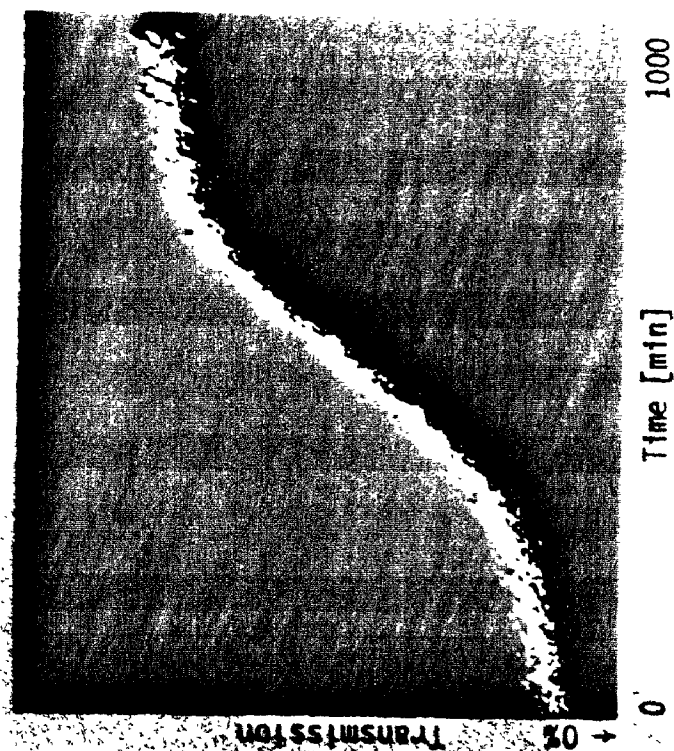


FIGURE 16 Integral reaction spectrum  
 $(\text{NH}_4)_2\text{Fe}(\text{SO}_4)_2 \cdot 6\text{H}_2\text{O} + 6\text{KCN}$   
 Acceleration:  $5 \text{ cm sec}^{-2}$   
 Dwell time :  $1 \text{ min ch}^{-1}$

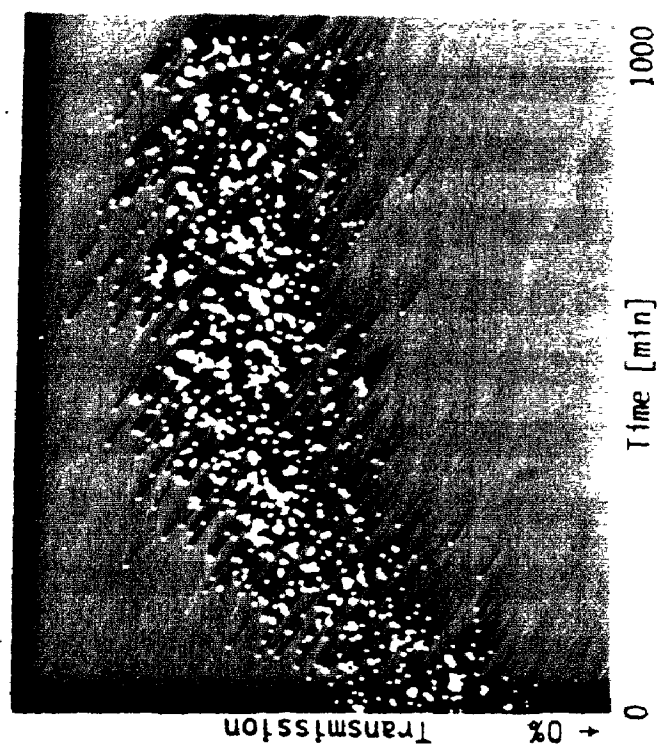
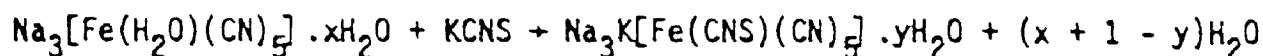


FIGURE 17 Integral reaction spectrum  
 $(\text{NH}_4)_2\text{Fe}(\text{SO}_4)_2 \cdot 6\text{H}_2\text{O} + 2\text{Mg}(\text{ClO}_4)_2$   
 Acceleration:  $5 \text{ cm sec}^{-1}$   
 Dwell time :  $1 \text{ min ch}^{-1}$

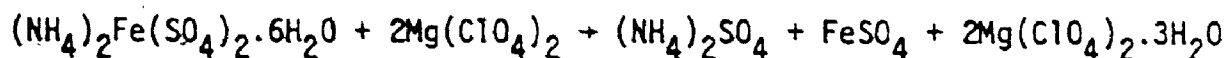
via the reaction



trying at the same time to parallel the second stage of the mechanism proposed by Gütllich and Hasselbach for the formation of  $[\text{Fe}(\text{CN})_6]^{4-}$ . However, in this system the reaction did not proceed. There was only a slight increase in transmission. The Mössbauer spectrum revealed only the presence of the starting material.

### Dehydration

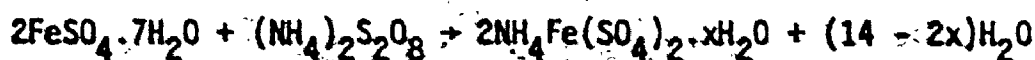
The following reaction was studied as an example of a reaction in which water was removed from the iron compound, but does not appear as free water:



The reaction was completed in about five hours (see Figure 17). The absorption change was -1% and afterwards fluctuated within statistical limits around that value over fourteen days. The Mössbauer spectrum contains two doublets, only partly resolved. The inner doublet belongs to the unreacted  $(\text{NH}_4)_2\text{Fe}(\text{SO}_4)_2 \cdot 6\text{H}_2\text{O}$ . After thirty days there remains less than about 30% of the starting material, but even after 200 days some slow structural changes are still going on.

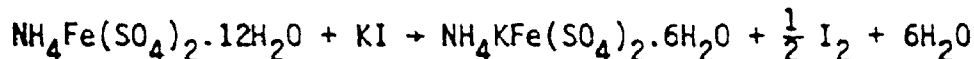
### Oxidation and Reduction

In the reaction



the oxidation was finished in a time just less than 1000 minutes (see Figure 18) giving a Mössbauer spectrum without a trace of  $\text{Fe}^{2+}$ . Also in this case the changes in the absorption during the reaction were larger than can be expected from the changes of the Mössbauer effect only and were caused by the changes of the non-Mössbauer resonance absorption. Unfortunately the reaction leads to an undefined mixture of lower hydrates, so that the observed value of  $\Delta A$  cannot at present be used in further calculations of non-Mössbauer resonance absorption.

The question of possible interference with the reaction caused by water freed in the reaction was clearly eliminated in the following reduction reaction:



which proceeded rapidly (completed in about 200 minutes) to the final product in one step (see Figure 19). The Mössbauer spectrum of the reaction product excludes the presence of the product originally expected:  $\text{FeSO}_4 \cdot 7\text{H}_2\text{O}$ . The peaks of  $\text{NH}_4\text{KFe}(\text{SO}_4)_2 \cdot 6\text{H}_2\text{O}$  are both within the integration interval and well separated.  $\Delta A$  for this reaction is positive (11.2%) and demonstrates the large non-Mössbauer resonance absorption of  $(\text{NH}_4)\text{KFe}(\text{SO}_4)_2 \cdot 6\text{H}_2\text{O}$  in comparison to  $(\text{NH}_4)\text{Fe}(\text{SO}_4)_2 \cdot 12\text{H}_2\text{O}$ . This  $\Delta A$  value will be used again on page 106. A decrease in absorption starts after about 300 minutes and is at least partly caused by the slow reaction of  $\text{I}_2$  with the wall of the cell (leading to the formation of  $\text{CuI}$ ) and causing the removal of a part of  $\text{I}_2$  from the optical path. The main process -- the reduction of  $\text{NH}_4\text{Fe}(\text{SO}_4)_2 \cdot 12\text{H}_2\text{O}$  -- is a first order reaction with

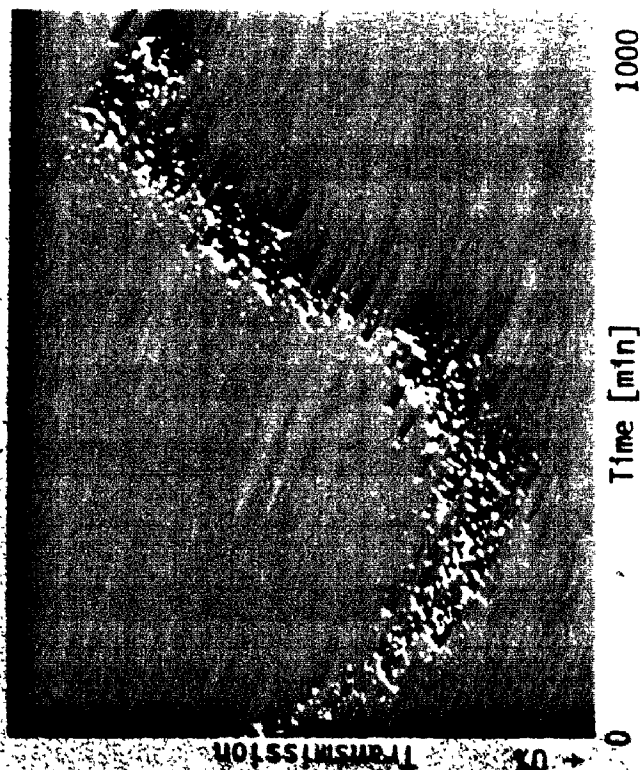


FIGURE 18 Integral reaction spectrum  
 $\text{FeSO}_4 \cdot 7\text{H}_2\text{O} + \frac{1}{2}(\text{NH}_4)_2\text{S}_2\text{O}_8$   
 Acceleration:  $5 \text{ cm sec}^{-2}$   
 Dwell time :  $1 \text{ min ch}^{-1}$

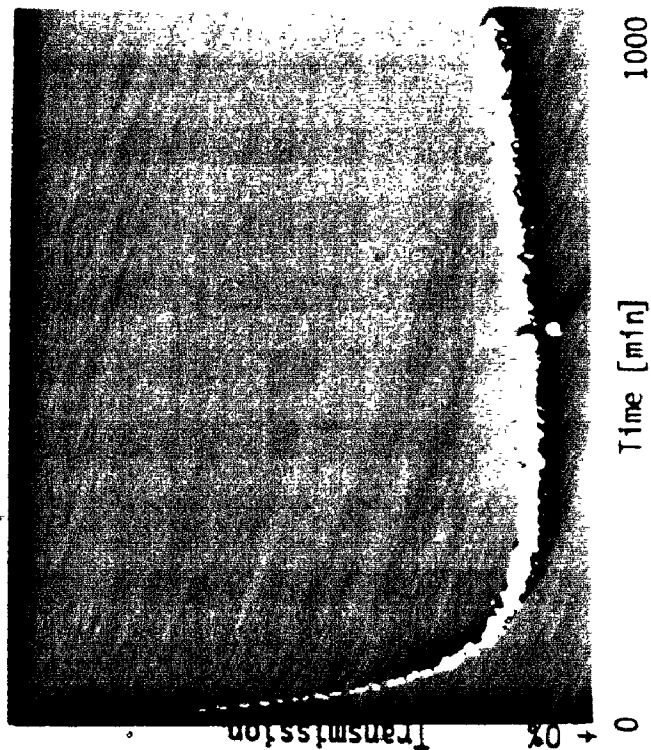
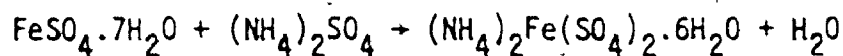


FIGURE 19 Integral reaction spectrum  
 $(\text{NH}_4)_2\text{Fe}(\text{SO}_4)_2 \cdot 12\text{H}_2\text{O} + \text{KI}$   
 Acceleration:  $5 \text{ cm sec}^{-2}$   
 Dwell time :  $1 \text{ min ch}^{-1}$



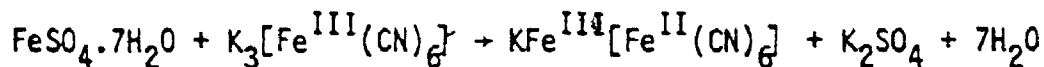
the half-life of about 30 minutes.

The formation of  $\text{NH}_4\text{KFe}(\text{SO}_4)_2 \cdot 6\text{H}_2\text{O}$  mentioned above led to an attempt to prepare similar compounds via the reaction



but this reaction proceeds only to a small extent and then stops. The Mössbauer spectra show a small, but clearly distinguishable doublet of the product and the stopped state of the reaction.

The reaction



proceeded for about 100 minutes and then apparently stopped. The sample was found by microscopic examination to be heterogeneous and contained some of the expected blue product, although this is not readily distinguishable from the Mössbauer spectrum.

#### Solid-Liquid Reactions: Ion Exchange

A number of reactions were studied in which one reactant was a solid while the other was in aqueous solution. This type of condition changes the kinetics in that the transport of reactants to the reaction site is much easier and more rapid. There are also problems, of course, and methods were required to preserve a certain rigidity of the sample in order to keep the same amount of material in the optical path.

An attempt was made to study the adsorption of  $\text{Fe}^{3+}$  from a saturated aqueous  $(\text{NH}_4)\text{Fe}(\text{SO}_4)_2$  solution on strong cation exchanger resin (Dowex 50W-X8, H-form, 100-200 mesh). According to Johansson

no changes were expected in the Integral Mössbauer spectrum.

Nevertheless very large changes were found. The absorption first increased rapidly by 1%, then smoothly in 100 minutes decreased to -2.4% and afterwards continuously, within the next 250 minutes, increased to the value of 19% and remained practically constant at that value (see Figure 20). This result indicated a strong absorption, but no Mössbauer spectrum was found, in agreement with Johansson's observations. This is the only case of pure non-Mössbauer resonance absorption changes (between two states of  $\text{Fe}^{3+}$ ), because it is known that neither initial nor the final material has a Mössbauer spectrum. The very large increase in absorption thus can be explained only in terms of strong non-Mössbauer resonance absorption by adsorbed iron.

Johansson also notes the appearance of the Mössbauer spectrum after removal of water from the ion exchanger. In order to follow the formation of the selectively absorbing species in the spectrum, by removal of the water, an absorber was prepared from a second batch of Dowex 50W-X8 saturated with  $\text{Fe}^{3+}$  and thoroughly washed with water. The excess of free water was removed and the sample placed in a cell with one porous window. Through this window the resin sample became slowly air dried, while not settling out of the optical path. The Integral Mössbauer spectrum shows only a decrease in absorption by 4.5% as a result of two simultaneous processes. The first effect, leading to decreased absorption, is caused by removal of water from the absorption path; the second effect (small in this case) leading to the increase in absorption, is caused by the appearance of selectively absorbing species. After 1000 minutes

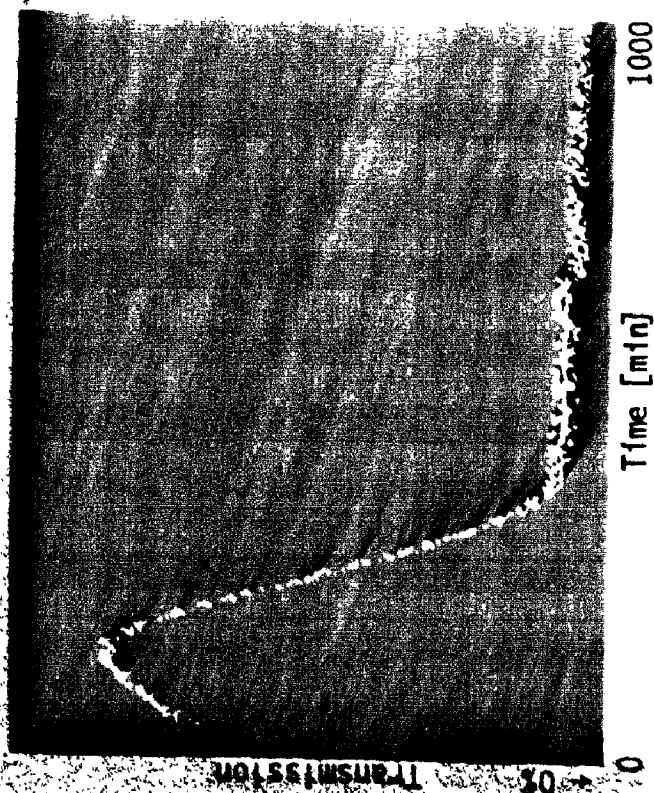


FIGURE 20

Integral reaction spectrum

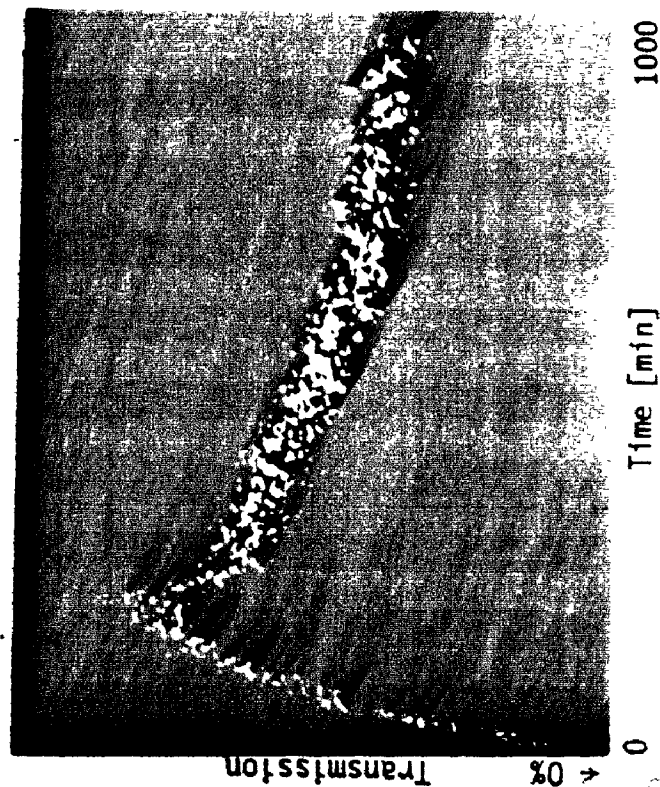
Absorption of  $\text{Fe}^{3+}$  on Dowex 50W + 8XAcceleration:  $65 \text{ cm sec}^{-2}$ Dwell time :  $1 \text{ min ch}^{-1}$ 

FIGURE 21

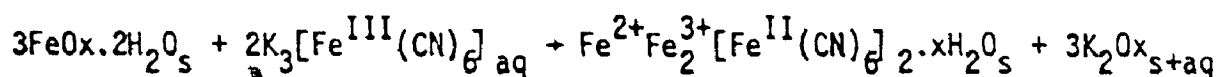
Integral reaction spectrum

 $3\text{FeOx} \cdot 2\text{H}_2\text{O} + 2\text{K}_3[\text{Fe}(\text{CN})_6]_{\text{aq}}$ Acceleration:  $5 \text{ cm sec}^{-2}$ Dwell time :  $1 \text{ min ch}^{-1}$

the cell was closed and the Mössbauer spectrum measured. It contains one small broad peak ( $\epsilon$  about 1%).

### Complex Redox and Exchange

Some reacting systems are described in the following experiments. The (precipitation) reaction between solid ferrous oxalate and potassium ferricyanide aqueous solution was studied according to the reaction

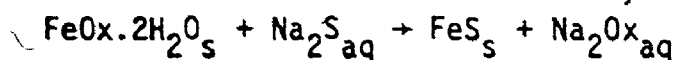


Since only one peak of the ferrous oxalate doublet lies within the integration interval and the other peak will move into the integration interval as a result of the reaction (for two atoms out of every three) an increased absorption in the Integral Mössbauer spectrum was expected. The expected increase is further promoted by the transfer of iron species (complex cyanide) from the solution into the solid (precipitate) with the characteristic Mössbauer spectrum also within the integration interval. However the observed change in the absorption over the first 200 minutes was a five per cent decrease, followed by a slow increase (see Figure 21). This absorption increase compensated for the original decrease after five days. The Mössbauer spectrum after 1,000 minutes of reaction contained only three peaks (due to overlapping), consistent with the expected spectrum of the reaction product. The  $\Delta A$  of the Integral reaction spectrum for first 200 minutes is -4.6%. As was already explained earlier, such a large change in absorption can occur only if an other, larger, resonance effect occurs namely, the non-Mössbauer

resonance absorption. The reacting system contains five different iron species and was not further analyzed.

### Reprecipitation

The Mössbauer spectrum of the reaction product for the previous reaction is complex (five iron species are present). To simplify the Mössbauer spectrum of the reaction product the following reaction was studied:



The absorption decreased also in this case (by 1% in 100 minutes) and then started to increase. The initial value of the absorption was reached in about 1000 minutes (see Figure 22) and then remained constant. The Mössbauer spectrum has one single peak. There is no  $\text{FeOx} \cdot 2\text{H}_2\text{O}$  left in the reaction product. The Integral Mössbauer spectrum could be explained by the precipitation of FeS in very fine form with very little Mössbauer absorption. This is finished in about 100 minutes, followed by the growth of microcrystals whose absorption will be greater.

This previous system reacted too rapidly for good experimental observation. A successful attempt was made to delay the start of the reaction and to slow the reaction down.  $\text{FeOx} \cdot 2\text{H}_2\text{O}$  was mixed with 1% agar-agar solution and poured into the cell and allowed to solidify, so as to half fill the cell. The saturated solution of  $\text{Na}_2\text{S}$  was then injected into the other half of the cell, and the cell was sealed. The Integral Mössbauer spectrum (see Figure 23) indicates the occurrence of four distinct processes. The absorption is generally decreasing. In 1000 minutes the change in the absorption is

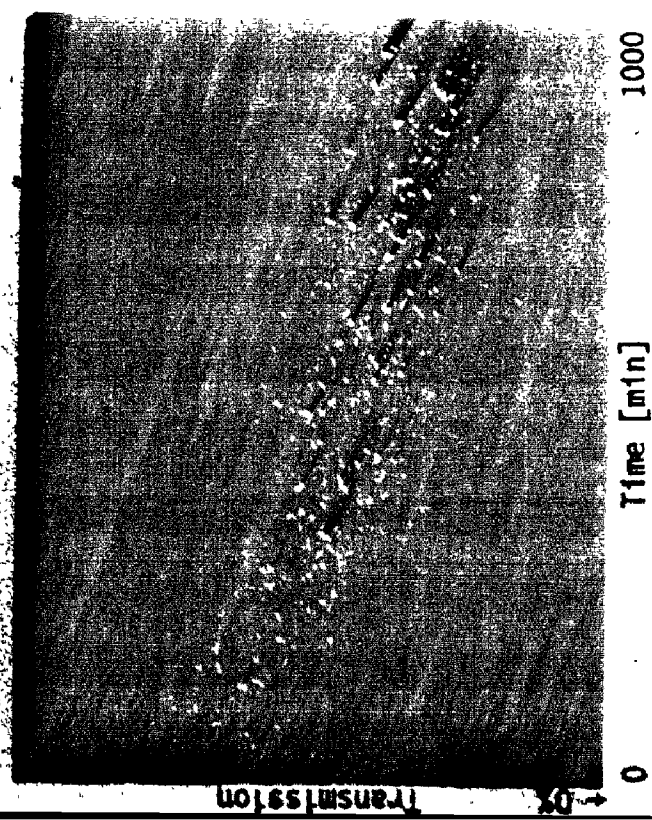


FIGURE 22 Integral reaction spectrum  
 $\text{FeOx} \cdot 2\text{H}_2\text{O} + \text{Na}_2\text{S}_{\text{aq}}$   
 Acceleration:  $5 \text{ cm sec}^{-2}$   
 Dwell time :  $1 \text{ min ch}^{-1}$

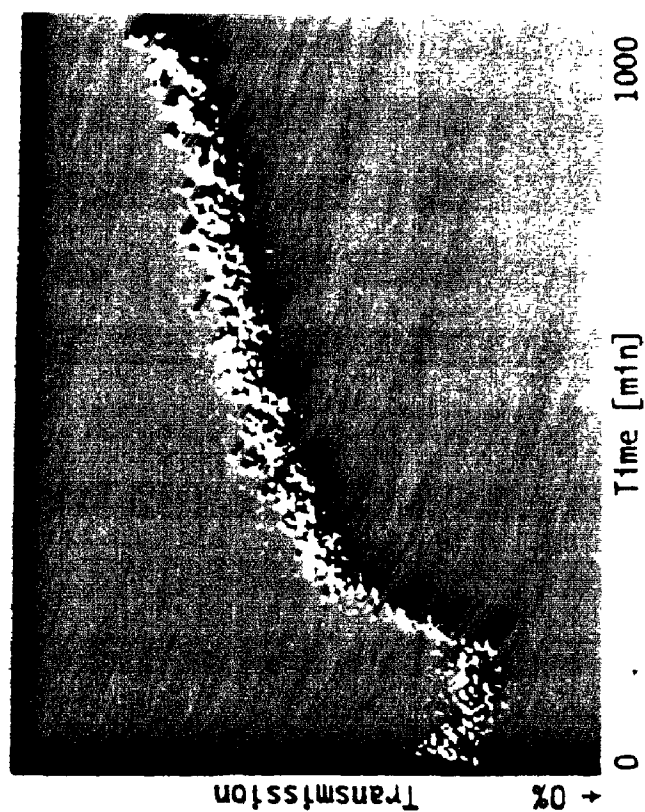


FIGURE 23 Integral reaction spectrum  
 $\text{FeOx} \cdot 2\text{H}_2\text{O} + \text{Na}_2\text{S}_{\text{aq}}$   
 In agar-agar  
 Acceleration:  $5 \text{ cm sec}^{-2}$   
 Dwell time :  $1 \text{ min ch}^{-1}$

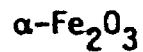
4.5%. The absorption does not become constant even after five days.

Thus the first visible process in the reprecipitation reaction without agar-agar which took about 100 minutes (see Figure 22) has been extended to more than five days (extension by factor larger than 70) by the use of agar-agar, and three earlier processes have become evident.

The Mössbauer spectrum shows practically only the presence of the excess of  $\text{FeOx} \cdot 2\text{H}_2\text{O}$ . The absence of the FeS peak can be explained only in the terms of the very small recoil-free fraction for very small particles. The growth of larger crystals is delayed by the presence of the agar-agar.

#### INTEGRAL THERMAL SCANS

Several compounds were studied using the method of Integral thermal scans. In these experiments, the sample was mounted at room temperature, and cooled to liquid nitrogen temperature. When the liquid nitrogen had evaporated, the sample temperature increased spontaneously up to room temperature. A typical temperature profile is shown in Figure 24. Integral spectrum measurements were started at room temperature and thus were able to follow the initial cooling as well as the slow temperature rise.



A set of measurements was done on  $\alpha\text{-Fe}_2\text{O}_3$ . A characteristic Integral thermal scan is shown in Figure 25 where an abrupt increase

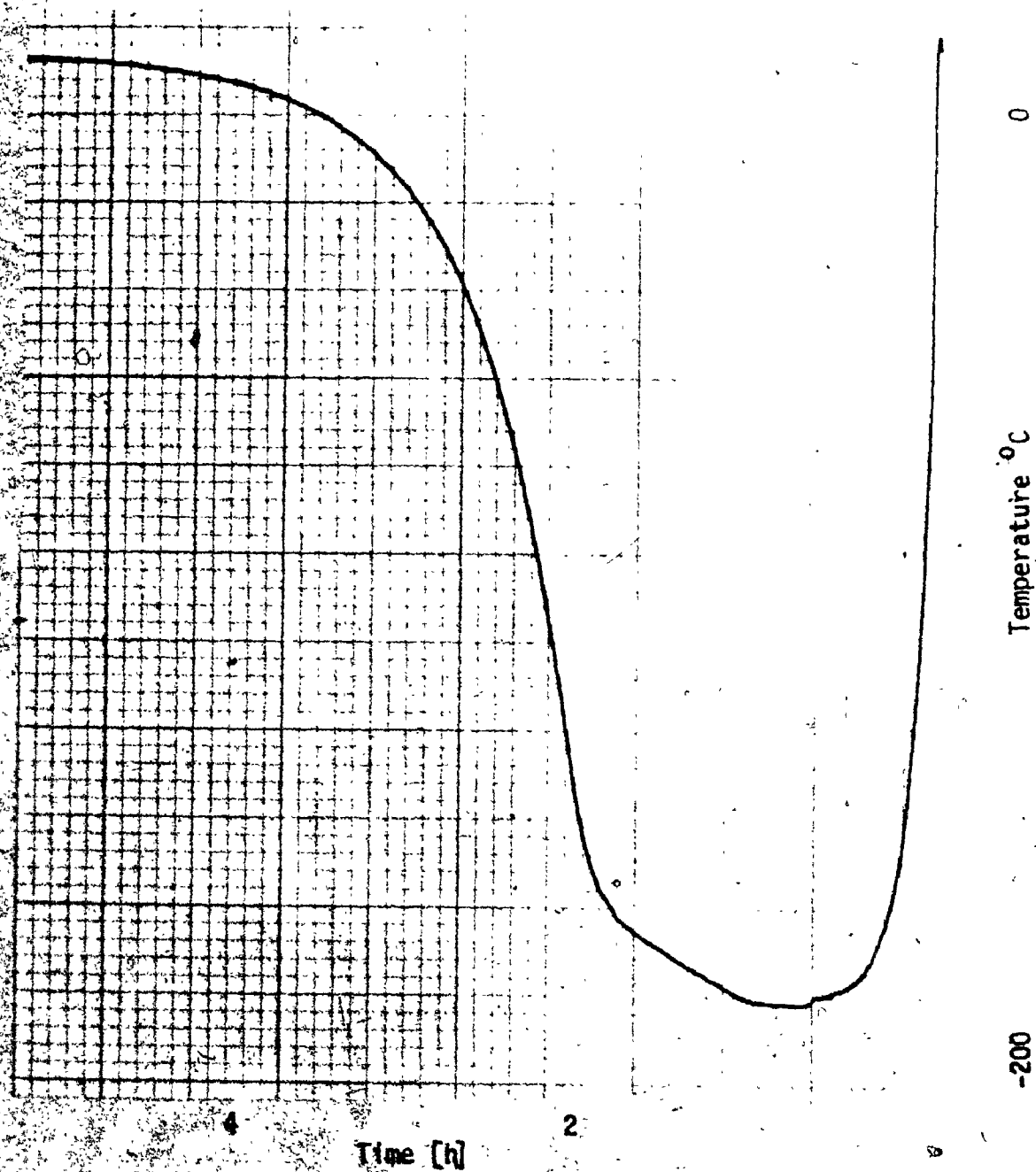


FIGURE 24 Temperature profile for cryostat



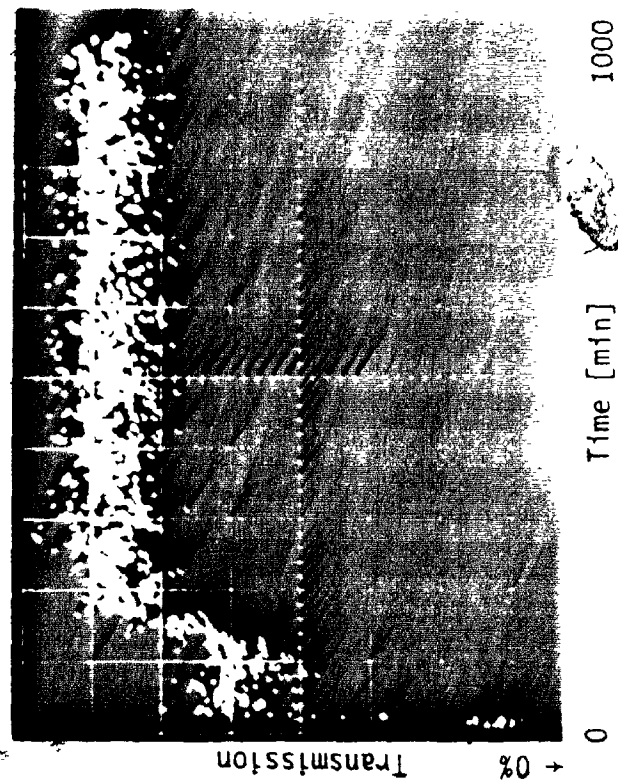


FIGURE 25 Integral thermal scan  
Stainless steel  $^{57}\text{Fe}$  enriched  
Acceleration:  $5 \text{ cm sec}^{-2}$   
Dwell time :  $1 \text{ min ch}^{-1}$

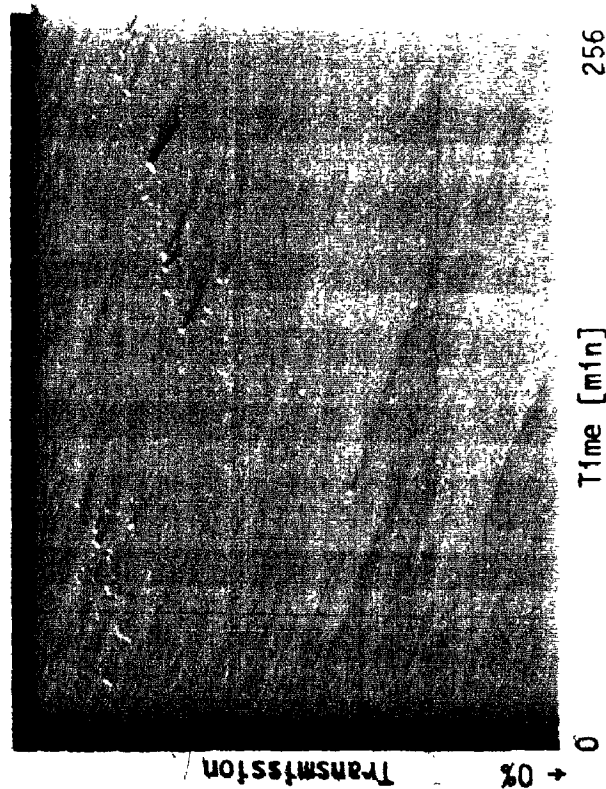


FIGURE 26 Integral thermal scan  $\alpha\text{-Fe}_2\text{O}_3$   
Acceleration:  $0 \text{ cm sec}^{-2}$   
Dwell time :  $1 \text{ min ch}^{-1}$

in absorption marked the time of cooling, and a slow recovery accompanied the warming. The results of some measurements are given in the following Table.

Acceleration (cm sec <sup>-2</sup> )	Absorption* (%)	Plateau	
		Low Temperature End (°C)	Room Temperature Start (°C)
0	6.4	-186	-157
16	5.2	-186	-154
65	5.8	-184	-153

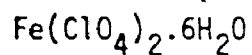
\* In the low temperature plateau

No changes in absorption had been expected in the Integral Thermal scan for an acceleration of 65 cm sec<sup>-2</sup>, and the size of the observed effect, as seen in the Table, was surprising. One plausible trivial explanation was the leakage of liquid nitrogen into the optical path or the condensation of liquid oxygen within the optical path. But these two effects are distinctly different, both lead to the increase in the absorption to the extent of about 35%.

The reality and reproducibility of the effect were confirmed by repeated measurements. The observation of the increased absorption at a low temperature indicates the occurrence of a temperature dependent non-Mössbauer resonance absorption in  $\alpha\text{-Fe}_2\text{O}_3$ . This effect was already postulated for other iron compounds and described in the previous part. The proof for the above statement lies in the independence of the effect on acceleration, its absence in the case where non-resonant  $\gamma$ -radiation was used for the measurement and a

good quantitative agreement of changes in the absorption calculated from the Mössbauer spectra measured (on another sample) at liquid nitrogen temperature and room temperature (9.3% measured and 11% calculated for the low temperature plateau). A low temperature absorption plateau, observed in all Integral thermal scans, is clearly seen in Figure 25 and runs to  $-186^{\circ}\text{C}$ . The following steep slope ends for  $\alpha\text{-Fe}_2\text{O}_3$  at about  $-154^{\circ}\text{C}$ .

Changes in the Mössbauer spectrum at liquid nitrogen temperature and room temperature are too small to have a measurable influence on the above measurements under used experimental conditions. (The thickness of absorbers was low.) The main change in the spectrum is a shift of the first peak to a higher velocity.



The first measurement was done with an acceleration of  $5 \text{ cm sec}^{-2}$ , where the Mössbauer spectrum shows only one peak within the velocity range used. The increase in absorption on cooling was small (1.6%). To achieve a larger change a new acceleration was selected ( $9.5 \text{ cm sec}^{-2}$ ). With this acceleration the room temperature Mössbauer spectrum contains both peaks, one at channel 182 and the second at channel 469 ( $\epsilon = 4.6\%$ ). Cooling to the liquid nitrogen temperature causes a shift of the first peak out of the interval of integration. The second peak shifts to the position 680 and its intensity increases by a factor of almost two (to 8.4%).

Additional improvement was realized by the use of the coincidence technique. In the first measurement under these conditions only the pulses present within the low temperature peak (around

channel 680) were counted. The absorption was 3.2% (maximum value at  $-196^{\circ}\text{C}$ ) and steadily approached 0% with increasing temperature. (0% absorption was reached at about  $-10^{\circ}\text{C}$ .) A second measurement was made, where only the pulses within the corresponding room temperature peak (around channel 469) were counted. The absorption started to decrease from about  $-30^{\circ}\text{C}$  and reached the extreme at  $-196^{\circ}\text{C}$  (-1.8%). It returned smoothly to the room temperature value with rising temperature. Room temperature measurements under both coincidence conditions showed a 1.1% difference in absorption. Unfortunately the statistical error was large (about 1%) due to the fact that only 1/8 of the real time was used for the counting. Nevertheless a continuous change of the absorption with temperature was proven. This excludes the possibility of a phase change as the explanation for the known difference between the room temperature and the liquid nitrogen temperature values of the quadrupole splitting,  $\Delta$ .

It is not possible to decide between the other two explanations; that is, between a continuous change of  $\Delta$  with the temperature and an increase (or decrease) of  $\epsilon$  for the peaks at their respective positions.

But still the two values of  $\Delta A$  (-1.8% and 3.2%) and the room temperature value of the difference in the absorption for both coincidence conditions (1.1%) made it possible to eliminate the Mössbauer effect changes and obtain the difference in the non-Mössbauer resonance absorption between  $-196^{\circ}\text{C}$  and  $24^{\circ}\text{C}$  which is -0.7%. That is, the calculated pure non-Mössbauer resonance absorption is lower at  $-196^{\circ}\text{C}$ .

### Stainless Steel

The room temperature and liquid nitrogen temperature Mössbauer spectra of a stainless steel absorber enriched in  $^{57}\text{Fe}$  (NEN) were measured under the following conditions: acceleration  $5 \text{ cm sec}^{-2}$ , dwell time  $200 \mu\text{sec}$  per channel, 256 channels. The characteristics of the single-peak spectra are:

Temperature ( $^{\circ}\text{C}$ )	Position (ch)	$\epsilon$ (%)
24	170	31
-196	155	23

The Mössbauer spectrum measured at room temperature under the usual conditions ( $5 \text{ cm sec}^{-2}$ ,  $50 \mu\text{sec}$ , 1024 channels) shows that the peak is not quite totally inside the measured interval but the measured interval is about three times the FWHM. For this reason coincidence measurement, as was used in the case of  $\text{Fe}(\text{ClO}_4)_2 \cdot 6\text{H}_2\text{O}$ , will not bring any advantage. Therefore the Integral thermal scan (see Figure 26) was measured over the whole velocity interval. The first (very short) plateau of 3.3% absorption starts at  $-196^{\circ}\text{C}$  and ends at  $-188^{\circ}\text{C}$ . The sudden decrease in the absorption to 1% stops at  $-184^{\circ}\text{C}$ . From there the absorption decreases until it reaches the final constant value (relative 0%) at  $-30^{\circ}\text{C}$ . An apparent plateau at 1% absorption is caused by the non-linearity in the temperature program. The higher value of the absorption at low temperatures and its temperature dependence are caused by a combination of three effects: two positive and one negative. Absorption decrease on rising temperature results from the decrease of the non-Mössbauer resonance absorption and the desymmetrization of the spectrum (the shift of

Reactants	$\Delta A$ (%)	$\epsilon$ Product (%)	$\Delta A$ Corr. (%)	Fe Amount (mmoles $\text{cm}^{-2}$ )
$\text{FeSO}_4 \cdot 7\text{H}_2\text{O} + 6\text{KCN} \rightarrow$	1.1	10	0.5	0.138
$\text{FeSO}_4 \cdot 7\text{H}_2\text{O} + 6\text{KCNO} \rightarrow$	- 0.6	<1	- 0.1	0.138
$\text{FeSO}_4 \cdot 7\text{H}_2\text{O} + 6\text{KCNS} \rightarrow$	-18.1	<1	-17.6	0.118
$(\text{NH}_4)_2\text{Fe}(\text{SO}_4)_2 \cdot 6\text{H}_2\text{O} + 6\text{KCNS} \rightarrow$	- 6.6	<1	- 5.5	0.0986
$(\text{NH}_4)\text{Fe}(\text{SO}_4)_2 \cdot 12\text{H}_2\text{O} + \text{KI} \rightarrow$	11.2	3.5	11.2	0.0986

Positive sign for  $\Delta A$  means that the absorption rose during the reaction. Included in the table are also  $\epsilon$  of the product as measured after the reaction and the amount of iron compound.  $\epsilon$  for the initial iron compound was 10% for  $\text{FeSO}_4 \cdot 7\text{H}_2\text{O}$  (value obtained from the Mössbauer spectra of systems which did not react) and about the same value should be expected for  $(\text{NH}_4)_2\text{Fe}(\text{SO}_4)_2 \cdot 6\text{H}_2\text{O}$ . The low value of  $\epsilon$  (expected value 10%) of the reaction product for fifth reaction is perhaps caused by the fine dispersion of the product. These values were used to calculate the pure non-Mössbauer resonance absorption (represented by  $\Delta A$  corr.), in which the influence of the Mössbauer effect changes is eliminated.

The non-Mössbauer resonance absorption of  $\text{NH}_4\text{Fe}(\text{SO}_4)_2 \cdot 12\text{H}_2\text{O}$  was lowest among the studied compounds.  $\text{NH}_4\text{Fe}(\text{SO}_4)_2 \cdot 12\text{H}_2\text{O}$  was therefore selected as relative zero non-Mössbauer resonance absorber.

The non-Mössbauer resonance absorption of other iron compounds can then be calculated from the absorption in the previous table and following values of the non-Mössbauer resonance absorption for 0.1 mmole  $\text{cm}^{-2}$  of individual compounds can be obtained (assuming that the non-Mössbauer resonance absorption of  $(\text{NH}_4)\text{KFe}(\text{SO}_4)_2 \cdot 6\text{H}_2\text{O}$  is equal to that of  $(\text{NH}_4)_2\text{Fe}(\text{SO}_4)_2 \cdot 6\text{H}_2\text{O}$ ).

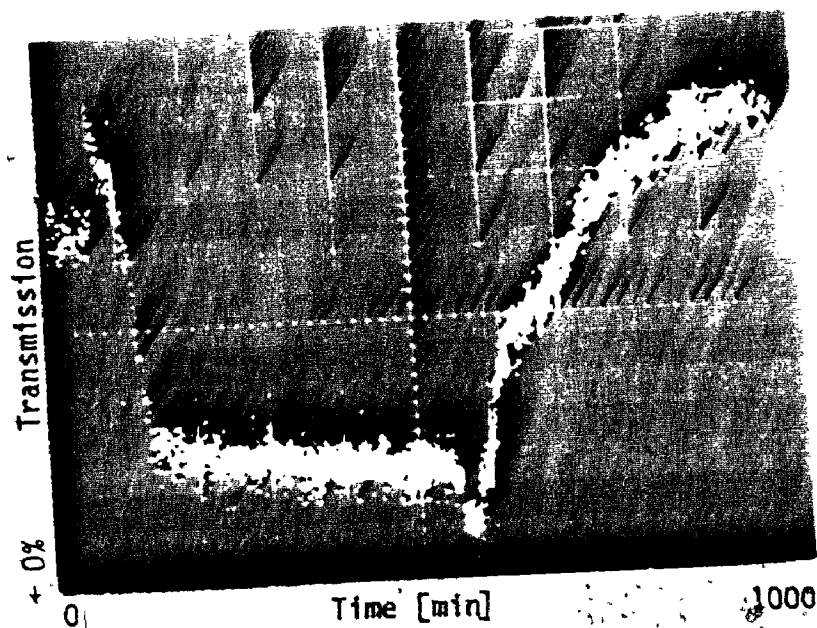


FIGURE 27 Integral thermal scan  $\text{NH}_4\text{Fe}(\text{SO}_4)_2$  aq  
(agar-agar)

Acceleration:  $5 \text{ cm sec}^{-2}$

Dwell time :  $1 \text{ min ch}^{-1}$

Measurement	Plateau		Spike Temperature			
	Start (°C)	Absorp. (%)	Start (°C)	Max. (°C)	End (°C)	Absorp. (%)
1	-190	2	-4.4	+3.6	+ 5.6	4
2	-191.5	5.7	-6.2	-1.0	+ 5.3	8
3*	- 20.1	5.6	-6.4	-5.0	24	7.5

\* cooled with solid CO<sub>2</sub> only -- lowest temperature reached -22.2°C

Similar spikes were observed from successive Mössbauer spectra by Keszthelyi and others. They had great difficulty with reproducibility in the spike formation. In view of this, the data in the Table are rather encouraging. Similar spikes were occasionally observed in saturated solutions of  $\text{NH}_4\text{Fe}(\text{SO}_4)_2$ .

#### NON-MÖSSBAUER RESONANCE ABSORPTION

Some of the previous results on the non-Mössbauer resonance absorption are further treated or presented again in this part. The main reason for such treatment is to summarize important, previously described results together with new evidence (the non-Mössbauer resonance absorption of pure compounds) in order to illustrate better the non-Mössbauer resonance absorption.

In the following table are the results of measured  $\Delta A$  as obtained from the integral reaction spectra which form an evaluable set due to the common reactants or products.



Reactants	$\Delta A$ (%)	$\epsilon$ Product (%)	$\Delta A$ Corr. (%)	Fe Amount (mmoles $\text{cm}^{-2}$ )
$\text{FeSO}_4 \cdot 7\text{H}_2\text{O} + 6\text{KCN} \rightarrow$	1.1	10	0.5	0.138
$\text{FeSO}_4 \cdot 7\text{H}_2\text{O} + 6\text{KCNO} \rightarrow$	- 0.6	<1	- 0.1	0.138
$\text{FeSO}_4 \cdot 7\text{H}_2\text{O} + 6\text{KCNS} \rightarrow$	-18.1	<1	-17.6	0.118
$(\text{NH}_4)_2\text{Fe}(\text{SO}_4)_2 \cdot 6\text{H}_2\text{O} + 6\text{KCNS} \rightarrow$	- 6.6	<1	- 5.5	0.0986
$(\text{NH}_4)\text{Fe}(\text{SO}_4)_2 \cdot 12\text{H}_2\text{O} + \text{KI} \rightarrow$	11.2	3.5	11.2	0.0986

Positive sign for  $\Delta A$  means that the absorption rose during the reaction. Included in the table are also  $\epsilon$  of the product as measured after the reaction and the amount of iron compound.  $\epsilon$  for the initial iron compound was 10% for  $\text{FeSO}_4 \cdot 7\text{H}_2\text{O}$  (value obtained from the Mössbauer spectra of systems which did not react) and about the same value should be expected for  $(\text{NH}_4)_2\text{Fe}(\text{SO}_4)_2 \cdot 6\text{H}_2\text{O}$ . The low value of  $\epsilon$  (expected value 10%) of the reaction product for fifth reaction is perhaps caused by the fine dispersion of the product.

These values were used to calculate the pure non-Mössbauer resonance absorption (represented by  $\Delta A$  corr.), in which the influence of the Mössbauer effect changes is eliminated.

The non-Mössbauer resonance absorption of  $\text{NH}_4\text{Fe}(\text{SO}_4)_2 \cdot 12\text{H}_2\text{O}$  was lowest among the studied compounds.  $\text{NH}_4\text{Fe}(\text{SO}_4)_2 \cdot 12\text{H}_2\text{O}$  was therefore selected as relative zero non-Mössbauer resonance absorber.

The non-Mössbauer resonance absorption of other iron compounds can then be calculated from the absorption in the previous table and following values of the non-Mössbauer resonance absorption for 0.1 mmole  $\text{cm}^{-2}$  of individual compounds can be obtained (assuming that the non-Mössbauer resonance absorption of  $(\text{NH}_4)\text{KFe}(\text{SO}_4)_2 \cdot 6\text{H}_2\text{O}$  is equal to that of  $(\text{NH}_4)_2\text{Fe}(\text{SO}_4)_2 \cdot 6\text{H}_2\text{O}$ ).

$(\text{NH}_4)\text{Fe}(\text{SO}_4)_2 \cdot 12\text{H}_2\text{O}$	0.0%
$\text{K}_4[\text{Fe}(\text{CNS})_6] \cdot x\text{H}_2\text{O}$	4.9%
$(\text{NH}_4)_2\text{Fe}(\text{SO}_4)_2 \cdot 6\text{H}_2\text{O}$	10.1%
$\text{FeSO}_4 \cdot 7\text{H}_2\text{O}$	19.1%
$\text{K}_4[\text{Fe}(\text{CNO})_6] \cdot x\text{H}_2\text{O}$	19.0%
$\text{K}_4[\text{Fe}(\text{CN})_6] \cdot 3\text{H}_2\text{O}$	19.4%

Among the strong non-Mössbauer resonance absorbers belongs also hydrated  $\text{Fe}^{3+}$  adsorbed on strong cation exchanger resin, with the non-Mössbauer resonance absorption at least 19%.

It was not possible for different reasons to derive comparative values for the non-Mössbauer resonance absorption for the following compounds:  $\text{FeS}$ ,  $\text{FeO} \cdot x\text{H}_2\text{O}$ ,  $\text{FeSO}_4$ ,  $\text{NH}_4\text{Fe}(\text{SO}_4)_2 \cdot x\text{H}_2\text{O}$  ( $x < 7$ ),  $\text{Na}_3[\text{Fe}(\text{H}_2\text{O})(\text{CN})_5] \cdot x\text{H}_2\text{O}$  and  $[\text{Fe}(\text{CN})_6]^{3-}$ . Nevertheless the first two compounds have practically the same non-Mössbauer resonance absorption.

In order to obtain the non-Mössbauer resonance absorption from direct measurements of pure compounds proper part of the "background" of the Mössbauer spectra (identical in all cases) was selected, the counting rate was corrected for differences in  $\gamma$ -ray absorption and dispersion of individual compounds (see Liebhaufsky, Pfeiffer, Winslow and Zemany) and the non-Mössbauer resonance absorption ( $\Delta A$ ) calculated relative to standard iron foil. The values of the non-Mössbauer resonance absorption in the following table obtained with source #5 are rather large and demonstrate the differences between different compounds. For definition of  $\Delta A$  see Appendix 2.

Compound (0.2 mmole cm <sup>-2</sup> )	$\Delta A$ (%)
Fe	( 0.0 )
K <sub>4</sub> [Fe(CN) <sub>6</sub> ].3H <sub>2</sub> O	10.6
(NH <sub>4</sub> ) <sub>2</sub> Fe(SO <sub>4</sub> ) <sub>2</sub> .6H <sub>2</sub> O	15.7
K <sub>3</sub> [Fe(CN) <sub>6</sub> ]	23.7

The size of the non-Mössbauer resonance absorption is similar to the values derived from Integral reaction spectra (see page 107). Two compounds present in both tables have different values and inversed order. That contradiction (among other facts) demonstrates the dependence of the non-Mössbauer resonance absorption on the state of absorber (matrix effects, or crystal size and other effects).

The following table contains another set of the non-Mössbauer resonance absorption values ( $\Delta A$ ) of pure compounds calculated relative to the non-Mössbauer resonance absorption of Fe(NO<sub>3</sub>)<sub>3</sub>.9H<sub>2</sub>O using source #4.

Compound (0.1 mmole cm <sup>-2</sup> )	$\Delta A$ (%)
Fe(NO <sub>3</sub> ) <sub>3</sub> .9H <sub>2</sub> O	0.0
Fe (bzac) <sub>3</sub>	3.0
$\alpha$ - Fe <sub>2</sub> O <sub>3</sub>	5.0 (for 0.05 mmole cm <sup>-2</sup> )
FeOx.2H <sub>2</sub> O	10.8
(NH <sub>4</sub> )Fe(SO <sub>4</sub> ) <sub>2</sub> .12H <sub>2</sub> O	15.3
FeSO <sub>4</sub> .7H <sub>2</sub> O	17.0
Na <sub>2</sub> [Fe(NO)(CN) <sub>5</sub> ].2H <sub>2</sub> O	22.2

There are again two compounds present which already appeared in the table of  $\Delta A$  derived from Integral reaction spectra (see page 107).

$\text{FeSO}_4 \cdot 7\text{H}_2\text{O}$  value is in good (accidental ?) agreement. The value of  $\Delta A$  for  $(\text{NH}_4)\text{Fe}(\text{SO}_4)_2 \cdot 12\text{H}_2\text{O}$  is much higher for the pure compound. Some explanations for this disagreement were already mentioned earlier. Integral thermal scan results demonstrated the thermal dependence of the non-Mössbauer resonance absorption and the different degrees thereof. The resonant character of the non-Mössbauer absorption was proven by the absence of the effect in Integral thermal scans of  $\alpha\text{-Fe}_2\text{O}_3$  using the non-resonant part of the  $\gamma$ -spectrum of  $^{57}\text{Co} + ^{57\text{m}}\text{Fe}$ . The "non-selective" character of the non-Mössbauer resonance absorption was proven also from the independence of results of Integral thermal scans on acceleration.

The non-Mössbauer resonance absorption is temperature dependent, different at least for some compounds, and is at least in some cases larger (by more than one order) than the Mössbauer absorption. It is present also under the conditions where the Mössbauer effect is not possible.

This absorption can be called in terms of Mössbauer spectroscopy a non-selective resonance absorption, or a "gray" absorption, which means that there exists a compound- and temperature-dependent specific absorption which does have a constant (or nearly constant) value over an energy interval much larger than the natural width of the Mössbauer peaks. At the same time this absorption is limited to a relatively narrow energy interval in terms of X-ray absorption spectroscopy.

Therefore this absorption forms a very broad peak with the FWHM which is (much) larger than  $3 \text{ cm sec}^{-1}$  ( $1.4 \times 10^{-6} \text{ eV}$ ) but smaller than 1 eV.

The existence of such peak(s) is consistent with the zero phonon non-Mössbauer transition or low energy one phonon or multi-phonon transitions.

Regular X-ray diffraction cannot cause the non-Mössbauer resonance absorption described because the intensities of diffracted lines are too small.

## CONCLUSIONS

The main result of this work has been the development of a new method of application of the Mössbauer effect to the study of systems which are changing as a function of time. This application which has essentially no direct forerunner in the literature (except the zero velocity work of Mössbauer and the constant non-zero velocity work of Preston, Hanna and Heberle) now enables us to follow the progress of chemical and physical changes with a closeness hitherto possible in only rare cases. The ease and simplicity of the work and the low sophistication of the equipment should make this method attractive to solid state chemists.

This work has not concerned itself with detailed understanding of the Integral Mössbauer spectra nor with the exhaustive interpretation of the changes in resonance absorption. These will wait for a further work.

It has been shown that this new method can be applied to a wide variety of reactions of iron-containing compounds in the solid state: coordination changes, oxidation and reduction, hydration changes. A wide variety of other possible reactions can doubtless be studied in this way. Similarly the method has been applied to processes occurring in the liquid state or on surfaces where even though no Mössbauer effect is displayed, the observed changes in transmission show the time dependence of the occurring reaction. Further, transitions occurring as a function of temperature have been observed by Integral Mössbauer spectroscopy. These seem likely to have their greatest application in identifying the temperature ranges over which to make more detailed Mössbauer studies.

A possibly very important result is that the background non-Mössbauer resonance absorption seems to vary strongly as a function of the state of the system. The effect has not yet been explained theoretically, but doubtlessly involves the phonon processes of the solid. Since the effect is in some cases larger than the Mössbauer effect, its use in off-resonance Integral Mössbauer spectroscopy is likely to give greater variability to this latter method. This result must originate in changes in the lattice rigidity and is also connected with the (micro) size of the sample assembly (crystal growth).

Within this work, the difficulty of obtaining the correct Mössbauer spectra was recognized, together with the fact, that a large amount of published data is not of very high quality. There are two reasons for it. Part of the work was done by physicists who usually do not appreciate problems with identity or purity of chemical compounds or in the case of chemists the problem was connected with the lack of computing capacity or lack of necessary sophistication of used programs.

For the part of Integral Mössbauer spectroscopy the presented results are rather phenomenological. The main concern was to establish the reality of Integral Mössbauer spectroscopy, to use it in different areas and specially to present original data without any "beneficial" computer trickery.

Nevertheless the computer was used heavily in the first part (Mössbauer spectra) and only through its use some important problems of Mössbauer spectroscopy were recognized and subsequently solved (non-equality of FWHM, incorrect intensity ratios for magnetically

split spectra et cetera).

Very important feature of procedures realized within this work is their convenience and easy applicability and usability also without extensive computer usage. The eventual (sometimes very useful) calculations are done only to extract as an example the kinetic law for isothermal measurements or the analytical function for the temperature dependence of corresponding parameter in varying temperature measurements.

Larger amount of work done in different areas of Mössbauer spectroscopy of  $^{57}\text{Fe}$  is not included in this work. The reasons for not presenting these topics are different. Usually it is because the continuation of work to publishable conclusion was asking for prohibitive amount of computer time or for realization of very difficult or expensive experimental techniques. The last reason was that it would have enlarged the scope of this work far beyond its feasibility. As an example only:

- (a) The analysis of silicate minerals (annites started in cooperation with R. Moore and G. Skippen from Department of Mineralogy and pyroxenes with S. Abbey from Geological Survey).
- (b) The measurements of Mössbauer spectra of viscous solutions (rather narrow low intensity peaks were discovered).
- (c) Very weak numerous peaks in Mössbauer spectra originating in the trace amounts of  $^{57}\text{Fe}$  in the beryllium window of the detector (or in the source) which are visible only after signal averaging and which can be instrumental artefacts.

In some cases of the Mössbauer spectroscopy either the absorber or the source will undergo very slow changes (reaction, phase



transition, thermal annealing) during the measurement of a spectrum. This is often not noticed because the differences in the measured Mössbauer spectrum are difficult to recognize as such. It is however strongly recommended to use an Integral Mössbauer spectrometer in parallel in all cases of serious Mössbauer spectroscopy work and accumulate the two spectra concurrently. The Integral Mössbauer spectrometer is in such case used as a control device only, whose function would be to demonstrate the absence of such changes.

## PERSPECTIVES

From the tremendous amount of possibilities in the study of Mössbauer effect only few are mentioned here.

In classical Mössbauer spectroscopy:

- (a) The study of the signal averaging, its significance, optimization and use (first for the solution of the origin and identification of numerous small peaks found in the background parabola).
- (b) The changes in the main curve fitting program to include results from the presented study in order to eliminate two variable parameters, which is important to every practising Mössbauer spectroscopist.

In Integral Mössbauer spectroscopy:

- (a) The realization of the Integral spectrometer without the use of multichannel analyzer. The publication should lead to the increase of accessibility (economic reasons -- saving of at least \$6,000) of Mössbauer effect studies.
- (b) Most interesting and important future work is in the field of concurrent measurements of successive ("short time") Mössbauer spectra and Integral Mössbauer spectra. The number of useful combinations is rather large and it is impossible to guess which one is more important and interesting. Only as an example an assembly of two Integral spectrometers, one set off resonance and second on resonance, will give the possibility to separate two components contributing to the large absorption

changes as described in this work, namely the small contribution from the Mössbauer component and the rather large non-Mössbauer component.

- (c) Also the possibilities of further fundamental exploratory studies with the present equipment, as realized in this laboratory, are far from being exhausted. To mention only one which seems quite interesting is to measure the phonon spectra of solids by using the non-Mössbauer resonance absorption, placing the absorber (source) in a sonic field and sweeping through proper range of frequencies.
- (d) In Integral Thermal Scans the basic necessary improvement is obvious -- the use of selectable linear temperature scans (values of the order of  $0.1^{\circ}\text{C}/1\text{ min}$  and lower are attractive).
- (e) But most of all for the advancement of the basic research the realization of universal multipurpose spectrometer system based on the minicomputer will be greatly enjoyed by the author. Nonetheless, the realization of such system anywhere else, predicted for the near future, will be equally appreciated. To that effect will this work and derived publications hopefully contribute.

## APPENDIX 1

## Signal-to-noise ratio

A Lorentzian function is an even function. For the determination of its area in the case of one peak is therefore enough to integrate from the position of the maximum and multiply the result by two. The position of the maximum can be shifted to the beginning of the coordinate system. The integration in the transposed system will be from  $x = 0$  to  $n/2$ , which leads to

$$\begin{aligned} 2Y_0^{n/2} &= 2/3 an^3 + bn^2 + 2cn - 2CA \arctan(nA/2A^2) \\ &= 2/3 an^3 + bn^2 + 2cn - 2CA \arctan(n/2A) \end{aligned}$$

Substitution of a dimensionless factor  $f$  defined as

$$n = 2fA$$

leads to

$$2Y_0^{n/2} = 2/3 an^3 + bn^2 + 2cn - 2CA \arctan(f)$$

The signal-to-noise ratio for the integral spectrum is then

$$S/N = \frac{\text{peak area}}{(n.\text{background} - \text{peak area})^{1/2}}$$

The peak area in the denominator can be made (by selection of  $C$ ) negligibly small compared to the area of the integrated background. The simplified expression for the  $S/N$  ratio is then

$$S/N = \frac{\text{peak area}}{(n.\text{background})^{1/2}}$$

Using the analytical expression for the peak area (after substitution of the dimensionless fraction  $f$ /reduced integration interval/

$f = n/2A$ ) and transferring the non-variable expressions into a constant, the expression

$$S/N = \text{const} \sqrt{A} [\text{Arctan}(f)] / \sqrt{f}$$

is obtained, where  $\sqrt{A}$  can be considered as a parameter which does not influence the position of the optimum of  $S/N$  in terms of  $f$ .

The final expression

$$S/N = \text{Const} [\text{Arctan}(f)] / \sqrt{f}$$

has a maximum for

$$\text{Arctan}(f) = 2f/(1 + f^2)$$

This last equation can only be solved numerically. The approximate value of  $f$  is 1.4.

It is thus shown that in Integral Mössbauer spectroscopy exists an optimum for the signal-to-noise ratio which lies at an  $f$  value about one order in magnitude greater than is possible in conventional Mössbauer spectroscopy and is in a methodically separate "non-dispersive" region of the dependence of  $S/N$  on  $f$ .

The existence of this optimum is not limited to the field of General Mössbauer spectroscopy. It is equally valid for all spectroscopies in which are found Lorentzian line shapes (and also for other line shapes - but with a different numerical value for  $f$ ).

At the same time this representation demonstrates that Mössbauer spectroscopy is a special case of Integral Mössbauer spectroscopy.

## APPENDIX 2

Definition of  $\Delta A$  for pure compounds

The initial intensity ( $I_0$ ) and the measured intensity ( $I_1$ ) of the standard iron foil are not compatible with transmitted intensities of pure compounds ( $I_i$ ) due to different counting conditions or different geometry of the standard sample. It is still possible to calculate (apparent) transmission ( $T_{1,i}$ , where  $i$  represents different samples with the exception of the first one). Logically the sample with the highest transmission ( $T_{1,2} \geq T_{1,i}$ ) can be selected as a sample with the relative transmission equal to one. This assumption makes it possible to transform the set  $T_{1,i}$  into a set  $T_{2,i}$  and from  $T_{2,i}$  to calculate relative absorptions forming a set  $\Delta A_i$ . (The symbol  $\Delta A$  was chosen to distinguish these values from the correct absorption.)

As an example:

$$T_{1,2} = \frac{I_2}{I_1} \longrightarrow T_{2,2} = 1$$

$$T_{1,3} = \frac{I_3}{I_1} \longrightarrow T_{2,3} = \frac{I_3}{I_2} = \frac{T_{1,3}}{T_{1,2}}$$

and generally

$$T_{1,i} = \frac{I_i}{I_1} \longrightarrow T_{2,i} = \frac{I_i}{I_2} = \frac{T_{1,i}}{T_{1,2}}$$

The relative absorptions are then

$$\Delta A_i = 1 - \frac{I_i}{I_2} = 1 - T_{2,i} = 1 - \frac{T_{1,i}}{T_{1,2}}$$

which can be expressed as

$$1 - \Delta A_i = \frac{1 - A_{1,i}}{1 - A_{1,2}}$$

or

$$\Delta A_i = \frac{A_{1,i} - A_{1,2}}{1 - A_{1,2}}$$

The former two assumptions are then

$$A_{1,2} \leq A_{1,i}$$

$$A_{2,2} = 0$$

and warrant that

$$\Delta A_i \leq A_i$$

which means that the correct absorption ( $A_i$ ) for any given compound will be larger than (or equal to) the tabulated relative absorption ( $\Delta A_i$ ).

At the same time on such sets the recalculation between different area concentrations is still meaningful.

## REFERENCES

1. A. Abragam, The Principles of Nuclear Magnetism, Clarendon Press, Oxford, 1961.
2. G. M. Bancroft, K. G. Dharmawardena, A. G. Maddock, Inorg. Chem., 9, 223 (1970).
3. P. Bertels, Carleton University, Chemistry Department, Electronics Workshop.
4. B. Brunot, V. Hauser, W. Neuwirth, Z. Physik, 249, 134 (1971).
5. D. W. Carson, personal communication.
6. E. R. Czerlinsky, Computational Techniques in Single Crystal Mössbauer Spectroscopy, Air Force Cambridge Research Laboratories Report 70-0010, 1969.
7. H. S. de Benedetti, G. Lang, R. Ingalls, Phys. Rev. Letters, 6, 60 (1961).
8. B. D. Dunlap, J. G. Dash, Phys. Rev., 155, 460 (1967).
9. L. W. Fagg, S. S. Hanna, Rev. Mod. Phys., 31, 711 (1959).
10. J. Fenger, RISØ Report No. 255, Danish Atomic Energy Commission, 1971.
11. H. Frauenfelder, D. E. Nagle, R. D. Raylor, D. R. F. Cochran, W. M. Visscher, Phys. Rev., 126, 1065 (1962).
12. K. Fröhlich, L. Keszthelyi, Z. Physik, 259, 301 (1973).
13. P. K. Gallagher, D. W. Johnson, F. Schrey, J. Amer. Ceram. Soc., 53, 666 (1970).
14. T. C. Gibb, N. N. Greenwood, M. D. Sastry, J. C. S. Dalton, 1896 (1972).
15. N. N. Greenwood, T. C. Gibb, Mössbauer Spectroscopy, Chapman and Hall Ltd., London, 1971.
16. P. Gütllich, K. M. Hasselbach, Angew. Chem. Internat. Ed., 8, 600 (1969).
17. R. H. Herber, in Mössbauer Effect Methodology, Vol. 1, Plenum Press, New York, 1965.
18. R. M. Housley, U. Gonser, R. Grant, Phys. Rev. Letters, 20, 1279 (1968).



19. A. Johansson, J. Inorg. Nucl. Chem., 31, 3273 (1969).
20. E. Kankaleit, unpublished results.
21. L. Keszthelyi, J. A. Cameron, G. Nagy, L. Kacsoh, J. Chem. Phys., 38, 4610 (1973).
22. O. C. Kistner, A. W. Sunyar, Phys. Rev. Letters, 4, 412 (1960).
23. W. Kuhn, Phil. Mag., 8, 625 (1929).
24. W. E. Lamb Jr., Phys. Rev., 55, 190 (1939).
25. H. A. Liebhafsky, H. G. Pfeiffer, E. H. Winslow, P. D. Zeman, X-Ray Absorption and Emission in Analytical Chemistry, John Wiley & Sons, New York, London, 1960.
26. P. B. Moon, Proc. Phys. Soc., 63, 1189 (1950).
27. R. F. Mössbauer, Z. Physik, 151, 124 (1958).
28. L. Pfeiffer, C. P. Lichtenwalner, Rev. Sci. Instrum., 45, 803 (1974).
29. R. V. Pound, G. A. Rebka, Phys. Rev. Letters, 3, 554 (1959).
30. R. S. Preston, S. S. Hanna, J. Heberle, Phys. Rev., 128, 2207 (1962).
31. Rayleigh, see R. W. Wood.
32. E. Rhodes, A. Pollinger, J. J. Spijkerman, B. W. Christ, Trans. Met. Soc. AIME., 242, 1922 (1968).
33. I. Solomon, Compt. Rend., 250, 3828 (1960).
34. R. Street, B. Window, Proc. Phys. Soc., 89, 589 (1966).
35. G. J. Thiessen, personal communication.
36. C. H. Townes, A. L. Shawlow, Microwave Spectroscopy, McGraw-Hill, New York, 1963.
37. H. Wegener, Der Mössbauer-effect und seine Anwendung in Physik und Chemie, Bibliographisches Inst., Mannheim, 1965.
38. B. Window, B. L. Dickson, P. Routcliffe, K. K. P. Srivastava, J. Phys. E.: Sci. Instrum., 7, 916 (1974).
39. F. Wittmann, F. Pobell, W. Wiedemann, Z. Angew. Phys., 19, 20 (1965).
40. R. W. Wood, Physical Optics, Macmillan, New York, 1934.
41. H. S. Word, personal communication.

END

1910377

FIN